

ISSN 1881-7815    Online ISSN 1881-7823

# BST

## BioScience Trends

Volume 12, Number 5  
October, 2018



[www.biosciencetrends.com](http://www.biosciencetrends.com)



**BioScience Trends** is one of a series of peer-reviewed journals of the International Research and Cooperation Association for Bio & Socio-Sciences Advancement (IRCA-BSSA) Group and is published bimonthly by the International Advancement Center for Medicine & Health Research Co., Ltd. (IACMHR Co., Ltd.) and supported by the IRCA-BSSA and Shandong University China-Japan Cooperation Center for Drug Discovery & Screening (SDU-DDSC).

**BioScience Trends** devotes to publishing the latest and most exciting advances in scientific research. Articles cover fields of life science such as biochemistry, molecular biology, clinical research, public health, medical care system, and social science in order to encourage cooperation and exchange among scientists and clinical researchers.

**BioScience Trends** publishes Original Articles, Brief Reports, Reviews, Policy Forum articles, Case Reports, News, and Letters on all aspects of the field of life science. All contributions should seek to promote international collaboration.

## Editorial Board

### Editor-in-Chief:

Norihiro KOKUDO  
*National Center for Global Health and Medicine, Tokyo, Japan*

*Toho University, Tokyo, Japan*

Ri SHO

*Yamagata University, Yamagata, Japan*  
Yasuhiko SUGAWARA  
*Kumamoto University, Kumamoto, Japan*  
Ling WANG  
*Fudan University, Shanghai, China*

### Co-Editors-in-Chief:

Xue-Tao CAO  
*Nankai University, Tianjin, China*  
Rajendra PRASAD  
*University of Delhi, Delhi, India*  
Arthur D. RIGGS  
*Beckman Research Institute of the City of Hope, Duarte, CA, USA*

### Managing Editor:

Jianjun GAO  
*Qingdao University, Qingdao, China*

### Chief Director & Executive Editor:

Wei TANG  
*National Center for Global Health and Medicine, Tokyo, Japan*

### Web Editor:

Yu CHEN  
*The University of Tokyo, Tokyo, Japan*

### Senior Editors:

Xunjia CHENG  
*Fudan University, Shanghai, China*  
Yoko FUJITA-YAMAGUCHI  
*Beckman Research Institute of the City of Hope, Duarte, CA, USA*  
Na HE  
*Fudan University, Shanghai, China*  
Kiyoshi KITAMURA  
*The University of Tokyo, Tokyo, Japan*  
Misao MATSUSHITA  
*Tokai University, Hiratsuka, Japan*  
Munehiro NAKATA  
*Tokai University, Hiratsuka, Japan*  
Takashi SEKINE

### Proofreaders:

Curtis BENTLEY  
*Roswell, GA, USA*  
Christopher HOLMES  
*The University of Tokyo, Tokyo, Japan*  
Thomas R. LEBON  
*Los Angeles Trade Technical College, Los Angeles, CA, USA*

### Editorial Office

Pearl City Koishikawa 603,  
2-4-5 Kasuga, Bunkyo-ku, Tokyo 112-0003, Japan  
Tel: +81-3-5840-8764 Fax: +81-3-5840-8765  
E-mail: office@biosciencetrends.com

# BioScience Trends

## Editorial and Head Office

Pearl City Koishikawa 603, 2-4-5 Kasuga, Bunkyo-ku,  
Tokyo 112-0003, Japan

Tel: +81-3-5840-8764, Fax: +81-3-5840-8765  
E-mail: office@biosciencetrends.com  
URL: www.biosciencetrends.com

## Editorial Board Members

Girdhar G. AGARWAL <i>(Lucknow, India)</i>	Takahiro HIGASHI <i>(Tokyo, Japan)</i>	Masatoshi MAKUCHI <i>(Tokyo, Japan)</i>	Tadatoshi TAKAYAMA <i>(Tokyo, Japan)</i>
Hirotugu AIGA <i>(Geneva, Switzerland)</i>	De-Fei HONG <i>(Hangzhou, China)</i>	Francesco MAROTTA <i>(Milano, Italy)</i>	Shin'ichi TAKEDA <i>(Tokyo, Japan)</i>
Hidechika AKASHI <i>(Tokyo, Japan)</i>	De-Xing HOU <i>(Kagoshima, Japan)</i>	Yutaka MATSUYAMA <i>(Tokyo, Japan)</i>	Sumihito TAMURA <i>(Tokyo, Japan)</i>
Moazzam ALI <i>(Geneva, Switzerland)</i>	Sheng-Tao HOU <i>(Ottawa, Canada)</i>	Qingyu MENG <i>(Beijing, China)</i>	Puay Hoon TAN <i>(Singapore, Singapore)</i>
Ping AO <i>(Shanghai, China)</i>	Yong HUANG <i>(Ji'ning, China)</i>	Mark MEUTH <i>(Sheffield, UK)</i>	Koji TANAKA <i>(Tsu, Japan)</i>
Hisao ASAMURA <i>(Tokyo, Japan)</i>	Hirofumi INAGAKI <i>(Tokyo, Japan)</i>	Satoko NAGATA <i>(Tokyo, Japan)</i>	John TERMINI <i>(Duarte, CA, USA)</i>
Michael E. BARISH <i>(Duarte, CA, USA)</i>	Masamine JIMBA <i>(Tokyo, Japan)</i>	Miho OBA <i>(Odawara, Japan)</i>	Usa C. THISYAKORN <i>(Bangkok, Thailand)</i>
Boon-Huat BAY <i>(Singapore, Singapore)</i>	Chunlin JIN <i>(Shanghai, China)</i>	Fanghua QI <i>(Ji'nan, Shandong)</i>	Toshifumi TSUKAHARA <i>(Nomi, Japan)</i>
Yasumasa BESSHOU <i>(Nara, Japan)</i>	Kimitaka KAGA <i>(Tokyo, Japan)</i>	Xianjun QU <i>(Beijing, China)</i>	Kohjiro UEKI <i>(Tokyo, Japan)</i>
Generoso BEVILACQUA <i>(Pisa, Italy)</i>	Ichiro KAI <i>(Tokyo, Japan)</i>	John J. ROSSI <i>(Duarte, CA, USA)</i>	Masahiro UMEZAKI <i>(Tokyo, Japan)</i>
Shiuan CHEN <i>(Duarte, CA, USA)</i>	Kazuhiro KAKIMOTO <i>(Osaka, Japan)</i>	Carlos SAINZ-FERNANDEZ <i>(Santander, Spain)</i>	Junming WANG <i>(Jackson, MS, USA)</i>
Yuan CHEN <i>(Duarte, CA, USA)</i>	Kiyoko KAMIBEPPU <i>(Tokyo, Japan)</i>	Yoshihiro SAKAMOTO <i>(Tokyo, Japan)</i>	Xiang-Dong Wang <i>(Boston, MA, USA)</i>
Naoshi DOHMAE <i>(Wako, Japan)</i>	Haidong KAN <i>(Shanghai, China)</i>	Erin SATO <i>(Shizuoka, Japan)</i>	Hisashi WATANABE <i>(Tokyo, Japan)</i>
Zhen FAN <i>(Houston, TX, USA)</i>	Bok-Luel LEE <i>(Busan, Korea)</i>	Takehito SATO <i>(Isehara, Japan)</i>	Lingzhong XU <i>(Ji'nan, China)</i>
Ding-Zhi FANG <i>(Chengdu, China)</i>	Mingjie LI <i>(St. Louis, MO, USA)</i>	Akihito SHIMAZU <i>(Tokyo, Japan)</i>	Masatake YAMAUCHI <i>(Chiba, Japan)</i>
Xiaobin FENG <i>(Beijing, China)</i>	Shixue LI <i>(Ji'nan, China)</i>	Zhifeng SHAO <i>(Shanghai, China)</i>	Aitian YIN <i>(Ji'nan, China)</i>
Yoshiharu FUKUDA <i>(Ube, Japan)</i>	Ren-Jang LIN <i>(Duarte, CA, USA)</i>	Judith SINGER-SAM <i>(Duarte, CA, USA)</i>	George W-C. YIP <i>(Singapore, Singapore)</i>
Rajiv GARG <i>(Lucknow, India)</i>	Lianxin LIU <i>(Harbin, China)</i>	Raj K. SINGH <i>(Dehradun, India)</i>	Xue-Jie YU <i>(Galveston, TX, USA)</i>
Ravindra K. GARG <i>(Lucknow, India)</i>	Xinqi LIU <i>(Tianjin, China)</i>	Peipei SONG <i>(Tokyo, Japan)</i>	Benny C-Y ZEE <i>(Hong Kong, China)</i>
Makoto GOTO <i>(Tokyo, Japan)</i>	Daru LU <i>(Shanghai, China)</i>	Junko SUGAMA <i>(Kanazawa, Japan)</i>	Yong ZENG <i>(Chengdu, China)</i>
Demin HAN <i>(Beijing, China)</i>	Hongzhou LU <i>(Shanghai, China)</i>	Hiroshi TACHIBANA <i>(Isehara, Japan)</i>	Xiaomei ZHU <i>(Seattle, WA, USA)</i>
David M. HELFMAN <i>(Daejeon, Korea)</i>	Duan MA <i>(Shanghai, China)</i>	Tomoko TAKAMURA <i>(Tokyo, Japan)</i>	<i>(as of February 26, 2018)</i>

**Policy Forum**

- 445 - 449** **China issues the National Essential Medicines List (2018 edition): Background, differences from previous editions, and potential issues.**  
*Jiangjiang He, Mi Tang, Ziping Ye, Xiaotong Jiang, Duo Chen, Peipei Song, Chunlin Jin*

**Original Article**

- 450 - 455** **Forecasting hand, foot, and mouth disease in Shenzhen based on daily level clinical data and multiple environmental factors.**  
*Ren Zhong, Yongsheng Wu, Yunpeng Cai, Ruxin Wang, Jing Zheng, Denan Lin, Hongyan Wu, Ye Li*
- 456 - 462** **Differential expression of APE1 in hepatocellular carcinoma and the effects on proliferation and apoptosis of cancer cells.**  
*Zhipeng Sun, Yubing Zhu, Aminbuhe, Qing Fan, Jirun Peng, Nengwei Zhang*
- 463 - 469** **The pregnancy outcomes of intrauterine insemination with husband's sperm in natural cycles versus ovulation stimulated cycles: A retrospective study.**  
*Feijun Ye, Wenli Cao, Jing Lin, Yan Du, Likun Lan, Ying Dong, Jun Zhu, Qi Zhou, Xinyao Pan, Youhui Lu, Fang Zeng, Bangshi Xia, Ling Wang*
- 470 - 475** **A novel compound heterozygous mutation in the *GJB2* gene is associated with non-syndromic hearing loss in a Chinese family.**  
*Haiou Jiang, Youya Niu, Lingfeng Qu, Xueshuang Huang, Xinlong Zhu, Genyun Tang*
- 476 - 483** **Impact of three-dimensional visualization technology on surgical strategies in complex hepatic cancer.**  
*Dong Zhao, Wan Yee Lau, Weiping Zhou, Jian Yang, Nan Xiang, Ning Zeng, Jun Liu, Wen Zhu, Chihua Fang*
- 484 - 490** **Total laparoscopic versus robot-assisted laparoscopic pancreaticoduodenectomy.**  
*Yuhua Zhang, Defei Hong, Chengwu Zhang, Zhiming Hu*
- 491 - 501** **Bao Yuan decoction and Tao Hong Si Wu decoction improve lung structural remodeling in a rat model of myocardial infarction: Possible involvement of suppression of inflammation and fibrosis and regulation of the TGF- $\beta$ 1/Smad3 and NF- $\kappa$ B pathways.**  
*Guozhen Yuan, Anbang Han, Jing Wu, Yingdong Lu, Dandan Zhang, Yuxiu Sun, Jian Zhang, Mingjing Zhao, Bingbing Zhang, Xiangning Cui*

**Brief Report**

- 502 - 506** **Novel compound heterozygous mutations in *SLC26A4* gene in a Chinese family with enlarged vestibular aqueduct.**  
*Xuelei Zhao, Xiaohua Cheng, Lihui Huang, Xianlei Wang, Cheng Wen, Xueyao Wang*

## Communication

---

- 507 - 509** **HIV/AIDS responses in China should focus on the impact of global integration.**  
*Qi Tang, Hongzhou Lu*
- 510 - 514** **Considerations on PCR-based methods for malaria diagnosis in China malaria diagnosis reference laboratory network.**  
*Jianhai Yin, Mei Li, He Yan, Shuisen Zhou*

## Letter

---

- 515 - 516** **The importance of non-tuberculous mycobacteria identification in Chinese patients infected with HIV.**  
*Li Liu, Renfang Zhang, Yang Tang, Tangkai Qi, Wei Song, Zhenyan Wang, Yinzhang Shen, Hongzhou Lu*
- 517 - 519** **Correlation between the use of antibiotics and development of a resistant bacterial infection in patients in the ICU.**  
*Yingxia Li, Xiyan Xia, Xiaohui Li, Ke Xiao, Xuewei Zhuang*
- 520 - 522** **The relation between social cohesion and the care burden of family healthcare providers.**  
*Yuki Naganuma, Sumiko Kihara, Yasuhiko Fujita, Kazue Yamaoka, Kenzo Takahashi*
- 523 - 525** **Prescription surveillance for early detection system of emerging and reemerging infectious disease outbreaks.**  
*Tamie Sugawara, Yasushi Ohkusa, Hirokazu Kawanohara, Miwako Kamei*

---

## Guide for Authors

---

---

## Copyright

---

# China issues the National Essential Medicines List (2018 edition): Background, differences from previous editions, and potential issues

**Jiangjiang He<sup>1,2</sup>, Mi Tang<sup>1</sup>, Ziping Ye<sup>3</sup>, Xiaotong Jiang<sup>3</sup>, Duo Chen<sup>1</sup>, Peipei Song<sup>1</sup>, Chunlin Jin<sup>1,\*</sup>**

<sup>1</sup> Department of Health Policy Research, Shanghai Health Development Research Center, Shanghai Medical Information Center, Shanghai, China;

<sup>2</sup> School of Public Health, Fudan University, Shanghai, China;

<sup>3</sup> College of Business Administration, Shenyang Pharmaceutical University, Shenyang, China.

## Summary

On October 25, 2018, the National Health Commission of China issued the National Essential Medicines List (2018 edition) [NEML (2018)]. The NEML (2018) contains 685 drugs, which consist of 417 chemicals and biological products and 268 Chinese patent medicines. Compared to the 2012 version of the NEML, a total number of 165 drugs were added, representing an increase of 31.7%. The biggest increase (90.9%) is in Chinese patent medicines for surgical use. The NEML (2018) set up the category of pediatric medications for the first time, and 11 cancer drugs were added. The NEML (2018) is characterized by: "basic" to "comprehensive" coverage, it includes both Chinese and Western medicines, it now includes pediatric drugs, and more cancer drugs have been added. There are several issues with the new NEML such as the link between the essential medicines system and the medical insurance system and establishment of firm support for implementation.

**Keywords:** National Essential Medicines List, essential medicines system, comparative analysis

## 1. Introduction

On October 25, 2018, the National Health Commission of the People's Republic of China issued the National Essential Medicines List (2018 edition) [NEML (2018)] (1). On May 1, 2013, China issued the 2012 edition of the National Essential Medicines List [NEML (2012)]. With further development of the national economy and continued healthcare reform, the NEML (2012) could not be fully adapted to meet the clinical need for essential drugs. On September 19, 2018, the General Office of the State Council issued its *Opinions on Improving the National Essential Medicines System* (2). In this context, the National Health Commission issued the NEML (2018).

Essential medicines are drugs that meet basic medical

and health needs, that come in suitable dosage forms, that are reasonably priced, that are in sure supply, and that are available to the public. Modifying the list of essential medicines will definitely play an important role in improving the drug supply system and ensuring the use of drugs by individuals. Moreover, the NEML (2018) is sure to have a positive impact on medical reform, to lower drug prices, and to reduce the medical economic burden on individuals.

The aim of this article was to describe four aspects of the NEML (2018): underlying policies, differences between the NEML (2018) and the NEML (2012), the characteristics of the NEML (2018), and potential issues.

## 2. Underlying policies

Creating a "Healthy China" has become a national strategy since the *Outline for the "Healthy China 2030"* Plan was issued and implemented on October 25, 2016 (3). In order to promote a "healthy China," the State Council promulgated and implemented the *13th Five-Year Plan for Hygiene and Health* on December 27, 2016

\*Address correspondence to:

Dr. Chunlin Jin, Shanghai Health Development Research Center, Shanghai Medical Information Center, Shanghai 200040, China.  
E-mail: jinchunlin@shdrc.org

(4). The *Outline for the "Healthy China 2030" Plan* and the *13th Five-Year Plan for Hygiene and Health* clearly seek to consolidate and improve the essential medicines system. Improvement of the national essential medicines system was listed as a key task for healthcare reform in 2018. On September 19, 2018, the General Office of the China State Council issued its *Opinions on Improving the National Essential Medicines System*.

China launched the National Essential Medicines Action Plan in 1979. The first edition of the National Essential Medicines List that included only Western drugs was completed in August 1981. A National Essential Medicines List that included both Chinese and Western drugs was issued in 1996, and the list was revised four times: in 1998, 2000, 2002, and 2004 (5). Amidst a new round of comprehensive healthcare reforms, China issued its *Opinions on Implementing the National Essential Medicines System* with a list of 307 essential medicines on August 18, 2009 (6), and the list was updated in 2012. On May 1, 2013, China officially implemented the NEML (2012) (7).

The establishment of an essential medicines system is a key component of the reform of China's healthcare system. Its implementation is first mainly placed on primary care facilities. The essential medicines system seeks to encourage patients to receive treatment from primary care facilities, to provide for basic coverage of drugs, and to reduce the burden of medication expenses, which will hopefully reduce the total cost for patients (8). However, the NEML (2012) could not be fully adapted to the meet the clinical need for essential medicines. Moreover, there is a gap between the quality of generics and brand name drugs. Furthermore, the drug supply mechanism is still with some flaws which need additional adjustment (9,10). A new edition of the National Essential Medicines List, which is the most important part of the essential medicines system, was recently issued.

### 3. The difference between the NEML (2018) and NEML (2012)

#### 3.1. Changes in the total number of drugs

The NEML (2018) is divided into three parts: chemicals and biological products, Chinese patent medicines, and Chinese herbal medicines. The list includes 417 chemicals and biological products and 268 Chinese patent medicines, for a total of 685 drugs. The NEML (2012) included 317 chemicals and biological products and 203 Chinese patent medicines, for a total of 520 drugs. As shown in Figure 1, a total number of 165 drugs were added, reflecting an increase of 31.7%. The added drugs include 100 chemicals (an increase of 31.5%) and 65 Chinese patent medicines (an increase of 32.0%). Section III of the NEML (2018) states that Chinese herbal medicines meet all standards for essential

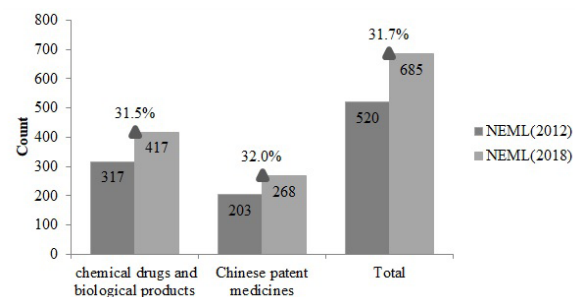


**Figure 1. Changes in the total number of drugs on the NEML (2018) and NEML (2012).** NEML, National Essential Medicines List.

medicines, but no detailed drugs' name is listed.

#### 3.2. Change in the types of drugs

One hundred and ninety-six new drugs were added and 31 drugs were removed from the NEML (2012). Nine of those drugs are listed under another classification in the NEML (2012), and indications for these drugs have been changed in the NEML (2018). In actuality, a total of 187 new drugs were added and 22 drugs were removed from the drugs listed in the NEML (2012).

Changes in chemicals and biological products are shown in Table 1. As is apparent from Table 1, the number change of types of most drugs have increased except for anti-allergic drugs, drugs to regulate water, electrolytes, and the acid-base balance, diagnostic agents, otolaryngologic drugs, and birth control. The biggest numerical increase was in cardiovascular drugs, hormones and endocrine drugs and antimicrobials. The biggest proportional increase was in vitamins and minerals, respiratory drugs, and hormones and endocrine drugs. A point particularly worth mentioning is that there are 3 new pediatric drugs and biological products and 11 new anti-tumor medications.

The number change of types of Chinese patent medicines is shown in Table 2. As is apparent from Table 2, types of Chinese patent medicines have increased to varying degrees. The biggest numerical increase was in internal medications, since 29 drugs were added to the list. The biggest proportional increase (90.9%) was in surgical medications. Pediatric Chinese patent medicines were not listed on the NEML (2012), but 13 pediatric Chinese patent medicines were added to the 2018 edition.

### 4. Characteristics of the NEML (2018)

#### 4.1. From "basic" to "comprehensive" coverage

When establishing its essential medicines system, China referenced the World Health Organization's Model List of Essential Medicines (denoted here simply as "the WHO List"). The WHO List is designed to help Member States select and purchase essential medicines and to meet national basic health needs with reasonable

**Table1. Changes in chemicals and biological products on the NEML (2018) and NEML (2012)**

Primary drug category	NEML (2018)	NEML (2012)	Number of new drugs added	Number of drugs removed	Net increase	Net increase as a percentage	Percent increase
Antimicrobial	54	43	13	2	11	11.0%	25.6%
Antiparasitic	8	7	1	0	1	1.0%	14.3%
Anesthetic	10	8	4	2	2	2.0%	25.0%
Analgesic, antipyretic, anti-inflammatory, anti-rheumatic, anti-gout medication	15	11	5	1	4	4.0%	36.4%
Nervous system medication	21	18	4	1	3	3.0%	16.7%
Psychiatric medication	32	22	10	0	10	10.0%	45.5%
Cardiovascular medication	48	34	17	3	14	14.0%	41.2%
Respiratory medication	16	10	7	1	6	6.0%	60.0%
Digestive system medication	29	24	8	3	4	5.0%	20.8%
Urinary system medication	9	7	2	0	3	2.0%	28.6%
Blood medication	26	21	7	2	5	5.0%	23.8%
Hormone and endocrine medication	36	24	14	2	12	12.0%	50.0%
Antiallergic medication	5	5	0	0	0	0.0%	0.0%
Immune system medication	4	3	1	0	1	1.0%	33.3%
Antineoplastic agent	35	26	11	2	9	9.0%	34.6%
Vitamins, minerals	11	6	5	0	5	5.0%	83.3%
Water, electrolyte, and acid-base balance regulator	8	8	0	0	0	0.0%	0.0%
Antidote	8	7	1	0	1	1.0%	14.3%
Biological products	5	4	1	0	1	1.0%	25.0%
Diagnostic agent	5	5	0	0	0	0.0%	0.0%
Skin medication	10	8	3	1	2	2.0%	25.0%
Ophthalmic medication	7	5	2	0	2	2.0%	40.0%
Otolaryngologic medication	4	4	1	1	0	0.0%	0.0%
Obstetric and gynecological agent	7	6	1	0	1	1.0%	16.7%
Birth control	1	1	0	0	0	0.0%	0.0%
Pediatric medication	3	0	3	0	3	3.0%	—
Total	417	317	121	21	100	100.0%	31.5%

NEML, National Essential medicines List.

**Table 2. Changes in the Chinese patent medicines on the NEML (2018) and NEML (2012)**

Primary drug category	NEML (2018)	NEML (2012)	Number of new drugs added	Number of drugs removed	Net increase	Net increase as a percentage	Percent increase
Internal medication	166	137	38	9	29	44.6%	21.2%
Surgical medication	21	11	10	0	10	15.4%	90.9%
Gynecological medication	24	20	4	0	4	6.2%	20.0%
Ophthalmic medication	8	7	2	1	1	1.5%	14.3%
Otolaryngologic medication	18	13	5	0	5	7.7%	38.5%
Orthopedic medication	18	15	3	0	3	4.6%	20.0%
Pediatric medication	13	0	13	0	13	20.0%	—
Total	268	203	75	10	65	100.0%	32.0%

NEML, National Essential medicines List.

pricing and reliable quality (11). China implemented its national essential medicines system in 2009. The first objective was to ensure that most people do not spend exorbitantly on basic medical care. Second, primary care facilities should play a fundamental role in providing basic medical care. Therefore, the 2009 edition and the 2012 edition of the NEML mainly list inexpensive drugs. However, a total number of 165 drugs were added to the NEML (2018), further expanding the diseases it covers. Different types of drugs to treat the same disease are included on the list. This indicates that the standard for including drugs in the list is no longer based solely on price but on

including as many drugs that treat common diseases as possible.

#### 4.2. Both Chinese and Western medicines are equally important

The NEML (2018) added a total number of 65 Chinese patent medicines, thus expanding indications and for Chinese medicines. The *Opinions on Improving the National Essential Medicines System* states that "Chinese and Western medicines are equally important and the appropriate number of essential medicines should be selected." Thus, one goal of the NEML (2018)

is to support the development of Chinese medicine industry and to spur the pharmaceutical industry to produce Chinese medicines (including ethnic medicines) and innovative domestic medicines.

#### *4.3. Addition of pediatric medications and expansion of cancer medications*

For a long time, the demand for basic medical and health services for children in China far exceeded what was on offer, indicating that the pediatric drug market needed to be enhanced. Irrational drug use on children is still common (12). There are few medications specifically for children. Even worse, pediatric medications are seriously inadequate, their ingredients are unclear, their indications are vague, their dosage forms are limited and they are difficult to administer, and relevant guidelines and catalogues of pediatric medications are lacking (13). The NEML (2018) now includes 22 pediatric medication in different types or dosage forms, which will hopefully promote the accessibility and safety of pediatric medications (14). A point worth mentioning with regard to the revised list is the increase in the number of anti-tumor medications. The Chinese Government has made every effort to lower taxes on and prices of anti-tumor drugs in 2018. There were no anti-tumor drugs in the NEML (2009) but 26 in the NEML (2012). Eleven new anti-tumor drugs have now been added to the list.

### **5. Potential issues**

The NEML (2018) covers a wider range of drugs than previous versions. It lists different types of drugs that can meet the multiple treatment needs of patients with different diseases. Moreover, further regulation of dosage forms and indications will greatly help to increase the production and distribution of essential medicines, it will facilitate their procurement and rational use, it will help determine how to reimburse their costs, and it will help to fully monitor those drugs. However, there are several issues with implementation of the NEML (2018).

#### *5.1. The link between the National Essential Medicines System and the Medical Insurance System*

The *Opinions on Implementing National Essential Medicines System* stipulates that all essential medicines should be included in the list of drugs to be reimbursed under medical insurance and that more of the cost of essential medicines should be reimbursed in comparison to non-essential medicines. The addition of 165 new drugs to the NEML (2018) will apply further financial pressure to the medical insurance system. The medical insurance system is not designed to address problems posed by pharmaceuticals. Therefore, the impact

that the new drug list and related policies will have on the medical insurance system is still unclear. The National Essential medicines system and the medical insurance system are complementary (15). Expansion of the essential medicines list will ensure that everyone benefits from basic medical and health services. However, the financial impact on the medical insurance system needs to be determined from the perspective of medical economics. The level of coordination between the two systems will have a huge impact on the implementation of National Essential Medicines List.

#### *5.2. Provision and improvement of support*

According to a document on interpretation of the NEML (2018), revision of the essential drug list is based on the clear and relatively perfect standard of inclusion and exclusion. This lays a solid foundation for future revision of the list. However, revision depends specifically on support from corresponding policies.

China's regulation of essential medicines can be divided into direct regulation and indirect regulation. Direct regulation includes control of the highest retail price and "zero markup" by chain stores, while indirect regulation includes a bidding system for procurement of essential drugs (16). The "zero markup" policy dictates that "the sales price will not differ from the purchase price" (17), so public medical and health care facilities will have no interest in the volume of drugs they sell. This will help to eliminate "prescriptions in volume" and other problems associated with superfluous treatment. However, effective support policies and system guarantees must be provided in order to smoothly transition to the "zero markup" policy. Important aspects include modification of medical prices and financial support for public health care providers.

Any reform of the healthcare system is a one-size-fits-all move, and reforms must be coordinated. This is especially true for the essential medicines system, which involves links such as production, distribution, use, and reimbursement of costs (18). Reforming each link will have an impact on existing interests. These interests must be properly handled, policies must be coordinated, and comprehensive support must be provided to effectively promote implementation of the NEML (2018).

### **References**

1. National Health Commission of the People's Republic of China. China's National Essential Medicines List (2018 edition) <http://www.nhfpc.gov.cn/zhus/ywml/201810/600865149f4740eb8ebe729c426fb5d7.shtml> (accessed on October 25, 2018) (in Chinese)
2. General Office of the State Council of the People's Republic of China. Opinions on improving the National

- Essential Medicines System. <http://www.nhfpc.gov.cn/yaozs/s7655/201809/feb1852027a949f7894b03394784dd3f.shtml> (accessed on October 26, 2018) (in Chinese)
3. Xinhua News Agency. Issuance of the Outline for the "Healthy China 2030" Plan. [http://www.xinhuanet.com/health/2016-10/25/c\\_1119786029.htm](http://www.xinhuanet.com/health/2016-10/25/c_1119786029.htm) (accessed on October 26, 2018) (in Chinese)
  4. Chinese Government Net. The State Council's notice on issuance of the 13th Five-year Plan for Hygiene and Health (Issued by the State Council, 2016 (No. 77). [http://www.gov.cn/zhengce/content/2017-01/10/content\\_5158488.htm](http://www.gov.cn/zhengce/content/2017-01/10/content_5158488.htm) (accessed on October 26, 2018) (in Chinese)
  5. Zhao WN, Xu LZ, Yang P, Zhou CC, Liu DM. A study on the status of a national system for essential drugs and improvements to that system. Chinese Health Service Management. 2011; 28:664-666. (in Chinese)
  6. National Health Commission of the People's Republic of China. Notice on issuance of the Opinions on Establishment of a National Essential Medicines System <http://www.nhfpc.gov.cn/tigs/s9660/200908/98b25d019fd/b4700b3409daf43f8bd81.shtml> (accessed on October 26, 2018) (in Chinese)
  7. National Health Commission of the People's Republic of China. China's National Essential Medicines List (2012 edition). <http://www.nhfpc.gov.cn/wsb/pwsyw/201303/f01fcc9623284509953620abc2ab189e.shtml> (accessed on October 26, 2018) (in Chinese)
  8. Ding LM. Impacts of the National Essential Medicines System on health care utilization and expenditures by patients covered by Basic Medical Insurance. Tianjin University. 2017. (in Chinese)
  9. Liu D, Yu ZH. The status and effect study of the policy implementation of essential drug in Chinese city community health institutions. China Practical Medicine. 2017; 12:182-183. (in Chinese w/ English abstract)
  10. Cai MY, Li YP, Dai CM, Li CX. Investigation on implementation of national essential medicine system in primary health care institutions of Shantou region. Evaluation and Analysis of Drug-Use in Hospitals of China, 2017, 17:254-256. (in Chinese w/ English abstract)
  11. Wang L, Zhang C, Yang Q, Zhang LL, Li YP. A comparative study between the newest essential medicine lists of China and the WHO in 2009. Chinese Journal of Evidence-Based Medicine. 2009; 9:1173-1184. (in Chinese w/ English abstract)
  12. Yu ML, Yang Y. Investigation of the availability of pediatric medication in China. Pharmaceutical Journal of Chinese People's Liberation Army. 2011; 27:368-370. (in Chinese)
  13. Wang YT. Pediatric medication in China: Status, problems, and solutions. Beijing University of Chinese Medicine. 2018. (in Chinese)
  14. National Health Commission of the People's Republic of China. Interpretation of the National Essential Medicines List (2018 edition). [http://www.nhfpc.gov.cn/yaozs/s3582/201810/de12303b26a046e49d725f375fb31315.shtml?wm=3333\\_2001](http://www.nhfpc.gov.cn/yaozs/s3582/201810/de12303b26a046e49d725f375fb31315.shtml?wm=3333_2001) (accessed on October 26, 2018). (in Chinese)
  15. Jiang SH, Zhang BY, Yang YK. Effects of a national essential medicines policy on the medical insurance system. China Health Industry. 2018; 15:191-193. (in Chinese)
  16. Li C, Wang WJ, Xiao LQ, Cui D, Zhang YX. Review of the status of implementation of an essential medicines system in China. Chinese Hospital Management. 2018; 38:28-31. (in Chinese)
  17. Liu JM. Enhancing coordination and promoting the adoption of an essential medicines policy. Health Economics Research, 2009; 1-1. (in Chinese)
  18. Xi XY, Chen PP, Ma DD, Mao NY. The validation of an indicator system of essential drug accessibility assessment in China. Chinese Journal of New Drugs. 2017; 26:620-625. (in Chinese w/ English abstract)

(Received October 28, 2018; Accepted October 31, 2018)

## Forecasting hand, foot, and mouth disease in Shenzhen based on daily level clinical data and multiple environmental factors

**Ren Zhong<sup>1,§</sup>, Yongsheng Wu<sup>2,§</sup>, Yunpeng Cai<sup>1</sup>, Ruxin Wang<sup>1</sup>, Jing Zheng<sup>3</sup>, Denan Lin<sup>3</sup>, Hongyan Wu<sup>1,\*</sup>, Ye Li<sup>1,\*</sup>**

<sup>1</sup> Shenzhen Institutes of Advanced Technology, Chinese Academy of Sciences, Shenzhen, China;

<sup>2</sup> Shenzhen Center for Disease Control and Prevention, Shenzhen, China;

<sup>3</sup> Shenzhen Health Information Center, Shenzhen, China.

### Summary

Hand, foot, and mouth disease (HFMD) is caused by a group of enteroviruses. It infects millions of children in the Southeast Asian area. An accurate forecasting of outbreaks of HFMD could facilitate public health officials to suggest public health actions earlier. Many researchers tried to develop an early warning system for HFMD to lower the damage caused by a HFMD outbreak. The research data based on daily level could help figure out the relationship between HFMD and environmental factors, but nevertheless is difficult to collect. In this study, we collected the daily clinical data from the Shenzhen Health Information Center and multiple environmental factors to analyze the outbreaks of HFMD. Considering the incubation period of HFMD, we fed the previous 60 days' HFMD rates, 7 days' temperature factors and 7 days' air-quality factors into the tree model, XGBoost. The following conclusions were drawn in this study: *i*) Compared with the model only using the previous HFMD rate and temperature factors, the addition of the air-quality factors could make the model better, improving MAE nearly 16.7%. *ii*) By analyzing the Pearson correlation, we found that the temperature showed a positive correlation and the air quality showed a negative correlation for the HFMD outbreaks. Improving the air quality, especially decreasing PM<sub>2.5</sub> and PM<sub>10</sub> could decrease the risk of HFMD outbreaks.

**Keywords:** Hand, foot, and mouth disease (HFMD), tree model, XGBoost, Correlation

### 1. Introduction

Hand, foot, and mouth disease (HFMD) is caused by a group of enteroviruses, of which the coxsackievirus type A and the enterovirus 71 (EV71) are the most frequently seen. This illness mainly occurs in children aged less than 5 years. Although a majority of patients have only mild symptoms, some patients rapidly develop neurological and cardiopulmonary symptoms that can be fatal, particularly when the cases are associated with EV71. Since 1997, numerous large outbreaks of HFMD have occurred in Eastern and Southeastern Asian

countries, including Singapore, Malaysia, Japan, and China (1-5). In China, the Chinese Ministry of Health has listed HFMD as a class C communicable disease and all doctors are required to report HFMD cases to the National Disease Surveillance Reporting and Management System.

Many researchers used data collected from the surveillance system to develop an early warning system of HFMD to lower the damage caused by a HFMD outbreak. A study by Nanjing Medical University attempted to predict the HFMD epidemics in Nanjing city, the main epidemic area of eastern China, by developing a weather-based forecasting model (6). A research team from Beijing explored the data collected in Beijing to find seasonal and other potential effects of weather factors on HFMD (7). In the southern part of China, some researchers from Guangzhou Center for Disease Control and Prevention also tried to estimate the effects of diverse climate variables on the incidence of HFMD (8). Another team from

<sup>§</sup>These authors contributed equally to this work.

\*Address correspondence to:

Drs. Hongyan Wu and Ye Li, Shenzhen Institutes of Advanced Technology, Chinese Academy of Sciences, 1068 Xueyuan Avenue, Shenzhen University Town, Nanshan, Shenzhen 518055, China.

E-mail: hy.wu@siat.ac.cn (Wu Y), ye.li@siat.ac.cn (Li Y)

Chongqing adopted multiple meteorological parameters to quantify the association of daily weather variation with HFMD incidence (9). Besides the meteorological parameters, studies from the Central South University also explored the relationship between HFMD and fine particulate matter less than 10 ( $PM_{10}$ ) (10). This research has achieved state-of-the-art models which deliver sufficiently accurate forecasts of HFMD. However, to the best of our knowledge, these studies on building HFMD monitoring and forecasting largely focus on weekly forecasts due to the lack of daily data.

Research data based on daily levels could help figure out the relationship between HFMD and environmental factors, but nevertheless is difficult to collect. In this study, we collected the daily clinical data from the Shenzhen Health Information Center and multiple environmental factors to analyze the outbreaks of HFMD. We consider three kinds of predictors: temperature, historical HFMD rate, and air quality. Considering the incubation period of HFMD, we fed the previous 60 days' HFMD rates, 7 days' temperature factors and 7 days' air-quality factors into the tree model, XGBoost. XGBoost is a highly sophisticated algorithm, powerful enough to deal with kinds of data irregularities. In addition, its feature importance functionality could help us understand the relationship between HFMD rate, temperature, and air quality.

## 2. Materials and Methods

### 2.1. Data sources

The weather and air-quality data were obtained from the Weather Underground app (<https://www.wunderground.com/>). The HFMD rate data were obtained from the Shenzhen Health Information Center, which collected the clinic visit information from January 1, 2010, to September 12, 2017, from 60 state hospitals, 6 mother and child care centers, and 619 community rehabilitation centers. Figure 1 illustrates the data, in which the Y-axis represents the daily HFMD rate and the X-axis represents the outbreak time.

### 2.2. Methodology

XGBoost, A scalable machine learning system for tree boosting, was first popularized by Tianqi Chen for improving the operating efficiency and reducing the memory space usage of the current tree boosting system. XGBoost is a kind of assembly algorithm, named gradient-boosted decision trees (GBDT), which creates and combines a high number of individually weak but complementary classifiers, to produce a robust estimator. In XGBoost, a new weak classifier is constructed to be maximally correlated with the negative gradient of the loss function associated with the whole assembly for each iteration. XGBoost belongs

to the group of widely used tree learning algorithms. A decision tree makes predictions on an output variable based on a series of rules arranged in a tree-like structure. They consist of a series of split points, the nodes, in terms of the value of an input feature and gives us the specific value of the output variable at the leaf node. As an efficient implementation of GBDT, XGBoost remarkably improves the efficiency of the training model but slightly decreases the accuracy of the model (11). In this study, three XGBoost models were built by gradually adding predictor factors into the predictor space to obtain the best model performance with minimum regression error.

*Predictor space.* In this study, three kinds of components were chosen as the predictor space: historical daily HFMD rate, temperature conditions, and air-quality conditions. Assuming the current predicted point was  $X_0$ , the first component was the sequence  $X_1, X_2, X_3, \dots, X_{t-1}, X_t$ , where  $t$  was 60 and was filled with the values of the previous 60 HFMD rate observations before  $X_0$ . The second components were maximum and minimum temperatures, which were the optimal-related factors with HFMD in previous studies (12). The third component was composed of the air-quality index (AQI), fine particulate matter less than 2.5 ( $PM_{2.5}$ ),  $PM10$ , sulfur dioxide ( $SO_2$ ), carbon monoxide (CO), nitrogen dioxide ( $NO_2$ ), and ozone ( $O_3$ ).

*Metrics.* The mean absolute error (MAE) was used to measure the prediction accuracy. MAE was defined using the following formula:

$$MAE(A_t, F_t) = \frac{1}{N} \sum_{t=0}^{N-1} |A_t - F_t|$$

Where  $A_t$  is the actual value and  $F_t$  is the forecast value.

*Variable importance.* Variable importance in XGBoost or GBDT is often called relative importance of predictor variables, which is useful to learn the relative importance or contribution of each input variable in predicting the response (13). In this study, XGBoost was tree-based, and therefore the variable importance was computed as follows:

(1) For a single decision tree  $T$ , the following formula was used:

$$I_l^2(T) = \sum_{t=1}^{J-1} i_t^2 i(t = l)$$

Calculating the relevance for each predictor variable  $F_i$ ; The sum was over the  $J - 1$  internal nodes of the tree. At each such node  $t$ , one of the input variables  $F_i$  was used to partition the region associated with that node into two subregions; within each, a separate constant was fit to the response values. The particular variable chosen was the one that gave the maximal estimated improvement  $i_t^2$  in squared error risk over that for a

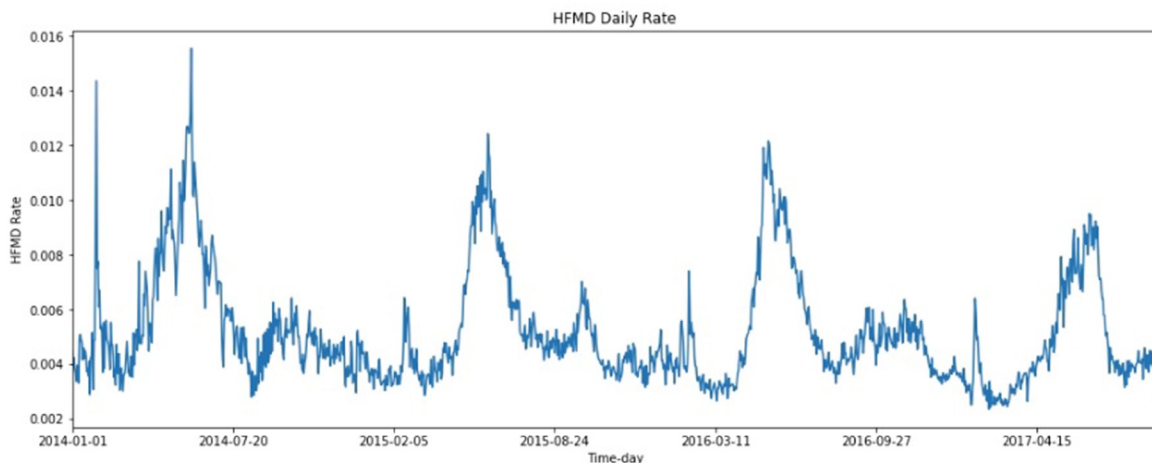


**Figure 1. Data from the Shenzhen Health Information Center.** The Y-axis represents the daily HFMD rate and the X-axis represents time.

constant fit over the entire region. The squared relative importance of variable  $F_l$  was the sum of such squared improvements over all internal nodes for which it was chosen as the splitting variable.  $i$  was the characteristic function whose value was 1 if  $t = l$  and 0 if  $t \neq l$ .

(2) As XGBoost used trees to predict, the variable importance was easily generalized to additive tree expansions. It was simply averaged over the trees as shown in the following formula:

$$I_l^2(T) = \frac{1}{M} \sum_{m=1}^M I_l^2(T_m)$$

### 3. Results

The data from January 1, 2014, to December 31, 2016, were used as the training data, and the half-year data from January 1, 2017, to September 1, 2017, were used as the test data. The experiments were performed by the training regression model using the training data and calculating the regression error between forecasted value and test data. The experiments were carried out three times by gradually combining more predictors into the predictor space to investigate the influence of different predictors on the prediction accuracy.

#### 3.1. Improved prediction accuracy

In the first process, the 14 recent temperature conditions (the maximum and minimum temperatures of the previous week) were chosen. In the second, 60 recent observation variables  $X_1, X_2, X_3, \dots, X_{59}, X_{60}$  were added. In the third, the air-quality factors and the foregoing predictor space were combined together as the last predictor space.

Figure 2A illustrates the result of the first experiment, which shows the model's ability to forecast the future HFMD trend, but the prediction accuracy was

not good. Figure 2B illustrates the second experiment of the daily HFMD rate with the predictor space of temperature and history HFMD rate, showing that the prediction accuracy was improved. Figure 2C shows that the prediction got better by adding air quality. Table 1 shows the improved forecast results by adding more predictor factors into the predictor space.

#### 3.2. Comparison of variable importance

As the final model provided the best result and the predictor space included all three kinds of factors, only the variables in the final model were checked. This study used the `get_fscore` function in the XGBoost package to calculate the variable's importance. The larger the value returned by the function, the greater the influence of a feature in the modeling process. According to their variable importance, the top 10 variables were obtained and are shown in Table 2. The following observations were made: (1) The historical HFMD rate, especially the nearest days' rate, seemed pretty important. (2) The air-quality factors showed more importance than the temperature factor. Two days ago,  $\text{NO}_2$  and AQI occupied the fourth and ninth places, respectively.

#### 3.3. Analysis of weather conditions

The three experiments revealed that the addition of air-quality conditions into the predictor space could efficiently improve the prediction accuracy. The analysis of variable importance also showed that the air-quality factors had an influence on the prediction. In this section, the Pearson correlation analysis between the HFMD rate and both temperature and air-quality factors was performed. Table 3 shows the correlation coefficients between the HFMD rate and these factors. The coefficient was a value that ranged from 1 to  $-1$ . The closer to 1 the coefficient was, the more linearly

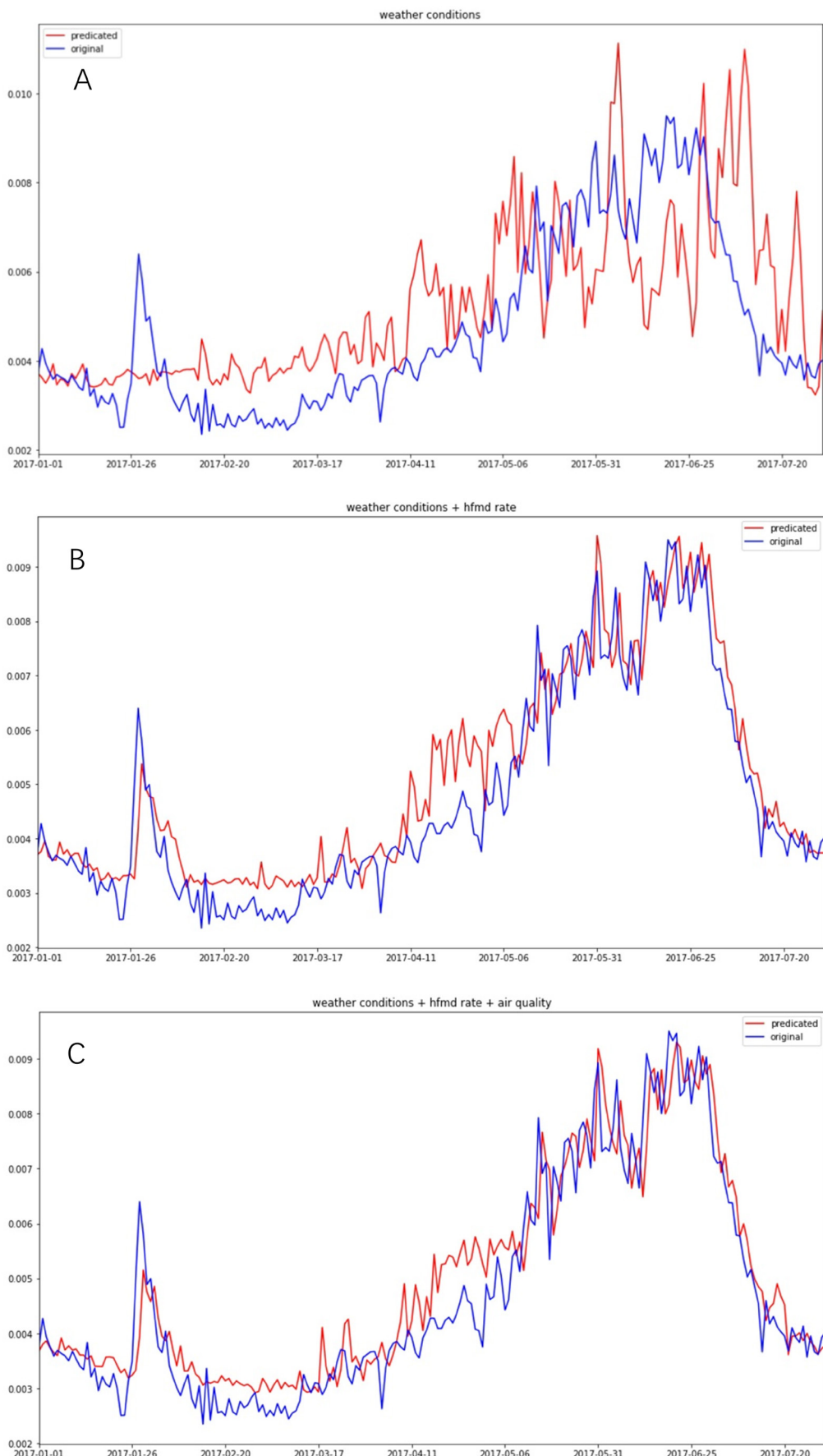


**Figure 2. Predication of Weekly ILI rate with different predictor spaces.** (A) Prediction of the daily HFMD rate using temperature factors. The blue line illustrates the original data, and the red line shows the corresponding predicted values. (B) Prediction of the daily HFMD rate using temperature factors and historical HFMD rate. The blue line illustrates the original data, and the red line shows the corresponding predicted values. (C) Prediction of the daily HFMD rate using temperature factors, historical HFMD rate, and air-quality factors. The blue line illustrates the original data, and the red line shows the corresponding predicted values.

**Table 1. Comparison of forecasting with different predictors**

Predictors space	MAE
Temperature	0.0013
Temperature + HFMD rate	0.0006
Temperature + HFMD rate + air quality	0.0005

HFMD, Hand, foot, and mouth disease; MAE, mean absolute error.

**Table 2. Comparison of variable importance**

Variables	V1	V2	V3	V4	V5	V6	V7	V8	V9	V10
Name	RATE <sub>1</sub>	RATE <sub>2</sub>	RATE <sub>7</sub>	NO <sub>2</sub>	RATE <sub>4</sub>	RATE <sub>59</sub>	RATE <sub>3</sub>	RATE <sub>48</sub>	AQI <sub>2</sub>	RATE <sub>57</sub>
VI	42	32	14	14	14	13	11	11	11	11

VI, Variable importance. Capital letters in name are the names of the features, and the suffix indicates how many days ago the value of the feature was obtained.

**Table 3. Analysis of correlation between the HFMD rate and other factors**

Variables	AQI	PM <sub>2.5</sub>	PM <sub>10</sub>	SO <sub>2</sub>	CO	NO <sub>2</sub>	O <sub>3</sub>	MAXT	MINT
Coefficient	-0.2968	-0.3653	-0.3249	-0.1324	-0.1808	-0.2564	-0.2063	0.4414	0.4743
P value	5.31e-28	1.45e-42	1.57e-33	1.55e-06	4.53e-11	4.47e-21	4.91e-14	1.8e-63	2.39e-74

AQI, Air-quality index; CO, carbon monoxide; NO<sub>2</sub>, nitrogen dioxide; O<sub>3</sub>, ozone; PM<sub>2.5</sub>, fine particulate matter less than 2.5; PM<sub>10</sub>, fine particulate matter less than 10; SO<sub>2</sub>, sulfur dioxide.

positive the feature was related to the HFMD rate; and the closer to -1 the coefficient was, the more linearly negative the feature was related to the HFMD rate. The closer the coefficient was to 0, the weaker was the linear correlation between the feature and the HFMD rate.

#### 4. Discussion

In this study, the daily maximum and minimum temperatures in the first experiment were chosen to examine the relationship between the temperature and HFMD. Figure 2A showed that the temperature could reflect the future HFMD trend, although the prediction accuracy was not good. The Pearson correlation in Table 3 also showed that the daily maximum and minimum temperature was correlated with HFMD, with the coefficients of 0.44 and 0.47, separately. Our conclusion is consistent with the previous studies (6-10), which shows outbreaks of HFMD in different areas.

Although some researchers found no strong correlation between air quality and HFMD, we still chose air quality factors as a part of feature space, considering that the air quality could impact on virus diffusion, people's travel and respiratory diseases etc. We added the air-quality index (AQI), fine particulate matter less than 2.5 (PM<sub>2.5</sub>), PM<sub>10</sub>, sulfur dioxide (SO<sub>2</sub>), carbon monoxide (CO), nitrogen dioxide (NO<sub>2</sub>), and ozone (O<sub>3</sub>) to the previous model, which improved MAE from 0.0006 to 0.0005, nearly 16.7%. The variable importance in this study shows the importance of air quality. The top 10 variables of the Shenzhen data were RATE<sub>1</sub>, RATE<sub>2</sub>, RATE<sub>7</sub>, NO<sub>2</sub>, RATE<sub>59</sub>,

RATE<sub>3</sub>, RATE<sub>48</sub>, AQI<sub>2</sub>, and RATE<sub>57</sub>. Furthermore, the Pearson correlation, some air-quality factors showed a negative correlation. The coefficient between PM<sub>2.5</sub> and HFMD is -0.37 while PM<sub>10</sub> is -0.33. Our study is not consistent with the conclusion in the previous study (10), which showed no significant relationship between PM<sub>10</sub> and HFMD (10).

The variable importance in our study showed that air quality seemed more important than temperature factors. We thought that the temperature factors could be collinear with historical rates, and therefore the importance of temperatures could be covered by the historical rates.

#### 5. Conclusions

The clinic and environmental data based on daily levels could help figure out the relationship between HFMD and environmental factors. Considering the incubation period of HFMD, in this study we fed the previous 60 days' HFMD rates, 7 days' temperature factors and 7 days' air-quality factors into the tree model, XGBoost. Our study showed that the addition of air-quality factors to the historical HFMD rate and temperature data, could improve forecasting of HFMD. In addition, air quality showed a negative correlation to HFMD outbreaks. Improving air quality, especially decreasing PM<sub>2.5</sub> and PM<sub>10</sub>, could decrease the risk of HFMD outbreaks.

#### Acknowledgements

This study was supported in part by the National High-tech R&D Program (863 Program) of China

(SS2015AA020109), Shenzhen Science and Technology Research Foundation (JCYJ20160229193120432), Major Special Project of Guangdong Province (2017B030308770), the National Natural Science Foundation of China (81601575), Layout of Shenzhen Basic Research Foundation, and the foundation from Shenzhen Healthy Big Data Analytics and Application Engineering Laboratory.

## References

1. Ang LW, Koh BK, Chan KP, Chua LT, James L, James L, Goh KT. Epidemiology and control of hand, foot and mouth disease in Singapore, 2001–2007. Ann Acad Med Singapore. 2009; 38:106-112.
2. Chan LG, Parashar UD, Lye MS, Ong FG, Zaki SR, Alexander JP, Ho KK, Han LL, Pallansch MA, Suleiman AB, Jegathesan M, Anderson LJ. Deaths of children during an outbreak of hand, foot, and mouth disease in Sarawak, Malaysia: Clinical and pathological characteristics of the disease. For the Outbreak Study Group. Clin Infect Dis. 2000; 31:678-683.
3. Fujimoto T, Chikahira M, Yoshida S, Ebira H, Hasegawa A, Totsuka A, Nishio O. Outbreak of central nervous system disease associated with hand, foot, and mouth disease in Japan during the summer of 2000: Detection and molecular epidemiology of enterovirus71. Microbiol Immunol. 2002; 46:621-627.
4. Chen KT, Chang HL, Wang ST, Cheng YT, Yang JY. Epidemiologic features of hand-foot-mouth disease and herpangina caused by enterovirus71 in Taiwan, 1998–2005. Pediatrics. 2007; 120:e244-252.
5. Yang F, Ren L, Xiong Z, Li J, Xiao Y, Zhao R, He Y, Bu G, Zhou S, Wang J, Qi J. Enterovirus 71 outbreak in the People's Republic of China in 2008. J Clin Microbiol. 2009; 47:2351-2352.
6. Liu S, Chen J, Wang J, Wu Z, Wu W, Xu Z, Hu W, Xu F, Tong S, Shen H. Predicting the outbreak of hand, foot, and mouth disease in Nanjing, China: A time-series model based on weather variability. Int J Biometeorol. 2018; 62:565-574.
7. Dong W, Li X, Yang P, Liao H, Wang X, Wang Q. The effects of weather factors on hand, foot and mouth disease in Beijing. Sci Rep. 2016; 6:19247.
8. Li T, Yang Z, DI B, Wang M. Hand-foot-and-mouth disease and weather factors in Guangzhou, southern China. Epidemiol Infect. 2014; 142:1741-1750.
9. Wang P, Zhao H, You F, Zhou H, Goggins WB. Seasonal modeling of hand, foot, and mouth disease as a function of meteorological variations in Chongqing, China. Int J Biometeorol. 2017; 61:1411-1419.
10. Ruixue Huang, Guolin Bian, Tianfeng He, Lv Chen, Guozhang Xu. Effects of Meteorological Parameters and PM10 on the Incidence of Hand, Foot, and Mouth Disease in Children in China. Int J Environ Res Public Health. 2016; 13:481.
11. Tianqi Chen, Carlos Guestrin. XGBoost: A Scalable Tree Boosting System. KDD '16 Proceedings of the 22<sup>nd</sup> ACM SIGKDD International Conference on Knowledge Discovery and Data Mining. 2016; 785-794.
12. Xiao X, Gasparini A, Huang J, Liao Q, Liu F, Yin F, Yu H, Li X. The exposure-response relationship between temperature and childhood hand, foot and mouth disease: A multicity study from mainland China. Environ Int. 2017; 100:102-109.
13. Trevor Hastie, Robert Tibshirani, Jerome Friedman. The Elements of Statistical Learning. Springer, Germany, 2009; pp. 367-369.

(Received June 8, 2018; Revised October 24, 2018;  
Accepted October 28, 2018)

# Differential expression of APE1 in hepatocellular carcinoma and the effects on proliferation and apoptosis of cancer cells

Zhipeng Sun, Yubing Zhu, Aminbuhe, Qing Fan, Jirun Peng\*, Nengwei Zhang\*

Oncology Surgery Department, Beijing Shijitan Hospital, Capital Medical University (Peking University Ninth School of Clinical Medicine), Beijing, China.

## Summary

This research aimed to investigate the differential expression of apurinic-apyrimidinic endonuclease 1 (APE1) in hepatocellular carcinoma (HCC) tissues and cells and the effects on proliferation and apoptosis of cancer cells. Immunohistochemical techniques were used to detect the expression of APE1 in 80 cases of HCC and the corresponding paracancerous tissue microarrays; meanwhile, Western blots were used to detect the expression of APE1 in both human HCC BEL-7402, BEL-7405, HCC-9204, Hep3B, HepG2, SMMC-7721 and Huh-7 cells, and normal hepatocyte L-02 cells. The relationship between APE1 expression and clinical pathological characteristics of HCC was statistically analyzed. APE1 shRNA vector was constructed in Hep 3B cells to establish a stably transfected cell line, using Western blots to determine the interference efficiency. Cell proliferation activity was detected with MTT assays, while apoptosis was detected with the Annexin V-FITC/PI double-labeling technique. The expression of APE1 in HCC tissues and cells was significantly up-regulated, and its expression was significantly different from TNM staging and histopathological grading. Down-regulation of APE1 expression significantly reduced the proliferative activity and increased the apoptosis rate of Hep 3B cells. In conclusion, APE1 demonstrates cancer progression potential at the clinical, tissue and cell level. It provides a new idea and theoretical basis for APE1-based clinical diagnosis, prognosis determination and molecular targeted therapy in treatment of HCC.

**Keywords:** APE1, hepatocellular carcinoma, differential expression, cell proliferation, apoptosis

## 1. Introduction

Hepatocellular carcinoma (HCC) is a type of primary liver cancer with high mortality clinically (1). As shown by the latest cancer statistics released by National Central Cancer Registry: In 2015, there were about 4.29 million new cases of malignant tumors and about 2.81 million deaths, which included about 461,100 new cases of HCC and 422,100 deaths (2), seriously threatening human life and health. Since uncontrolled growth, deterioration and metastasis were the main causes of high cancer mortality, the hotspots of HCC research in recent years have focused on exploring the molecular mechanisms of carcinogenesis and development of HCC, and searching

for the biomarkers of malignant proliferation and interventional targets of HCC (3-5). Many studies have shown that apurinic-apyrimidinic endonuclease 1 (APE1) was expressed in a variety of tumors such as lung cancer, colorectal cancer, ovarian cancer and multiple myeloma (6), but in-depth study reports in HCC were very limited. This study was designed to investigate the expression characteristics of APE1 in HCC, analyze its relationship with clinical pathological characteristics, and determine its effects on HCC cell proliferation and apoptosis.

## 2. Materials and Methods

### 2.1. Tissue samples and main reagents

**Tissue samples and experimental cells:** HCC tissue microarrays were purchased from Shanghai Outdo Biotech (model HLivH160CS01); there were 80 cases of HCC, 1 each at cancer/paracancerous site. TNM staging was available, clinical phase 1, 2, 3 and 4,

\*Address correspondence to:

Dr. Jirun Peng and Dr. Nengwei Zhang, Oncology Surgery Department, Beijing Shijitan Hospital, Capital Medical University (Peking University Ninth School of Clinical Medicine), Beijing 100038, China.  
E-mail: pengjr@medmail.com.cn or zhangnw1@sohu.com

pathological grade I, II and III (AJCC, 7th Edition). The specific display arrangement is shown in Figure 1B. Both human HCC BEL-7402, BEL-7405, HCC-9204, Hep3B, HepG2, SMMC-7721 and Huh-7 cells and normal hepatocyte L-02 cells APE1 were purchased from Institute of Basic Medical Sciences of Peking Union Medical College.

**Main reagents:** Total RNA extraction reagent TRIzol, SYBR® PrimeScript™ RT-PCR Kit and mRNA SYBR Green fluorescence quantification PCR reagent were purchased from Takara of Japan; protein extraction RIPA lysate, BCA protein concentration kit, SDS-PAGE gel preparation reagent, MTT cell proliferation kit and Annexin V-FITC/PI double-labeling apoptosis kit were purchased from Jiangsu Beyotime Biotechnology; cell transfection reagent Lipo 3000 was purchased from Invitrogen of the United States; APE1 antibody and GAPDH antibody were purchased from ABCAM of the United Kingdom.

## 2.2. Methods

**Detection of APE1 expression level in HCC tissue microarrays with immunohistochemistry:** After baking, hydration and antigen-repairing, the primary and secondary antibodies were added dropwise to tissue microarrays, followed by DAB color development and mounting with neutral balsam. After microphotography under a light microscope, IPP software was used to acquire integrated content density (IOD).

**Detection of cellular APE1 expression with Western blots:** The cells were collected to extract total proteins for quantification using the BCA technique. Following SDS-PAGE gel electrophoresis, the proteins were transferred to the membrane and blocked with 5% skim milk powder-TBST blocking solution at room temperature for 1 h. Then, diluted APE1 and GADPH primary antibodies were separately added to the NC membrane, which was incubated at 4°C overnight on a shaker; the corresponding secondary antibodies (1:100 dilution) were added, followed by incubation at 37°C constant temperature for 1 h on a shaker before color development.

**Construction of APE1 shRNA vector:** APE1 shRNA sequences were designed and synthesized, the forward primer was: 5'-CCGGCCTGGATTAAGAAGAAAGGA TCTCGAGATCCTTCTTAATCCAGGTTTT-3', the reverse primer was: 5'-AATTCAAAACCTGGAT TAAGAAGAAAGGATCTGAGATCCTTCTTCTT AATCCAGG-3', the clone was ligated to pLKO.1-GFP plasmid, followed by sequencing verification.

**Detection of cell proliferation with MTT assay:** The cells in each group were stably sub-cultured for passaging and then cultured in complete medium. MTT assay was conducted for 72 h. Four duplicates were used in each group. A 20 µL MTT (dissolved in 5mg/mL PBS) was added to each well, and the supernatant

was discarded after incubation for 4 h. Then, 150 µL Formazan solution was added to shake for 10 min until the crystals were fully dissolved. The absorbance was measured with a microplate reader (570 nm).

**Detection of apoptosis with Annexin V-FITC/PI double-labeling technique:** The cells were collected, placed on a 100 mesh copper sieve and rubbed gently. After rinsing with normal saline, the cells were centrifuged at 2500 r/min, then the cell suspension was obtained after the supernatant and cell debris were discarded. Flow cytometry was employed for the analysis according to "Annexin V-FITC/PI Double-Labeling Detection Kit".

## 2.3. Statistical processing

SPSS 17.0 software was employed for statistical analysis, and  $\bar{x} \pm s$  was used for statistical description. One-way ANOVA was conducted to compare inter-group differences, if the results showed that the inter-group difference had statistical significance, *t*-test was further conducted for pairwise comparison of inter-group differences. All statistical analysis test levels were set at  $\alpha = 0.05$ .

## 3. Results

### 3.1. Differential expression of APE1 in HCC tissues

Immunohistochemical technique was used to detect APE1 expression in HCC of the 80 cases and the corresponding paracancerous tissue microarrays; the IOD values are shown in Figure 1A. The results showed that APE1 expression was significantly up-regulated in HCC tissues (Figure 1C), and the difference had statistical significance ( $p < 0.0001$ ). The results suggested that APE1 may play an important role in the development of HCC. The immunohistochemical results of 4 cases were selected from each group (Figure 2).

### 3.2. Differential expression of APE1 in HCC cells

Western blots were used to detect APE1 expression in human HCC BEL-7402, BEL-7405, HCC-9204, Hep3B, HepG2, SMMC-7721 and Huh-7 cells as well as in normal hepatocyte L-02 cells. The results showed that APE1 expression was higher in HCC cells than in normal hepatocytes to varying levels, APE1 expression in HCC cells was 2.5-3.6 times higher than in hepatocytes (Figure 3). The changes of differential expression of APE1 in HCC cells were consistent with that in HCC tissues, showing significant over-expression in both cases.

### 3.3. Relationship between APE1 expression and pathological characteristics of HCC

According to the statistical analysis of case data in

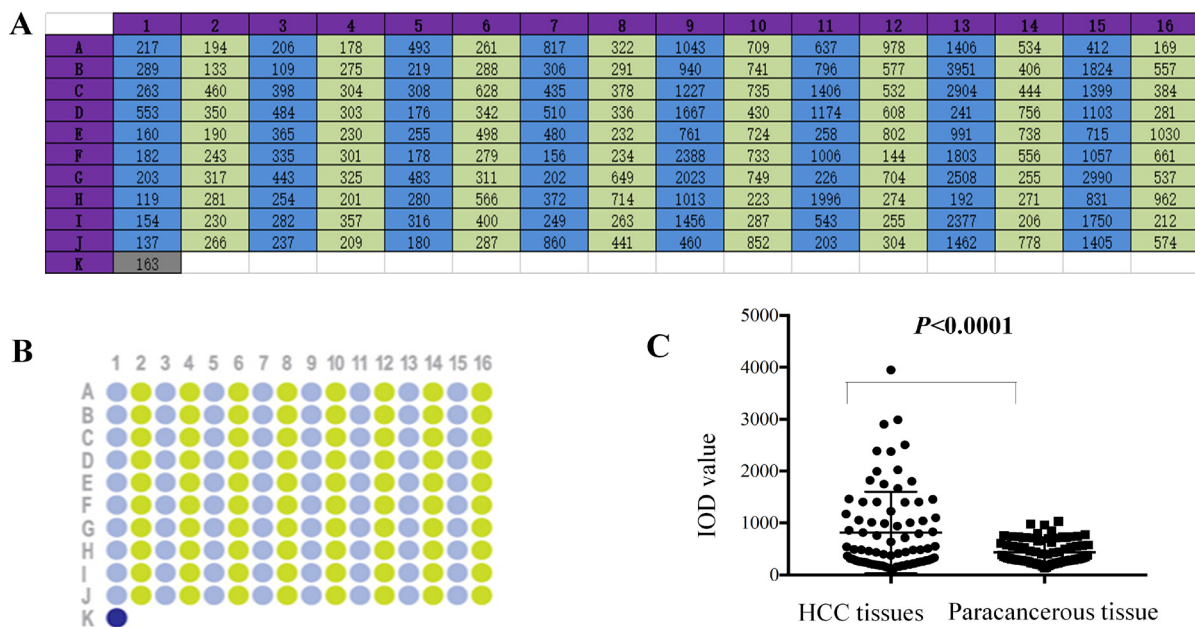


**Figure 1. Differential expression of APE1 in HCC tissues.** (A): IOD for APE1 expression in HCC of the 80 cases and the corresponding paracancerous tissue microarrays as detected with immunohistochemistry (Blue indicates HCC tissues, green indicates paracancerous tissues). (B): Schematic diagram for the distribution of HCC and paracancerous tissues in the microarrays (blue indicates HCC tissues, green indicates paracancerous tissues). (C): Statistical analysis of APE1 expression in HCC tissues.

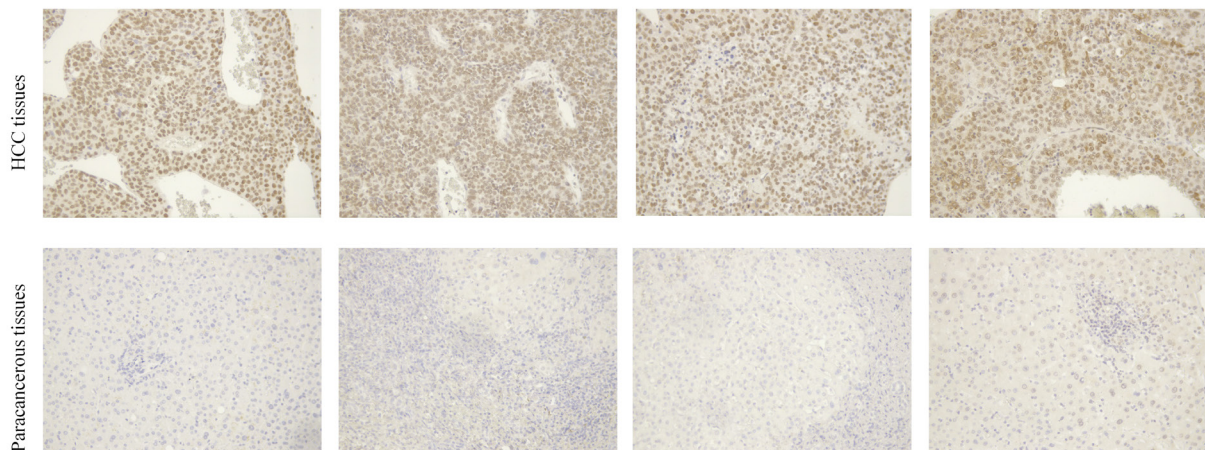


**Figure 2. The immunohistochemical results of 4 cases were selected from HCC and paracancerous tissues in the microarrays.** The immunohistochemistry results showed that the APE1 positive rate of HCC was much higher than paracancerous tissues in the microarrays. It was the same with the IOD result.

tissue microarrays, APE1 expression in HCC tissues of the 80 cases had no statistically significant correlation with patient's gender and age ( $p > 0.05$ ), but its correlation with the differences in TNM staging and histological grading had statistical significance ( $p < 0.05$ ) (Table 1).

#### 2.4. Silencing APE1 expression and transfection efficiency evaluation

The silencing of APE1 mRNA expression in HCC Hep 3B cells was detected with real-time PCR. The results showed that the mRNA expression level was significantly lower in APE1 shRNA group than in

control shRNA group and blank group ( $p < 0.05$ ), and there was no significant difference between control shRNA group and blank group ( $p > 0.05$ ) (Figure 4A). Meanwhile, protein expression detected with Western blotting was consistent with mRNA level, and the protein expression was significantly lower in APE1 shRNA group than in control shRNA group and blank group, demonstrating the efficacy of the designed shRNA interfering sequence (Figure 4B). Various groups of Hep 3B cell lines with stably transfected plasmids were established, the transfection efficiency as detected by fluorescence microscopy was  $> 70\%$ , accordingly, the cell lines could be used for subsequent detections (Figure 4C).

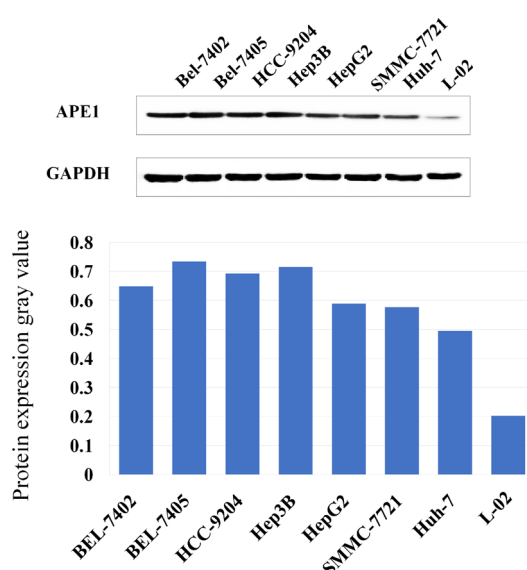


**Figure 3. Detection of APE1 expression in human HCC cells with Western blot.** APE1 expression in human HCC BEL-7402, BEL-7405, HCC-9204, Hep3B, HepG2, SMMC-7721 and Huh-7 cells as well as in normal hepatocytes L-02 cells. The results showed that APE1 expression was higher in HCC cells than in normal hepatocytes to varying levels, APE1 expression in HCC cells was 2.5-3.6 times higher than in hepatocytes.

### 2.5. Effects of silencing APE1 on Hep 3B cell proliferation ability

MTT assay was used to detect cell proliferation in each group after culture for 72 h. The results showed that the cell absorbance in blank group, control shRNA group and APE1 shRNA group was  $1.525 \pm 0.079$ ,  $1.497 \pm 0.072$  and  $0.981 \pm 0.063$ , respectively, based on the results of one-way ANOVA, the inter-group differences had statistical significance ( $F = 109.7$ ,  $p < 0.001$ ). The cell proliferation activity was significantly lower in APE1 shRNA group than in control shRNA group, and the difference had statistical significance ( $p < 0.001$ ), while the difference in cell proliferation activity between blank group and control shRNA group had no statistical significance ( $p > 0.05$ ). The results showed that silencing APE1 expression could significantly reduce cell proliferation activity in HCC Hep 3B cells (Figure 5).

### 2.6. Effects of silencing APE1 expression on HCC Hep 3B apoptosis

An Annexin V-FITC/PI double-labeling technique was

**Table 1. Relationship between APE1 expression and clinical pathological characteristics of HCC**

Group	No. of cases ( <i>n</i> = 80)	Positive expression ( <i>n</i> = 31)	Negative expression ( <i>n</i> = 49)	$\chi^2$ value	<i>p</i> value
Sex					
Male	64	25	39	0.013	0.908
Female	16	6	10		
Age					
≤ 50 years	20	7	13	0.158	0.691
> 50 years	60	24	36		
TNM staging					
I-II	39	10	29	5.975	0.014
III-IV	41	21	19		
Histopathological grading					
Good (I)	2	0	2	7.167	0.027
Medium (II, III)	67	23	44		
Poor (IV)	11	8	3		

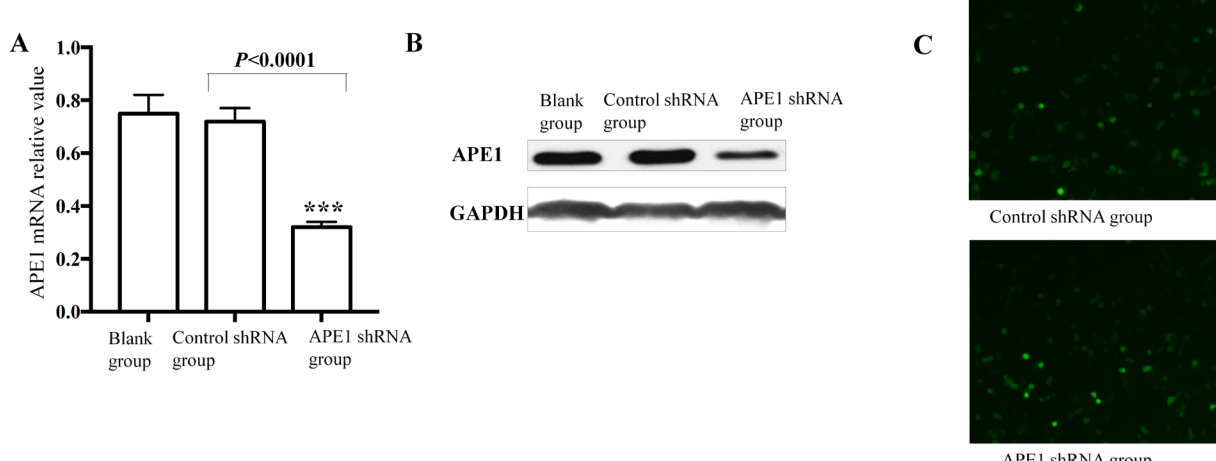


**Figure 4. Silencing APE1 expression in HCC Hep 3B cells and transfection efficiency evaluation.** (A): The mRNA expression level was significantly lower in APE1 shRNA group than in control shRNA group and blank group ( $p < 0.05$ ), and there was no significant difference between control shRNA group and blank group ( $p > 0.05$ ). (B): The APE1 protein expression was significantly lower in APE1 shRNA group than in control shRNA group and blank group. (C): The transfection efficiency as detected by fluorescence microscopy was  $> 70\%$  in both experimental and control group.

used to detect apoptosis in each group. The results showed that the total apoptosis rate in blank group, control shRNA group and APE1 shRNA group was  $9.91\% \pm 0.61\%$ ,  $10.96\% \pm 0.75\%$  and  $20.06\% \pm 1.73\%$ , respectively. Based on one-way ANOVA, the inter-group differences had statistical significance ( $F = 46.63$ ,  $p < 0.01$ ). The apoptosis rate was significantly higher in APE1 shRNA group than in control shRNA group, and the difference had statistical significance ( $p < 0.01$ ); the difference in apoptosis rate between blank group and control shRNA group had no statistical significance ( $p > 0.05$ ) (Figure 6). The results showed that silencing APE1 expression was able to significantly increase the apoptosis of HCC Hep 3B, suggesting that APE1 may promote tumor growth by inhibiting apoptosis.

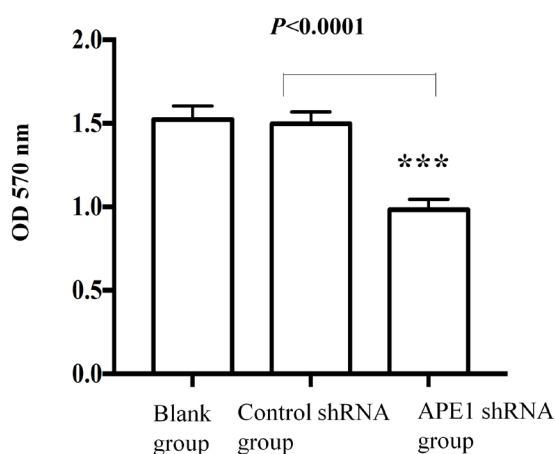


**Figure 5. Effects of silencing APE1 expression on HCC Hep 3B cell proliferation ability.** MTT assay was used to detect cell proliferation in each group after culture for 72 h. The results showed that the cell absorbance in blank group, control shRNA group and APE1 shRNA group was  $1.525 \pm 0.079$ ,  $1.497 \pm 0.072$  and  $0.981 \pm 0.063$ , respectively, based on the results of one-way ANOVA, the inter-group differences had statistical significance ( $F = 109.7$ ,  $p < 0.0001$ ).

#### 4. Discussion

The carcinogenesis and development of HCC is a complex multi-factor multi-stage pathogenesis process that involves abnormal expression of many related genes (7). An important part of tumor biology is to identify the key genes of HCC and search for new therapeutic targets based on the study of mechanisms of action (8). APE1 is a protein that plays a role in DNA repair and redox function, and is able to regulate a variety of transcription factors associated with cancer-related pathways (9,10). Its open reading frame consisting of 954bp encodes 318 amino acid residues (Figure 7) for protein diagram (11). On the one hand, APE1 functions as an endonuclease involved in DNA base excision repair, it is closely related to tumor cell proliferation; on the other hand, it regulates the activity of redox-sensitive transcription factors (12). Many studies showed APE1 over-expression in a variety of tumors (13-15). Some scholars used enzyme-linked immunosorbent assay to detect serum APE1 in patients suffering from bladder cancer without chemotherapy or radiotherapy (51 cases) and in a non-tumor control group (55 cases). The correlation between clinical factors and serum APE1 was determined by the area of subject's characteristics under the curve. The results showed significant over-expression of serum APE1 in patients with bladder cancer, the sensitivity and specificity were 93% and 59%, respectively, and serum APE1 expression was related to tumor staging, grading, myometrial invasion and recurrence, suggesting that serum APE1 may serve as a potential serum marker of bladder cancer (16). Some studies also found that serum APE1 level was significantly elevated in 229 of 412 patients with non-small cell lung cancer and was correlated with tissue level ( $r^2 = 0.639$ ,  $p < 0.001$ ). Elevation of APE1 level in patient's tissues and serum prior to chemotherapy was related to progression-

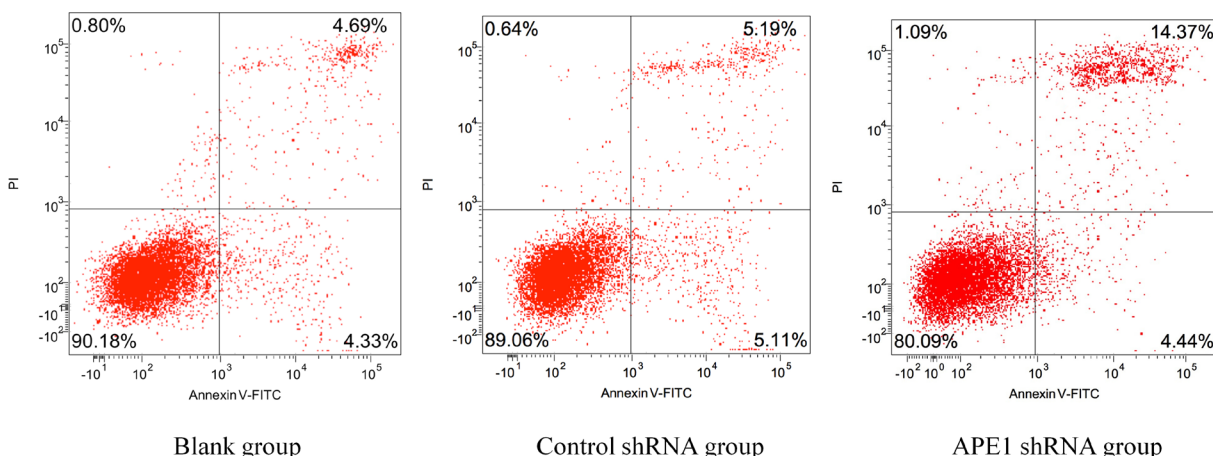


**Figure 6. Silencing APE1 expression significantly increases HCC Hep 3B apoptosis.** Annexin V-FITC/PI double-labeling technique was used to detect apoptosis in each group. The results showed that the total apoptosis rate in blank group, control shRNA group and APE1 shRNA group was  $9.91\% \pm 0.61\%$ ,  $10.96\% \pm 0.75\%$  and  $20.06\% \pm 1.73\%$ , respectively.

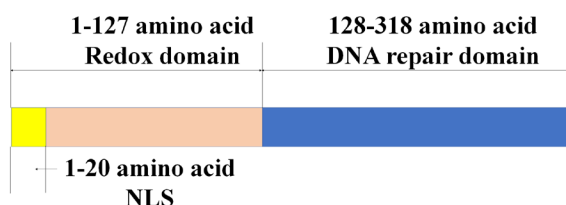


**Figure 7. APE1 protein schematic diagram.** The open reading frame of APE1 consisted of 954bp encoding 318 amino acid residues. The Redox domain, DNA repair domain are shown in this picture. So APE1 functions as an endonuclease involved in DNA base excision repair; on the other hand, it regulates the activity of redox-sensitive transcription factors.

free survival (HR: 2.165,  $p < 0.001$ , HR: 1.421,  $p = 0.012$ ), but unrelated to overall survival; after 6 cycles of chemotherapy, low APE1 serum level was related to better overall survival (HR: 0.497,  $p = 0.010$ ) (17).

With the rapid development of molecular biology technologies, some new methods such as shRNA technique are used in targeted intervention of APE1. RNA interference is a typical technique that uses double-stranded RNA to specifically inhibit gene expression of the corresponding complementary bases. This technique characterized by high specificity, small molecularity and transitivity can specifically silence gene expression. It has been widely used to explore gene functions and provide gene therapy for the treatment of malignant tumors (18). Bhat AA *et al.* knocked out APE1 with shRNA to study the pathogenesis of esophageal adenocarcinoma; they found that APE1 was essential for phosphorylation, nuclear localization and transcriptional activation of STAT3, further suggesting that APE1 plays a key role in inducing the activation of the EGFR-STAT3 signaling axis. It also responded to acidic bile salts and is a major risk factor for esophageal adenocarcinoma (19). Shah F *et al.* knocked out APE1 with siRNA in pancreatic cancer cells and found that some new genes and pathways affected APE1 expression using a single-cell sequencing technique, they also determined the specificity of tumor subtypes; these findings will facilitate hypothesis-driven methods to generate combination therapies. For example, pancreatic and other cancers can be treated with APE1 inhibitor APX33 30 in combination with other drugs approved by the FDA (20).

Since there were few study reports on the roles of APE1 in HCC pathogenesis, this study investigated its functions in human HCC high metastatic cells by silencing APE1. First of all, we examined the level of APE1 expression in 80 cases of HCC and the corresponding paracancerous tissue microarrays using immunohistochemical techniques. Meanwhile, we detected APE1 expression in human HCC BEL-7402, BEL-7405, HCC-9204, Hep3B, HepG2, SMMC-7721 and Huh-7 cells as well as in normal hepatocyte L-02 cells using Western blotting. The results showed that

APE1 expression in HCC was significantly up-regulated and different from TNM staging and histological grading. An APE1 shRNA vector was further constructed in HCC Hep3B cells to establish stably transfected cell lines. Then, cell proliferative activity was detected with MTT assay while apoptosis was detected with an Annexin V-FITC/PI double-labeling technique. The results showed that down-regulation of APE1 expression significantly reduced the proliferative activity of Hep3B cells and increased the apoptosis rate. Apoptosis is not only an important means in the regulation of cell growth and differentiation but also an important protective mechanism against the tumors. The apoptotic potential is usually extremely low in cancerous cells, but the proliferative ability is enhanced, which directly leads to rapid pathologic division and proliferation of tumor cells, suggesting that APE1 may promote tumor growth by inhibiting apoptosis.

In summary, this experiment applied a RNA interference technique and successfully introduced an APE1 siRNA expression plasmid into human HCC cells, leading to down-regulation of cellular APE1 expression. It is confirmed that down-regulation of APE1 protein can inhibit proliferation and promote apoptosis of HCC cells. These findings provide an experimental basis and show certain prospects for clinical application of APE1 in the treatment of HCC, justifying further in-depth research.

## Acknowledgements

This study was supported by China Railway Corporation science and technology development project, No.: J2017Z609 and the fund of Beijing Key Lab of Therapeutic Cancer Vaccines, No.: 2017-KF02. We thank these foundations.

## References

- Clark T, Maximin S, Meier J, Pokharel S, Bhargava P. Hepatocellular Carcinoma: Review of Epidemiology, Screening, Imaging Diagnosis, Response Assessment, and Treatment. *Curr Probl Diagn Radiol.* 2015; 44:479-486.
- Chen W, Zheng R, Baade PD, Zhang S, Zeng H, Bray F, Jemal A, Yu XQ, He J. Cancer statistics in China, 2015. *CA Cancer J Clin.* 2016; 66:115-132.
- Gao XH, Zhang SS, Chen H, Wang K, Xie W, Wang FB. Lipoprotein (a): A promising prognostic biomarker in patients with hepatocellular carcinoma after curative resection. *Onco Targets Ther.* 2018; 11:5917-5924.
- Xiao H, Zhou B, Jiang N, Cai Y, Liu X, Shi Z, Li M, Du C. The potential value of CDV3 in the prognosis evaluation in Hepatocellular carcinoma. *Genes Dis.* 2018; 5:167-171.
- Amr KS, Elmawgoud Atia HA, Elazeem Elbnhawy RA, Ezzat WM. Early diagnostic evaluation of miR-122 and miR-224 as biomarkers for hepatocellular carcinoma. *Genes Dis.* 2017; 4:215-221.
- Li Q, Wei X, Zhou ZW, Wang SN, Jin H, Chen KJ, Luo J, Westover KD, Wang JM, Wang D, Xu CX, Shan

- JL. GADD45alpha sensitizes cervical cancer cells to radiotherapy via increasing cytoplasmic APE1 level. *Cell Death Dis.* 2018; 9:524.
7. Singh AK, Kumar R, Pandey AK. Hepatocellular Carcinoma: Causes, Mechanism of Progression and Biomarkers. *Curr Chem Genom Transl Med.* 2018; 12:9-26.
8. Lim, II, Farber BA, LaQuaglia MP. Advances in fibrolamellar hepatocellular carcinoma: A review. *Eur J Pediatr Surg.* 2014; 24:461-466.
9. Tell G, Quadrifoglio F, Tiribelli C, Kelley MR. The many functions of APE1/Ref-1: Not only a DNA repair enzyme. *Antioxid Redox Signal.* 2009; 11:601-620.
10. Fairlamb MS, Whitaker AM, Freudenthal BD. Apurinic/apyrimidinic (AP) endonuclease 1 processing of AP sites with 5' mismatches. *Acta Crystallogr D Struct Biol.* 2018; 74:760-768.
11. Guerreiro PS, Estacio SG, Antunes F, Fernandes AS, Pinheiro PF, Costa JG, Castro M, Miranda JP, Guedes RC, Oliveira NG. Structure-based virtual screening toward the discovery of novel inhibitors of the DNA repair activity of the human apurinic/apyrimidinic endonuclease 1. *Chem Biol Drug Des.* 2016; 88:915-925.
12. Fung H, Demple B. A vital role for Ape1/Refl protein in repairing spontaneous DNA damage in human cells. *Mol Cell.* 2005; 17:463-470.
13. Logsdon DP, Shah F, Carta F, Supuran CT, Kamocka M, Jacobsen MH, Sandusky GE, Kelley MR, Fishel ML. Blocking HIF signaling via novel inhibitors of CA9 and APE1/Ref-1 dramatically affects pancreatic cancer cell survival. *Sci Rep.* 2018; 8:13759.
14. Hudson AL, Parker NR, Khong P, Parkinson JF, Dwight T, Ikin RJ, Zhu Y, Chen J, Wheeler HR, Howell VM. Glioblastoma Recurrence Correlates With Increased APE1 and Polarization Toward an Immuno-Suppressive Microenvironment. *Front Oncol.* 2018; 8:314.
15. Yang X, Peng Y, Jiang X, et al. The regulatory role of APE1 in epithelial-to-mesenchymal transition and in determining EGFR-TKI responsiveness in non-small-cell lung cancer. *Cancer Med.* 2018; 7:4406-4419.
16. Shin JH, Choi S, Lee YR, Park MS, Na YG, Irani K, Lee SD, Park JB, Kim JM, Lim JS, Jeon BH. APE1/Ref-1 as a Serological Biomarker for the Detection of Bladder Cancer. *Cancer Res Treat.* 2015; 47:823-833.
17. Zhang S, He L, Dai N, et al. Serum APE1 as a predictive marker for platinum-based chemotherapy of non-small cell lung cancer patients. *Oncotarget.* 2016; 7:77482-77494.
18. Xin Y, Huang M, Guo WW, Huang Q, Zhang LZ, Jiang G. Nano-based delivery of RNAi in cancer therapy. *Mol Cancer.* 2017; 16:134.
19. Bhat AA, Lu H, Soutto M, Capobianco A, Rai P, Zaika A, El-Rifai W. Exposure of Barrett's and esophageal adenocarcinoma cells to bile acids activates EGFR-STAT3 signaling axis via induction of APE1. *Oncogene.* 2018.
20. Shah F, Goossens E, Atallah NM, Grimard M, Kelley MR, Fishel ML. APE1/Ref-1 knockdown in pancreatic ductal adenocarcinoma - characterizing gene expression changes and identifying novel pathways using single-cell RNA sequencing. *Mol Oncol.* 2017; 11:1711-1732.

(Received September 27, 2018; Revised October 18, 2018;

Accepted October 21, 2018)

# The pregnancy outcomes of intrauterine insemination with husband's sperm in natural cycles versus ovulation stimulated cycles: A retrospective study

**Feijun Ye<sup>1,§</sup>, Wenli Cao<sup>1,§</sup>, Jing Lin<sup>2,3,4,§</sup>, Yan Du<sup>2,3,5</sup>, Likun Lan<sup>6</sup>, Ying Dong<sup>7</sup>, Jun Zhu<sup>8</sup>, Qi Zhou<sup>9</sup>, Xinyao Pan<sup>2,3,4</sup>, Youhui Lu<sup>2,3,4</sup>, Fang Zeng<sup>1</sup>, Bangshi Xia<sup>1</sup>, Ling Wang<sup>2,3,4,\*</sup>**

<sup>1</sup> Department of Reproductive Center, Zhoushan Maternity and Child Healthcare Hospital, Zhejiang, China;

<sup>2</sup> Laboratory for Reproductive Immunology, Hospital & Institute of Obstetrics and Gynecology, Shanghai Medical College, Fudan University, Shanghai, China;

<sup>3</sup> The Academy of Integrative Medicine of Fudan University, Shanghai, China;

<sup>4</sup> Shanghai Key Laboratory of Female Reproductive Endocrine-related Diseases, Shanghai, China;

<sup>5</sup> Office of Clinical Epidemiology, Obstetrics and Gynecology Hospital of Fudan University, Shanghai, China;

<sup>6</sup> Second Affiliated Hospital of Hexi University, Gansu, China;

<sup>7</sup> Putuo District Institute of Maternity and Child Health of Shanghai, Shanghai, China;

<sup>8</sup> Department of Obstetrics and Gynecology, Wenling People's Hospital, Wenzhou Medical University, Zhejiang, China;

<sup>9</sup> Yangpu Hospital of Traditional Chinese Medicine, Shanghai, China.

## Summary

To compare the clinical outcomes of intrauterine insemination (IUI) with or without ovulation induction (OI), IUI cycles from January 2008 to December 2017 in Zhoushan Maternity and Child Healthcare Hospital were included, consisting of 455 natural cycles and 536 OI cycles. The overall clinical pregnancy rate did not differ between the two groups ( $P > 0.05$ ). Stratified by OI medications such as clomiphene (CC), human menopausal gonadotropin (HMG) and follicle stimulating hormone (FSH), the pregnancy rates in HMG, CC, CC+HMG, and FSH/FSH+HMG groups were 11.70%, 13.58%, 15.95%, and 13.46%, respectively, but the difference was not significant compared with natural cycles ( $P > 0.05$ ). Stratified by infertility etiology, the pregnancy rate was significantly higher in stimulated cycles than natural cycles with ovulation disorders ( $P < 0.01$ ) and unexplained factors ( $P < 0.01$ ) while it was significantly lower regarding cervical factors ( $P < 0.01$ ), endometriosis ( $P < 0.05$ ), male factor ( $P < 0.01$ ) and other female factors. There was no strong difference of pregnancy rate for biparental causes ( $P > 0.05$ ). Stratified by age category, women over 35 had higher pregnancy rate in stimulated cycles compared with natural cycles (18.75 vs. 12.24%;  $P < 0.05$ ), while women under 35 had no significant difference of pregnancy rate between the two groups (13.65 vs 13.05%;  $P > 0.05$ ). However, there was no significant difference between each ovarian stimulation group and natural cycle group regardless of the infertility causes or age categories. To conclude, IUI-OI could achieve a higher overall pregnancy rate for women over 35 and infertile patients with ovulation disorders and unexplained factors.

**Keywords:** Intrauterine insemination (IUI), ovulation induction (OI), stimulated cycles, natural cycles, clinical pregnancy rate

<sup>§</sup>These authors contributed equally to this work.

\*Address correspondence to:

Dr. Ling Wang, Laboratory for Reproductive Immunology, Hospital & Institute of Obstetrics and Gynecology, Fudan University, 419 Fangxie Road, Shanghai 200011, China.  
E-mail: Dr.wangling@fudan.edu.cn

## 1. Introduction

Intrauterine insemination (IUI) is an assisted conception technique offering hope to many infertile couples based on the finding of a striking reduction in sperm

number with the length of the female reproductive tract after intercourse (1). It is performed by transferring a processed motile semen sample into a female's uterus, which increases the number of sperm that reaches the oviduct and subsequently increases the chances of *in vivo* fertilization.

IUI with or without ovulation induction (OI) is a relatively cost-effective and noninvasive treatment, indicated for selected couples with infertility due to female factors including ovulation disorders and cervical factor, mild male factor, ejaculatory disorders, immunological factor and unexplained factors with an unfavorable prognosis for natural conception. As the effectiveness of IUI-OI is a result of multiple ovulations compared with natural cycles, concerns exist about the associated OI complications such as ovarian hyperstimulation syndrome (OHSS) and multiple pregnancies, leading to maternal and perinatal risks. Predictive indicators of IUI success include maternal age, infertility etiology, infertility duration, stimulation medications, follicle number, endometrial thickness, semen characteristics, timing of insemination, number of cycles, etc. (2).

In order to address the question of whether and when OI is required in IUI, a retrospective study was conducted to provide evidence regarding the fertility treatment.

## 2. Materials and Methods

### 2.1. Study design

The clinical data of 991 IUI cycles with husband's sperm present at the Reproductive Center of Zhoushan Maternity and Child Healthcare Hospital in China from January 2008 to December 2017 were reviewed retrospectively. A complete couple workup was performed, including health history, physical examination, laboratory and radiological investigations. Semen analysis was repeated three times if an abnormal sperm result occurred. Inclusion criteria consisted of: 1) married couples failing to achieve a clinical pregnancy after one-year (or longer) of regular unprotected sexual intercourse; 2) patency of at least one fallopian tube confirmed by hysterosalpingography, laparoscopy or ultrasound-guided hydrotubation. Exclusion criteria included: 1) failed ovulation after IUI under ultrasound monitoring; 2) total motile sperm count  $< 5 \times 10^6$  (grade a+b) after semen processing. The study was approved by the ethics committee of Zhoushan Maternity and Child Healthcare Hospital (No. 2018-004).

### 2.2. Natural or stimulated IUI cycles

Females with regular menstrual cycles could adopt IUI in natural cycles. Follicular development was monitored by transvaginal ultrasound from day 10-12 of the cycle

onward according to the menstrual cycle length.

Patients with ovulation disorders, irregular menstruation or abnormal follicle development received ovarian stimulation medications from cycle day 3-5 under the monitoring of transvaginal ultrasonography.

**Human menopausal gonadotropin (HMG):** daily injection of 75-150 IU HMG from day 3-5 of the menstrual cycle for 4-5 days consecutively. The dosage was adjusted according to the ultrasonic monitoring of follicle and endometrial development.

**Clomiphene Citrate (CC):** daily oral administration of 50-100 mg CC starting from day 5 of the cycle for 5 days with subsequent ultrasonic monitoring.

**CC+HMG:** CC 100 mg/day (cycle day 5) for 5 days, followed by daily injection of 150 IU HMG for 2 days. According to the ultrasonic monitoring for ovary response and dominant follicle size, CC/HMG could be administered repeatedly.

**Follicle stimulating hormone (FSH)/FSH+HMG:** daily injection of 150 IU FSH from day 3 of the cycle. To prevent OHSS, the dosage was adjusted accordingly.

### 2.3. Operative time of IUI

Urinary luteinizing hormone (LH) test paper (Yunnan University Biopharmaceutical Co., Ltd.) and vaginal ultrasound were measured day by day from when the lead follicle diameter reached 16-18 mm. Ovulation was triggered with 5000-10000 IU of human chorionic gonadotropin (HCG) when a follicle with a diameter of 18 mm was observed and the number of dominant follicles was controlled at  $\leq 3$ . IUI was implemented based on the detection of LH surge or at 24-36 hours post HCG. If the follicle diameter was over 20 mm without the presence of a urinary LH peak, HCG 10000 IU was injected and IUI was planned 24-36 hours thereafter. Non-ovulators detected by ultrasound at 24 hours after operation required a second IUI.

### 2.4. Semen collection and processing

In accordance with laboratory guidelines of the World Health Organization (WHO) for sperm collection and preparation, semen was collected by masturbation after abstinence for 3-7 days, placed in  $\text{CO}_2$  incubator at 37°C and liquefied for about 30 minutes. After semen analysis, the upstream or density gradient centrifugation method was adopted to yield 0.5 mL of semen suspension.

### 2.5. Insemination

The patient was placed in a lithotomy position. After routine disinfection of the vulva and placement of a sterile towel, the cervix was exposed with a vaginal speculum and wiped with a cotton ball containing saline. 0.5 mL of semen suspension was injected into

the uterine cavity through a disposable syringe. The patient was instructed to immobilization in a supine position for 30 minutes after the operation.

### 2.6. Postoperative corpus luteum support and follow-up

Routine corpus luteum support for all patients started from the third day after ovulation with oral administration of dydrogesterone tablets 10 mg, twice a day, and continued up to postoperative day 15. A clinical pregnancy was confirmed by HCG level with urine test and detection of a gestational sac and embryonic heartbeat via ultrasound on postoperative day 15 and day 30, respectively. Patients were followed up to the time of delivery.

### 2.7. Statistical analysis

Data were expressed as mean  $\pm$  standard deviation (SD). Statistical Package for the Social Sciences (SPSS) 13.0 software was used for statistical analysis. Student's *t* test was used for measurement data, and chi-square test was used for count data. A *p*-value  $< 0.05$  was considered statistically significant.

## 3. Results

### 3.1. Study demographics

A total of 991 IUI cycles with husband's sperm present at the Reproductive Center of Zhoushan Maternity and Child Healthcare Hospital from 2008 to 2017 were reviewed. The average age of women was  $30.48 \pm 3.29$  years (range: 22–43 years), and the average infertility period was  $3.69 \pm 2.48$  years (range: 1–13 years). 547 cycles (55.2%) were diagnosed as primary infertility and 444 cycles were secondary infertility. Female infertility etiology included ovulation disorders ( $N = 245$ ), cervical factor ( $N = 100$ ), endometriosis ( $N = 40$ ) and other female factors ( $N = 33$ ). In addition, male

factor contributed to 188 cycles of infertility; biparental factor caused 196 cycles of infertility; and there were 189 cycles of unexplained causes. From a total of 991 IUI cycles, the clinical pregnancy rate was 13.32%.

### 3.2. Natural cycles versus stimulated cycles

In natural cycles ( $N = 455$ ), the average female age was  $30.59 \pm 3.59$  years and the average infertility period was  $3.65 \pm 2.57$  years. 536 were stimulated cycles with an average female age of  $30.39 \pm 3.03$  years and an average infertility period of  $3.73 \pm 2.41$  years. The two groups were comparable for baseline characteristics regarding female age, body mass index (BMI), infertility period and infertility type ( $P > 0.05$ ) (Table 1). The overall clinical pregnancy rate did not differ between stimulated cycles and natural cycles (13.62 vs. 12.97%;  $P > 0.05$ ).

The pregnancy outcomes of different ovarian stimulation protocols are shown in Table 2. The pregnancy rates in HMG, CC, CC+HMG, and FSH/FSH+HMG groups were 11.70%, 13.58%, 15.95%, and 13.46%, respectively. However, the difference was not statistically significant as compared with the natural cycle group ( $P > 0.05$ ).

### 3.3. Pregnancy outcomes stratified according to infertility etiology

The pregnancy outcomes pertaining to different causes of infertility are shown in Table 3. Stratified according to infertility etiology, the clinical pregnancy rate significantly increased in stimulated cycles compared to natural cycles with ovulation disorders (14.22 vs. 9.76%;  $P < 0.01$ ) and unexplained factor (14.08 vs. 10.17%;  $P < 0.01$ ) while it decreased regarding cervical factor (7.27 vs. 15.56%;  $P < 0.01$ ), endometriosis (19.05 vs. 21.05%;  $P < 0.05$ ), other female factors (0.00 vs. 12.00%) and male factor (7.84 vs. 13.14%;  $P < 0.01$ ), in contrast with a lack of a strong difference of pregnancy

**Table 1. Comparison of natural cycles versus stimulated cycles**

Groups	Female age, years, mean $\pm$ SD	Infertility period, years, mean $\pm$ SD	Body mass index (BMI), mean $\pm$ SD	Primary infertility, N (%)	Secondary infertility, N (%)
Natural cycles ( $N = 455$ )	$30.59 \pm 3.59$	$3.65 \pm 2.57$	$21.03 \pm 2.39$	284 (62.4)	171 (37.6)
Stimulated cycles ( $N = 536$ )	$30.39 \pm 3.03$	$3.73 \pm 2.41$	$23.60 \pm 4.23$	263 (49.1)	273 (50.9)

**Table 2. Pregnancy outcomes of ovulation induction regimens**

Groups	Cycles, N	Pregnancy, N	Pregnancy rate, %
Natural cycles	455	59	12.97
Stimulated cycles	536	73	13.62
HMG	188	22	11.70
CC	81	11	13.58
CC+HMG	163	26	15.95
FSH/FSH+HMG	104	14	13.46

**Table 3. Pregnancy outcomes stratified according to infertility etiology**

Infertility etiology	Natural cycles				HMG				CC				Stimulated cycles			
	Cycles, N		Pregnancy rate, N (%)		Cycles, N		Pregnancy rate, N (%)		Cycles, N		Pregnancy rate, N (%)		Cycles, N		Pregnancy rate, N (%)	
Female factors	130	18 (13.85)	82	10 (12.20)	57	8 (14.04)	62	8 (12.90)	87	11 (12.64)	288	37 (12.85)				
Cervical factor	45	7 (15.56)	21	2 (9.52)	18	2 (11.11)	8	0 (0.00)	8	0 (0.00)	55	4 (7.27)**				
Endometriosis	19	4 (21.05)	0	0 (0.00)	5	1 (20.00)	10	2 (20.00)	6	1 (16.67)	21	4 (19.05)*				
Ovulation disorders	41	4 (9.76)	58	8 (13.80)	33	5 (15.15)	40	6 (15.00)	73	10 (13.70)	204	29 (14.22)**				
Others	25	3 (12.00)	3	0 (0.00)	1	0 (0.00)	4	0 (0.00)	0	0 (0.00)	8	0 (0.00)				
Male factor	137	18 (13.14)	16	2 (12.50)	10	0 (0.00)	20	2 (10.00)	5	0 (0.00)	51	4 (7.84)**				
Biparental factor	70	11 (15.71)	48	6 (12.50)	10	2 (20.00)	60	11 (18.33)	8	3 (37.50)	126	22 (17.46)				
Unexplained causes	118	12 (10.17)	42	4 (9.52)	4	1 (25.00)	21	5 (23.81)	4	0 (0.00)	71	10 (14.08)**				

Note: \* $P < 0.05$  compared with natural cycle group; \*\* $P < 0.01$  compared with natural cycle group.**Table 4. Pregnancy outcomes stratified according to age categories**

Age category	Natural cycles				HMG				CC				Stimulated cycles			
	Cycles, N		Pregnancy rate, N (%)		Cycles, N		Pregnancy rate, N (%)		Cycles, N		Pregnancy rate, N (%)		Cycles, N		Pregnancy rate, N (%)	
Aged ≤ 35	406	53 (13.05)	179	20 (11.17)	80	11 (13.75)	158	25 (15.82)	103	14 (13.59)	520	70 (13.65)				
Aged > 35	49	6 (12.24)	9	2 (22.22)	1	0 (0.00)	5	1 (20)	1	0 (0.00)	16	3 (18.75)*				

Note: \* $P < 0.05$  compared with natural cycle group.

rate for biparental causes (17.46 vs. 15.71%;  $P > 0.05$ ). Further stratified according to OI regimes, there was no significant difference between each ovarian stimulation group and natural cycle group regardless of the infertility causes ( $P > 0.05$ ).

#### 3.4. Pregnancy outcomes stratified according to age categories

The pregnancy outcomes of different age categories are shown in Table 4. The overall pregnancy rate did not differ between the over-35s and the under-35s (13.85 vs. 13.28%;  $P > 0.05$ ). Women over 35 years old had a higher pregnancy rate in stimulated cycles compared with natural cycles (18.75 vs. 12.24%;  $P < 0.05$ ), while women under 35 had no significant difference of pregnancy rate between the two groups (13.65 vs. 13.05%;  $P > 0.05$ ). Further stratified according to OI regimes, there was no significant difference between each ovarian stimulation group and natural cycle group regardless of the age categories ( $P > 0.05$ ).

## 4. Discussion

IUI with or without OI is currently one of the most common assisted conception technologies for the treatment of infertility. Compared with monofollicular growth in natural cycles, the rationale of OI prior to IUI was to achieve multifollicular growth, which resulted in a notably higher pregnancy rate (3). IUI-OI treatment could increase the number of mature follicles and improve the development of follicles. In addition, the non-synchronous rupture of multiple follicles by HCG as well as the optimal timing of insemination could increase the fertilization rate and thus increase the pregnancy rate of IUI. Ovarian stimulation therapy might correct the unfavorable factors in the process of follicular maturation, fertilization and implantation. Researchers who held this view believed that the pregnancy rate of IUI in the stimulated cycles was higher than that in the natural cycles, which was verified in a meta-analysis (OR: 1.47, 95% CI: 1.26-1.72;  $P < 0.00001$ ) (4) and a randomized clinical trial (13.7 vs. 9.5%;  $P < 0.05$ ) (5).

However, a recent retrospective study discovered that the pregnancy rate did not differ between IUI and IUI-OI ( $\chi^2=1.55$ ;  $P > 0.05$ ) and suggested that natural cycles would be a more reasonable treatment in prevention of multiple pregnancies (6). Agreeing with this finding, our study also showed that the difference of overall clinical pregnancy rate between the stimulated cycles and the natural cycles was not significant. Subdividing stimulated cycles into HMG, CC, CC+HMG and FSH/FSH+HMG groups according to different OI regimens, still, no strong difference was found as compared with the natural cycle group. Opposed to the idea that OI induced multifollicular

growth, the current ovarian stimulation medications could control the number of dominant follicles. Meanwhile, the developmental motivation of follicles in IUI-OI was due to exogenous drug stimulation, which was different from the natural physiological condition, therefore the risk of abnormal follicle development remained. The endocrine environment altered by OI might impair fertilization potential and endometrial receptivity as well.

We therefore recommended that the indications for IUI-OI be strictly controlled and natural cycle-IUI be the preferred choice for females with normal ovulation. For patients with abnormal ovulation or repeated failures of getting pregnant in natural cycle-IUI, OI prior to IUI could be adopted with reasonable regimen, mild doses and optimal timing of HCG. It was appropriate to have one or two dominant follicles developed in OI cycles to avoid multiple pregnancies. Ovulation trigger and IUI would be withheld or shifted to oocyte retrieval and in vitro fertilization-embryo transfer (IVF-ET) when more than 3 follicles with a diameter of 16 mm or more than 5 follicles with a diameter of 12 mm were present.

Our study showed that the clinical pregnancy rate significantly increased in stimulated cycles compared to natural cycles for females presenting with ovulation disorders while it decreased regarding cervical factor, endometriosis and other female factors. It was further strengthened by a retrospective study in 2014 that higher clinical pregnancy rates per cycle were observed in patients with ovulation disorders versus other female indications ( $P = 0.03$ ) (7). For infertility caused by cervical factors, our study found a significant difference in favor of natural cycles. However, Fu *et al.* believed that OI combined with IUI positively influenced the pregnancy outcomes (22.40 vs. 14.62%;  $P < 0.05$ ) because the ovarian stimulation treatment increased the follicle number and estrogen level and improved cervical mucus, subsequently increased the pregnancy rate (8), which was inconsistent with Steures's results in terms of ongoing pregnancy rate (21 vs. 17%; RR: 1.2, 95% CI: 0.75-2.0) (9). Endometriosis could affect pregnancy by disturbing ovulation, endometrial receptivity, uterus microenvironment and luteal function. Surgery remained an important option to reduce ectopic lesions, restore normal anatomy, prevent recurrence of ectopic lesions and relieve symptoms. Some believed that IUI combined with FSH could obtain a better pregnancy rate than anti-estrogens for infertile females with mild endometriosis, mild male infertility and unexplained factor (OR: 1.8, 95% CI: 1.2-2.7) (10). However, our study showed a significant benefit of natural cycles for patients with endometriosis, which required further investigation.

IUI-OI has been routinely offered as a first-line treatment for couples with unexplained infertility in most fertility clinics of China. Our findings showed that clinical pregnancy rate significantly increased in

stimulated cycles compared to natural cycles regarding unexplained factor, consistent with an updated Cochrane review by Veltman-Verhulst in 2016, which reported a beneficial effect of IUI-OI on live birth rate compared to the natural cycles (OR: 0.48, 95% CI: 0.29-0.82) (11). However, because there was still a chance of natural conception through expectant management in couples with unexplained infertility and a good prognosis, the 2013 guideline from the UK National Institute for Health and Care Excellence recommended extended expectant management instead of IUI-OI for these patients. More recently, a randomized, controlled, two-center study in New Zealand in 2018 revealed that IUI-OI had a higher cumulative livebirth rate than three cycles of expectant management (31 vs. 9%; RR: 3.41, 95% CI: 1.71-6.79;  $p = 0.0003$ ) in this particular population (12). Large multi-center trials comparing IUI in natural unstimulated cycles or stimulated cycles to extended expectant management were necessary to draw a firm conclusion.

IUI for male infertility was under huge debate because large high-quality randomized studies were lacking. There was neither a strict cut-off value of sperm quality nor a clear definition of mild, moderate and severe male infertility (13). Our study showed that the clinical pregnancy rate significantly decreased in stimulated cycles compared to natural cycles regarding male factor, which was insufficient evidence to recommend for or against IUI-OI in couples with poor sperm parameters. In patients with unexplained or mild male infertility and an unfavorable prognosis, IVF with elective single embryo transfer was as effective as IUI-OI in terms of livebirth rate per couple (52 vs. 47%), demonstrated by Bensdorp *et al.* in 2015 (14).

Age is one of the most important factors of pregnancy achievement in IUI. Women's fertility potential declined with advancing reproductive age (15). As aging, there was a decrease in women's ovarian reserve, follicle number, oocyte quality, endometrial receptivity, function of corpus luteum and uterine blood flow, while an increase in the incidence of chromosomal abnormalities in oocytes was noted, leading to compromised capability of fertilization, development and implantation (16). The prolonged infertility duration and repeated failures in IUI brought psychological stress, depression and iatrogenic injuries, which seriously affected the success rate of IUI (17).

Our study revealed that the overall pregnancy rate did not differ between the over-35s and the under-35s, which might be explained by the individual treatment plans chosen for each patient from different age groups. Women over 35 years old had higher pregnancy rate in stimulated cycles compared with natural cycles, while women under 35 had no significant difference of pregnancy rate between the two groups. It was contradicted by another retrospective cohort study that females younger than 38 years old obtained a

better clinical pregnancy rate in the stimulated cycles than their older counterparts ( $P = 0.02$ ) (18). It argued that due to the irreversibility of ovarian function that accompanied aging, it would be impossible to yield high-quality oocytes and improve endometrial receptivity with ovulation induction, resulting in an unfavorable clinical pregnancy rate.

With a lack of high quality studies on pregnancy outcomes comparing IUI with or without OI in different age groups, the question of whether IUI-OI should be recommended for or against in the aged population deserved consideration and a clear age cut-off level was needed. With failed attempts of assisted reproductive technologies, women with age-related infertility probably labeled with unexplained infertility which led to inappropriate therapies (19). We therefore suggested that infertile women should be treated as early as possible and ovulation induction in females above 35 years should be used with caution.

Our study retrospectively reviewed all the IUI cycles with husband's sperm at our center in a ten-year period. It was noteworthy that the outcome measure in the study was solely pregnancy rate, whereas the European Society for Human Reproduction and Embryology (ESHRE) recommended birth of a single healthy child as the primary outcome (20). Our study was strengthened by complete data, strict criteria for clinical pregnancy, standard clinical routine and laboratory procedures. Pregnancies achieved with natural conception or additional interventions were carefully identified and excluded from the analysis.

## 5. Conclusion

To conclude, IUI-OI could achieve a higher overall pregnancy rate for women over 35 and infertile patients with ovulation disorders and unexplained factors. Natural cycle-IUI had better performance in the pregnancy outcome for patients with cervical factor, endometriosis, other female factors and male infertility. Our study provided draft recommendations for answering whether and when to provide ovulation induction in IUI.

## Acknowledgements

This work was supported by the National Natural Science Foundation of China No. 31571196 (to L Wang), the Science and Technology Commission of Shanghai Municipality YIXUEYINGDAO project No. 15401932200 and No. 18401902200 (to L Wang), the FY2008 JSPS Postdoctoral Fellowship for Foreign Researchers P08471 (to L Wang), the National Natural Science Foundation of China No. 30801502 (to L Wang), the Shanghai Pujiang Program No. 11PJ1401900 (to L Wang), Development Project of Shanghai Peak Disciplines-Integrative Medicine No. 20150407.

## References

1. Settlage DS, Motoshima M, Tredway DR. Sperm transport from the external cervical os to the fallopian tubes in women: A time and quantitation study. *Fertil Steril.* 1973; 24:655-661.
2. Merviel P, Heraud MH, Grenier N, Lourdel E, Sanguinet P, Copin H. Predictive factors for pregnancy after intrauterine insemination (IUI): An analysis of 1038 cycles and a review of the literature. *Fertil Steril.* 2010; 93:79-88.
3. van Rumste MME, Custers IM, van der Veen F, van Wely M, Evers JLH, Mol BWJ. The influence of the number of follicles on pregnancy rates in intrauterine insemination with ovarian stimulation: A meta-analysis. *Hum Reprod Update.* 2008; 14:563-570.
4. Cao J, Li A, Niu T, Shen L, Chen L. Effectiveness of natural cycle and ovulation induction cycle in intrauterine Insemination: A meta analysis. *Chin J Birth Health Heredity.* 2015; 23:98-101. (in Chinese)
5. Yang L. Pregnancy outcome of intrauterine insemination combined with ovarian stimulation: A clinical trial. *J Practical Gynecol Endocrinol.* 2018; 5:71-72. (in Chinese)
6. Shi Y, Zhang F, Liang Y, Zhang F, Zhi Y, Li Y, Li H, Song C, Guo X. Analysis on pregnancy outcomes of 2103 artificial insemination cycles. *Maternal & Child Health Care of China.* 2017; 32:4473-4476. (in Chinese)
7. Dinelli L, Courbière B, Achard V, Jouve E, Devezé C, Gnisci A, Grillo JM, Paulmyer-Lacroix O. Prognosis factors of pregnancy after intrauterine insemination with the husband's sperm: Conclusions of an analysis of 2,019 cycles. *Fertil Steril.* 2014; 101:994-1000.
8. Fu Z, Zhu W, Chen X, Li X, Tan Z, Zhou Y. Effect of ovarian hyperstimulation on pregnant rate in intrauterine insemination. *Chin J Clin Obstet & Gynecol.* 2008; 9:332-335. (in Chinese)
9. Steures P, van der Steeg JW, Hompes PGA, Bossuyt PMM, Habbema JDF, Eijkemans MJC, Koks CAM, Boudrez P, van der Veen F, Mol BWJ. The additional value of ovarian hyperstimulation in intrauterine insemination for couples with an abnormal postcoital test and a poor prognosis: A randomized clinical trial. *Fertil Steril.* 2007; 88:1618-1624.
10. ESHRE Capri Workshop Group. Intrauterine insemination. *Hum Reprod Update.* 2009; 15:265-277.
11. Veltman-Verhulst SM, Hughes E, Ayeleke RO, Cohen BJ. Intra-uterine insemination for unexplained subfertility. *Cochrane Database Syst Rev.* 2016; 2:CD001838.
12. Farquhar CM, Liu E, Armstrong S, Arroll N, Lensen S, Brown J. Intrauterine insemination with ovarian stimulation versus expectant management for unexplained infertility (TUI): A pragmatic, open-label, randomised, controlled, two-centre trial. *Lancet.* 2018; 391:441-450.
13. Cohen B, Bikerk A, Van der Poel S, Ombelet W. IUI: Review and systematic assessment of the evidence that supports global recommendations. *Hum Reprod Update.* 2018; 24:300-319.
14. Bensdorp AJ, Tjon-Kon-Fat RI, Bossuyt PMM, et al. Prevention of multiple pregnancies in couples with unexplained or mild male subfertility: Randomised controlled trial of in vitro fertilisation with single embryo transfer or in vitro fertilisation in modified natural cycle compared with intrauterine insemination with controlled ovarian hyperstimulation. *BMJ.* 2015; 350:g7771.
15. Younis JS. Ovarian aging and implications for fertility female health. *Minerva Endocrinol.* 2012; 37:41-57.
16. Crawford NM, Steiner AZ. Age-related infertility. *Obstet Gynecol Clin North Am.* 2015; 42:15-25.
17. Chow KM, Cheung MC, Cheung IK. Psychosocial interventions for infertile couples: A critical review. *J Clin Nurs.* 2016; 25:2101-2113.
18. Viardot-Foucault V, Tai BC, Prasath EB, Lau MSK, Chan JK, Loh SF. Younger women with ovulation disorders and unexplained infertility predict a higher success rate in superovulation (SO) intrauterine insemination (IUI). *Ann Acad Med Singap.* 2014; 43:225-231.
19. Somigliana E, Paffoni A, Busnelli A, Filippi F, Pagliardini L, Vigano P, Vercellini P. Age-related infertility and unexplained infertility: An intricate clinical dilemma. *Hum Reprod.* 2016; 31:1390-1396.
20. Land JA, Evers JLH. Risks and complications in assisted reproduction techniques: Report of an ESHRE consensus meeting. *Hum Reprod.* 2003; 18:455-457.

(Received July 17, 2018; Revised October 12, 2018;  
Accepted October 22, 2018)

## A novel compound heterozygous mutation in the *GJB2* gene is associated with non-syndromic hearing loss in a Chinese family

Haiou Jiang<sup>§,\*</sup>, Youya Niu<sup>§</sup>, Lingfeng Qu, Xueshuang Huang, Xinlong Zhu, Genyun Tang

*Department of Cellular Biology and Genetics, Hunan Provincial Key Laboratory of Dong Medicine, Hunan University of Medicine, Huaihua, China.*

### Summary

Autosomal recessive (AR) non-syndromic hearing loss (NSHL) is the most common form of hereditary deafness. Mutations in the gap junction protein beta 2 (*GJB2*) gene encoding connexin 26 (Cx26) account for about 50% of cases of ARNSHL. In the current study, a combination of exome sequencing and Sanger sequencing in a Chinese Dong family with ARNSHL allowed identification of a novel compound heterozygous mutation c.240G>C(p.Q80H)/C.109G>A(p.V37I) in exon 2 of the *GJB2* gene, which co-segregated with the disease phenotype in this family and was not evident in 100 healthy controls. Bioinformatic analysis revealed that the two mutations in the *GJB2* gene were probably pathogenic. Results indicated that the compound heterozygous variants, p.Q80H and p.V37I, in the *GJB2* gene are associated with ARNSHL. The Q80H variant was initially identified in patients of Dong Chinese origin with NSHL. The current results broaden the spectrum of *GJB2* mutations responsible for NSHL and have important implications for molecular diagnosis, treatment, and genetic counseling for this family.

**Keywords:** Exome sequencing, hearing loss, *GJB2* gene, mutation

### 1. Introduction

Hearing loss is the most frequent human sensory disorder, affecting 1 in 1,000 newborns (1). More than 50% of the cases of hearing loss are attributable to genetic causes that may be non-syndromic or syndromic (2). Non-syndromic hearing loss (NSHL) generally refers to deafness without other clinical symptoms, and accounts for 70% of inherited deafness. Approximately 80% of NSHL is autosomal recessive (AR), about 20% is autosomal dominant (AD), and less than 1% is inherited in an X chromosome-linked or a mitochondrial manner (3). To the extent known, at least 59 genes associated with ARNSHL have been identified (<http://hereditaryhearingloss.org>). For many populations, the most common cause of ARNSHL is a mutation in the gap junction protein beta 2 (*GJB2*)

gene that encodes connexin 26 (Cx26) (4-6). Cx26 is highly expressed in epithelial supporting cells of the mammalian cochlea and is believed to play an important role in the recycling of the K<sup>+</sup> ion from the hair cells to the endolymph (7-9). So far, over 100 pathogenic mutations in the *GJB2* gene have been reported (The Connexin-deafness Homepage: <http://davinci.crg.es/deafness>). The p.V37I variant is highly prevalent in East Asian deafness, but the pathogenic role of p.V37I is debated. p.V37I was previously reported to be a polymorphism without pathogenicity in some studies; nevertheless, results have increasingly revealed that a homozygous p.V37I mutation or a compound p.V37I mutation with some other *GJB2* pathogenic variation is associated with mild to moderate hearing loss (10-12).

Using conventional Sanger sequencing to identify variants causing ARNSHL is extremely time-consuming and expensive due to the condition's high level of genetic heterogeneity; in contrast, exome sequencing is a powerful and cost-effective tool with which to reveal the genetic basis of Mendelian diseases (13). The current study used a combination of exome sequencing and Sanger sequencing, and results revealed a novel compound heterozygous mutation c.240G>C(p.Q80H)/

<sup>§</sup>These authors contributed equally to this work.

\*Address correspondence to:

Dr. Haiou Jiang, Department of Cellular Biology and Genetics, Hunan University of Medicine, 492#, Jinxi South Road, Huaihua, Hunan 418000, China.  
E-mail: hhjiangh@126.com

c.109G>A(p.V37I) of the *GJB2* gene in a Chinese Dong family with ARNSHL.

## 2. Materials and Methods

### 2.1. Subjects

Subjects were a nonconsanguineous Chinese Dong family with ARNSHL from an ethnic minority region of western Hunan Province, China. Five members of the family, including three affected siblings (II:1, II:2, and II:3, Figure 1A) and two unaffected parents (I:1, I:2, Figure 1A), were included in this study. Clinical evaluations were conducted and pure tone audiometry (PTA) was performed at the First People's Hospital of Huaihua, China. Auditory function was divided into normal hearing (< 20 dBHL), mild deafness (20-40 dBHL), moderate deafness (41-70 dBHL), severe deafness (71-95 dBHL), and profound deafness (> 95 dBHL) (14). Three patients (II:1, aged 12 years; twins, II:2 and II:3, aged 8 years) had congenital hearing loss, and PTA indicated moderate bilateral sensorineural deafness (Figure 2). Audiometric data are summarized in Table 1. The parents (I:1, aged 38 years; I:2, aged 35 years) and 100 ethnicity-matched unrelated normal controls had bilateral normal hearing according to PTA. The study was approved by the Ethics Committee of Hunan University of Medicine, Huaihua, China. Written informed consent were obtained from all participants or guardians in accordance with the principles of the

Declaration of Helsinki.

### 2.2. Exome sequencing

A genomic extraction kit (Tiangen Biotech Co. Ltd, Beijing, China) was used to isolate genomic DNA from leukocytes in peripheral venous blood from all participants. The proband (II:1) in the family was subjected exome sequencing. According to the manufacturer's protocol, no less than 1.5 µg of genomic DNA was used to construct the exome library. Genomic DNA of the proband was fragmented using Covaris sonication, and the DNA library was pooled and hybridized for enrichment of exons using Agilent SureSelect Human All Exon V5. Enriched exome fragments were sequenced on the HiSeq 2000 platform. A mean sequencing depth of 128.16× was obtained to

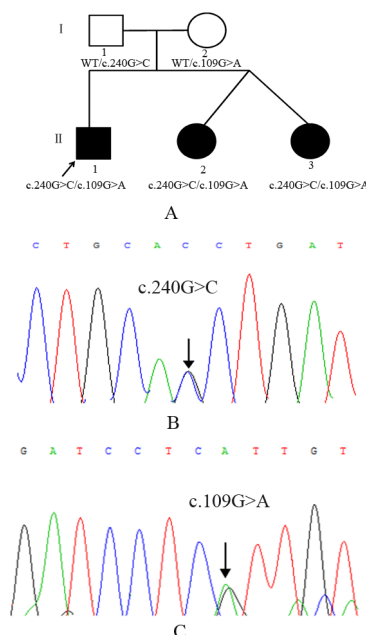


**Figure 1. Pedigree and mutation analysis.** (A) A Dong family with ARNSHL. The black arrow indicates the proband (II:1) of the family, and the filled symbols represent affected members. The patients (II:1, II:2, II:3) have compound heterozygote mutations in the *GJB2* gene. (B) A heterozygous *GJB2* c.240G>C mutation of the proband. (C) A heterozygous *GJB2* c.109G>A mutation of the proband.

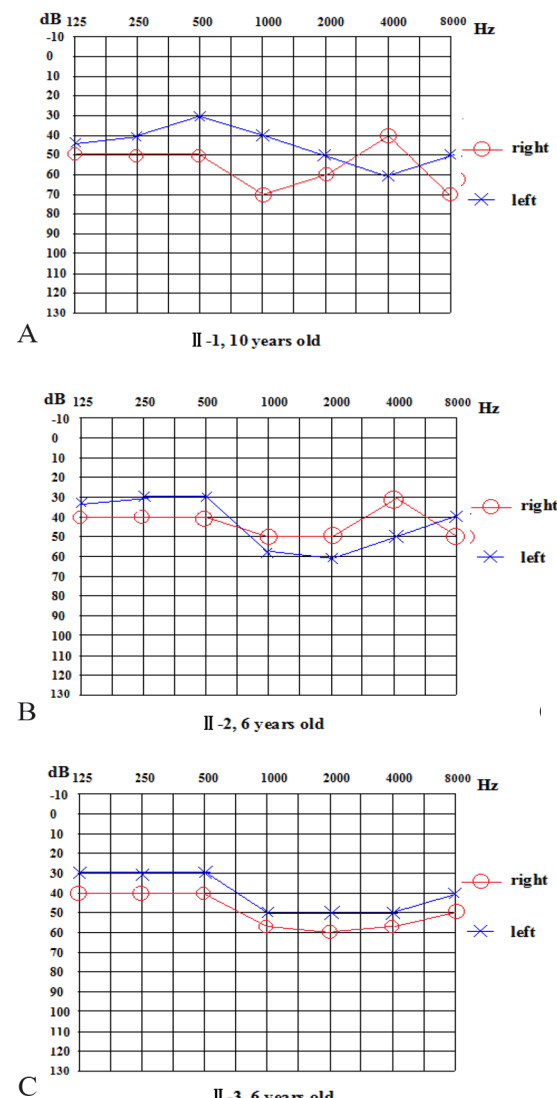


**Figure 2. Pure tone audiograms of three affected family members.** Hearing thresholds are the hearing level in decibels. The patients display moderate bilateral deafness. The patient age at diagnosis is indicated at the bottom of the audiogram. The "o" and "x" symbols represent air conduction pure-tone thresholds at different frequencies in the right and left ear. dB, decibels; Hz, Hertz.

**Table 1. Characterization of the audiometric data for three affected family members**

Individual	Gender	Current age	Newborn hearing screening	Age of onset	Age at initial visit	Age at audiometric testing	Degree of hearing loss	Other symptoms
II1	M	12	moderate	birth	10	10	moderate	N
II2	F	8	moderate	birth	6	6	moderate	N
II3	F	8	moderate	birth	6	6	moderate	N

F, female; M, male; N, without other symptoms

accurately determine variants at 99.20% of the targeted exome.

The sequence reads were aligned to a human genome reference obtained from the UCSC database version hg19 (<http://genome.ucsc.edu>) using the Burrows-Wheeler Alignment tool. SAMtools was used to detect single nucleotide polymorphisms (SNPs) and insertions/deletions, and Picard was used to delete duplicate reads (produced mainly during PCR). Possible variants were filtered against databases including SNP database version 137 (dbSNP137), 1000 Genomes data (April 2012 version), HapMap8, the YanHuang1 (YH1) project, and synonymous mutations. For bioinformatic analysis, four in-silico tools were used to predict potential deleterious effects of missense mutations, including PolyPhen-2 (<http://genetics.bwh.harvard.edu/pph2/>), SIFT (<http://sift.jcvi.org>), Mutation Taster (<http://www.mutationtaster.org/>) and the American College of Medical Genetics and Genomics (ACMG). The software ANNOVAR (Annotate Variation) was used to annotate possible variants. In order to confirm the conservation of amino acid substitutions during species evolution, typical protein sequences from multiple species were aligned using the online tool Clustal W to compare mutation sites with conserved domains.

### 2.3. Verification with Sanger sequencing

After exome sequencing, Sanger sequencing was used to verify genetic defects. Sequences of primers for potential causative mutations in the *GJB2* gene (NM\_004004.5) were designed and synthesized as follows: 5'-ACACGTTCAAGAGGGTTGG-3' and 5'-GGGAAATGCTAGCGACTGAG-3'. The size of the PCR product was 1,003 bp, and the product contained the coding sequence of the *GJB2* gene. PCR was performed with 30-μL reaction mixtures containing 40 ng of genomic DNA, 1.0 μM of the forward and reverse primers, and 15 μL of 2X Taq Master Mix (Huiling Biotech Co. Ltd, Shanghai, China). Thermocycling was performed using the following program: initial denaturation at 95°C for 2 min, followed by 35 cycles of 94°C for 10 s, 60°C for 30 s, and 72°C for 1 min, and final extension at 72°C for 5 min. PCR products were purified with the Cycle-Pure Kit (OMEGA; Bio-Tek, Doraville, GA) and sequenced using an ABI PRISM 3730 automated sequencer (Applied Biosystems). Co-

segregation analysis was subsequently performed with available DNA samples from family members. A mutation was considered to be novel if it was not in the National Center for Biotechnology Information dbSNP database (<http://www.ncbi.nlm.nih.gov/projects/SNP/index.html>), the Human Mutation Database (HGMD) (<http://www.hgmd.cf.ac.uk/ac>), or the Exome Variant Server (<http://evs.gs.washington.edu>) and had not been published.

### 2.4. Structure-based model building and analysis

Human wild-type and mutant proteins were modeled using SWISS-MODEL online (<https://swissmodel.expasy.org>), and PyMOL Viewer was used to visualize the effects of mutated residues on the structure of proteins.

## 3. Results

### 3.1. Exome sequencing

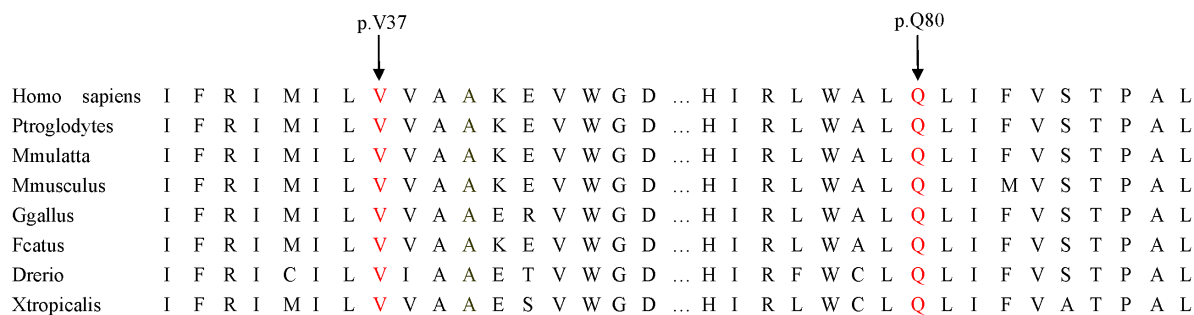
The proband generated 60,456,963 raw reads with a mean read length of 150 bp according to exome sequencing; 98.14% (59332463) of these raw reads were aligned to the human reference genome. Synonymous variants and known common variants described in dbSNP137, 1000 Genomes data, HapMap8, and the YH1 project were excluded. Non-synonymous variants were predicted using SIFT, PolyPhen-2, and Mutation Taster to eliminate benign variants or tolerated variants. In the known genes for hearing loss, a novel compound heterozygous mutation, c.240G>C(p.Q80H) /c.109G>A(p.V37I), in the *GJB2* gene was identified in the proband.

### 3.2. Identification of causative mutations

The compound heterozygous variants c.240G>C(p.Q80H) and c.109G>A(p.V37I) in the *GJB2* gene (Figure 1B and 1C) were found in all three affected family members according to Sanger sequencing, and the heterozygous variants c.240G>C(p.Q80H) and c.109G>A(p.V37I) were found in the unaffected father and mother, respectively, but were absent in the 100 ethnically matched normal controls. The compound heterozygous variants in the *GJB2* gene co-segregated with the ARNSHL phenotype in this family, suggesting

**Table 2. Prediction of the functionality of compound heterozygous mutations**

Variants	AA change	PolyPhen2	SIFT	Mutation Taster	ACMG
c.240G>C	p.Q80H	Probably damaging (1.00)	Damaging (0.00)	Disease-causing	Likely pathogenic
c.109G>A	p.V37I	Probably damaging (1.00)	Tolerated (0.66)	Disease-causing	Pathogenic

**Figure 3. A multiple-sequence alignment of the amino acid sequence in Cx26 from different species.** Results indicate that both V37 and Q80 in Cx26 protein are highly conserved among many species.

that the c.240G>C(p.Q80H) and c.109G>A(p.V37I) variants were likely responsible for ARNSHL in this family.

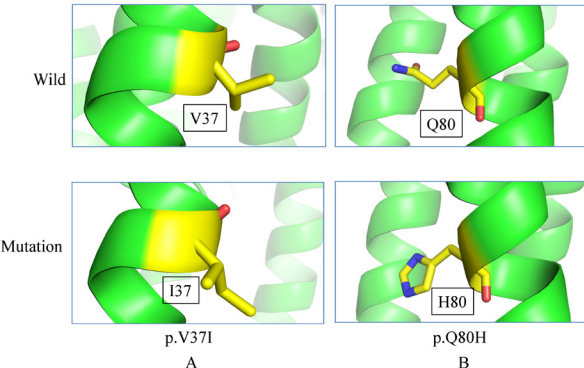
The p.Q80H variant of the *GJB2* gene was predicted to be probably damaging according to PolyPhen-2, SIFT, MutationTaster, and ACMG (Table 2), and this mutation was novel since it had not been previously reported nor was it present in dbSNP, HGMD, or Exome Variant Server. The p.V37I variant in the *GJB2* gene was predicted to affect the features of the protein and it was predicted to be disease-causing according to MutationTaster, PolyPhen-2, and ACMG (Table 2). Both p.Q80 and p.V37 in Cx26 were highly conserved amino acid residues among different species (Figure 3), indicating their importance structurally and functionally.

### 3.3. Structural modeling

A 3D model was constructed for structural analysis of WT/Mut Cx26 proteins to determine the pathogenicity of mutant Cx26 according to SWISS-MODEL. When amino acid 37 is changed to isoleucine, the side chains of Cx26 also change as a result and tend to be longer than those of a structure in which amino acid 37 is valine (Figure 4A). The variant H80 protein has a different side chain than the wild-type protein as a result of a heterocyclic histidine being substituted for an aliphatic glutamine (Figure 4B). Therefore, the compound heterozygous mutations are predicted to affect the amino acid side chain. This might disrupt Cx26 function and interactions with other molecules and residues.

## 4. Discussion

The novel compound heterozygous mutations

**Figure 4. Protein molecular models of wild types and GJB2 mutations.** (A) The mutated I37 protein has a longer side chain than the wild-type V37 protein. (B) The mutated H80 protein has a different side chain than the wild-type Q80 protein.

c.240G>C(p.Q80H) and c.109G>A(p.V37I) in the *GJB2* gene were likely responsible for ARNSHL in a Chinese family because the variants co-segregated with the disease phenotype in this family and because these variants were predicted to be disease-causing mutations. Moreover, the current study indicated that the compound mutations may give rise to the moderate hearing loss present in this family.

*GJB2* mutations were first identified in three consanguineous pedigrees from Pakistan with ARNSHL in 1997 (8). Following dominant or recessive deafness, mutations in *GJB2* are considered to be the most common cause of nonsyndromic deafness (14,15). Over 50% of cases of ARNSHL are associated with *GJB2* mutations (3). The *GJB2* gene encodes the gap-junction protein Cx26, which is highly expressed in the cochlear cells (16). The sequences of Cx26 are extremely conserved with four transmembrane domains (TM1-4), two extra-cellular loops (E1 and E2), a cytoplasmic

loop (CL), and the N- and C-terminal cytoplasmic ends (17). Cx26 belongs to a large family of proteins that constitute intercellular channels and that contribute to the rapid exchange of small molecules between adjacent cells (18,19). Cx26 is essential for auditory transduction by recycling endolymphatic potassium ions and also for cell survival within the cochlea. Cx26-deficient mice have marked hearing impairment and cell death in the cochlea (20).

*GJB2* mutations may affect the function of the Cx26 protein in various ways and may depend on the position and type of amino acid substituted. Previous studies suggested that hemichannels (hexamers) played an important role in the smooth functioning of ion channels in the WT-Cx26 protein. The novel c.240G>C mutation in the *GJB2* gene led to a positively charged histidine (His) being substituted for an uncharged glutamine (Gln) at amino acid 80 (p.Q80H), which is located in the TM2 segment of Cx26 protein. Therefore, the rare mutation may generate a functional null protein by disrupting the normal formation of hexamers (21). Three missense mutations (Q80K, Q80P and Q80R) and one nonsense mutation (Q80X) at the same position (The Connexin-deafness Homepage: <http://davinci.crg.es/deafness>) were reported to be responsible for hearing loss. For example, the variants c.238C>A (Q80K) and 35delG were identified as compound heterozygous mutations in a patient with severe hearing loss (22). In the current study, the novel p.Q80H variant of the *GJB2* gene was predicted to be deleterious according to SIFT, PolyPhen-2, MutationTaster, and ACMG. The c.109G>A variant, resulting in substitution of isoleucine for valine at position 37 (p.V37I), was initially reported as a polymorphic change in one study (23). However, greater awareness of *GJB2* has led to several studies describing p.V37I as a variant causing diverse hearing phenotypes, ranging from severe-to-profound hearing loss to normal hearing and from congenital onset to delayed-onset (24-28). In contrast, the homozygous p.V37I variant and the compound p.V37I variant with some other *GJB2* disease-causing mutation are rare (25). A study by Huang *et al.* (28) indicated that the p.V37I variant of the *GJB2* gene is mainly associated with mild or moderate hearing impairment in the Chinese population. The *GJB2* p.V37I variant was also predicted to be a pathogenic mutation according to PolyPhen-2, MutationTaster, and ACMG. Both the p.V37I and p.Q80H variants of the *GJB2* gene, located in the TM1 and TM2 domains, respectively, might interfere with the interaction of transmembrane regions or the proper folding and/or oligomerization of connexins or they might generate defective channels and thus cause hearing loss (17). In addition, both p.Q80 and p.V37 in Cx26 are highly conserved throughout all members of the connexin family, indicating their importance structurally and functionally.

In summary, the current results indicated that novel

compound heterozygous variants (p.Q80H and p.V37I) in the *GJB2* gene were associated with congenital moderate hearing loss in a Chinese family. The p.Q80H variant was initially identified in patients of Dong Chinese origin with ARNSHL. The current study further supports the hypothesis that the p.V37I variant is devoid of functional activity and causes hearing loss (29). Exome sequencing is a rapid, exact, and cost-effective method with which to identify genes causing hearing impairment. The current findings broaden the spectrum of *GJB2* mutations associated with NSHL and may also shed new light on genetic counseling for individuals with hearing loss.

### Acknowledgements

This study was supported by a grant from the Natural Science Foundation of Hunan Province, China (no. 2018JJ2278). The authors wish to sincerely thank the patients and their family members for their participation in this study.

### References

1. Morton NE. Genetic epidemiology of hearing impairment. Ann N Y Acad Sci. 1991; 630:16-31.
2. Marazita ML, Ploughman LM, Rawlings B, Remington E, Arnos KS, Nance WE. Genetic epidemiological studies of early-onset deafness in the U.S. school-age population. Am J Med Genet. 1993; 46:486-491.
3. Hilgert N, Smith RJ, Van Camp G. Forty-six genes causing non-syndromic hearing impairment: Which ones should be analyzed in DNA diagnostics? Mutat Res. 2009; 681:189-196.
4. Estivill X, Fortina P, Surrey S, Rabionet R, Melchionda S, D'Agruma L, Mansfield E, Rappaport E, Govea N, Milà M, Zelante L, Gasparini P. Connexin-26 mutations in sporadic and inherited sensorineural deafness. Lancet. 1998; 351:394-398.
5. Gabriel H, Kupsch P, Sudendey J, Winterhager E, Jahnke K, Lautermann J. Mutations in the connexin26/*GJB2* gene are the most common event in non-syndromic hearing loss among the German population. Hum Mutat. 2001; 17:521-522.
6. Yuan Y, You Y, Huang D, Cui J, Wang Y, Wang Q, Yu F, Kang D, Yuan H, Han D, Dai P. Comprehensive molecular etiology analysis of nonsyndromic hearing impairment from typical areas in China. J Transl Med. 2009; 7:79.
7. Kikuchi T, Kimura RS, Paul DL, Adams JC. Gap junctions in the rat cochlea: Immunohistochemical and ultrastructural analysis. Anat Embryol. 1995; 191:101-118.
8. Kelsell DP, Dunlop J, Stevens HP, Lench NJ, Liang JN, Parry G, Mueller RF, Leigh IM. Connexin 26 mutations in hereditary non-syndromic sensorineural deafness. Nature. 1997; 387:80-83.
9. Chang EH, Van Camp G, Smith RJ. The role of connexins in human disease. Ear Hear. 2003; 24:314-323.
10. Li L, Lu J, Tao Z, Huang Q, Chai Y, Li X, Huang Z, Li Y, Xiang M, Yang J, Yao G, Wang Y, Yang T, Wu

- H. The p.V37I exclusive genotype of *GJB2*: A genetic risk-indicator of postnatal permanent childhood hearing impairment. *PLoS One*. 2012; 7:e36621.
11. Snoeckx RL, Huygen PL, Feldmann D, et al. *GJB2* mutations and degree of hearing loss: A multicenter study. *Am J Hum Genet*. 2005; 77:945-957.
  12. Dahl HH, Tobin SE, Poulakis Z, Rickards FW, Xu X, Gillam L, Williams J, Saunders K, Cone-Wesson B, Wake M. The contribution of *GJB2* mutations to slight or mild hearing loss in Australian elementary school children. *J Med Genet*. 2006; 43:850-855.
  13. Xia H, Xu HB, Deng X, Yuan L, Xiong W, Yang Z, Deng H. Compound heterozygous *GJB2* mutations associated to a consanguineous Han family with autosomal recessive non-syndromic hearing loss. *Acta Otolaryngol*. 2016; 136:782-785.
  14. Bae SH, Baek JI, Lee JD, Song MH, Kwon TJ, Oh SK, Jeong JY, Choi JY, Lee KY, Kim UK. Genetic analysis of auditory neuropathy spectrum disorder in the Korean population. *Gene*. 2013; 522:65-69.
  15. Chan DK, Chang KW. *GJB2*-associated hearing loss: Systematic review of worldwide prevalence, genotype, and auditory phenotype. *Laryngoscope*. 2014; 124:E34-E53.
  16. Morle L, Bozon M, Alloisio N, Latour P, Vandenberghe A, Plauchu H, Collet L, Edery P, Godet J, Lina-Granade G. A novel C202F mutation in the connexin 26 gene (*GJB2*) associated with autosomal dominant isolated hearing loss. *J Med Genet*. 2000; 37:368-370.
  17. Maeda S, Nakagawa S, Suga M, Yamashita E, Oshima A, Fujiyoshi Y, Tsukihara T. Structure of the connexin 26 gap junction channel at 3.5 Å resolution. *Nature*. 2009; 458:597-602.
  18. Bruzzone R, White TW, Paul DL. Connections with connexins: The molecular basis of direct intercellular signaling. *Eur J Biochem*. 1996; 238:1-27.
  19. Kumar NM, Gilula NB. The gap junction communication channel. *Cell*. 1996; 84:381-388.
  20. Cohen-Salmon M, Ott T, Michel V, Hardelin JP, Perfettini I, Eybalin M, Wu T, Marcus DC, Wangemann P, Willecke K, Petit C. Targeted ablation of connexin 26 in the inner ear epithelial gap junction network causes hearing impairment and cell death. *Curr Biol*. 2002; 12:1106-1111.
  21. Wei Q, Liu Y, Wang S, Liu T, Lu Y, Xing G, Cao X. A novel compound heterozygous mutation in the *GJB2* gene causing non-syndromic hearing loss in a family. *Int J Mol Med*. 2014; 33:310-316.
  22. Kalay E, Caylan R, Kremer H, de Brouwer AP, Karaguzel A. *GJB2* mutations in Turkish patients with ARNSHL: Prevalence and two novel mutations. *Hear Res*. 2005; 203:88-93.
  23. Kelley PM, Harris DJ, Comer BC, Askew JW, Fowler T, Smith SD, Kimberling WJ. Novel mutations in the connexin 26 gene (*GJB2*) that cause autosomal recessive (DFNB1) hearing loss. *Am J Hum Genetic*. 1998; 62:792-799.
  24. Kim SY, Park G, Han KH, Kim A, Koo JW, Chang SO, Oh SH, Park WY, Choi BY. Prevalence of p.V37I variant of *GJB2* in mild or moderate hearing loss in a pediatric population and the interpretation of its pathogenicity. *PLoS One*. 2013; 8:e61592.
  25. Dai P, Yu F, Han B, et al. *GJB2* mutation spectrum in 2,063 Chinese patients with nonsyndromic hearing impairment. *J Transl Med*. 2009; 7:26.
  26. Dahl HH, Tobin SE, Poulakis Z, Rickards FW, Xu X, Gillam L, Williams J, Saunders K, Cone-Wesson B, Wake M. The contribution of *GJB2* mutations to slight or mild hearing loss in Australian elementary school children. *J Med Genet*. 2006; 43:850-855.
  27. Chai Y, Chen D, Sun L, Li L, Chen Y, Pang X, Zhang L, Wu H, Yang T. The homozygous p.V37I variant of *GJB2* is associated with diverse hearing phenotypes. *Clin Genet*. 2014; 87:350-355.
  28. Huang Y, Yang XL, Chen WX, Duan B, Lu P, Wang Y, Xu ZM. Prevalence of p.V37I variant of *GJB2* among Chinese infants with mild or moderate hearing loss. *Int J Clin Exp Med*. 2015; 8:21674-21678.
  29. Bruzzone R, Veronesi V, Gomes D, Bicego M, Duval N, Marlin S, Petit C, D'Andrea P, White TW. Loss-of-function and residual channel activity of connexin 26 mutations associated with non-syndromic deafness. *FEBS Lett*. 2003; 533:79-88.

(Received July 7, 2018; Revised August 19, 2018;  
Accepted October 7, 2018)

# Impact of three-dimensional visualization technology on surgical strategies in complex hepatic cancer

Dong Zhao<sup>1,2</sup>, Wan Yee Lau<sup>3,\*</sup>, Weiping Zhou<sup>4</sup>, Jian Yang<sup>1,2</sup>, Nan Xiang<sup>1,2</sup>, Ning Zeng<sup>1,2</sup>, Jun Liu<sup>1,2</sup>, Wen Zhu<sup>1,2</sup>, Chihua Fang<sup>1,2,\*</sup>

<sup>1</sup> Department of Hepatobiliary Surgery, Zhujiang Hospital, Southern Medical University, Guangzhou, China;

<sup>2</sup> Guangdong Provincial Clinical and Engineering Center of Digital Medicine, Guangzhou, China;

<sup>3</sup> Faculty of Medicine, the Chinese University of Hong Kong, Shatin, New Territories, Hong Kong SAR, China;

<sup>4</sup> The Third Department of Hepatic Surgery, Eastern Hepatobiliary Surgery Hospital, Second Military Medical University, Shanghai, China.

## Summary

Surgical resection is still the mainstay of treatment for primary liver cancer (PLC). It is unclear whether three-dimensional visualization (3DV) preoperative evaluation and simulated liver resection would affect the surgical strategies and improve the R0 resection rates of patients with complex PLC when compared with the 2D evaluation using computed tomography or magnetic resonance imaging. In the study, patients with complex PLC who were subjected to laparotomy underwent both 2D and 3DV evaluation before operation. A comparison between the 2D and 3DV evaluation was compared with the gold standard of laparotomy findings. In this study, of 335 patients with complex PLC, 71 were assessed to have resectable tumors. 2D and 3DV assessments determined 63 and 71 patients to have resectable PLC, respectively. At laparotomy 69 of the 71 patients were found to have resectable PLC, but 2 patients were found to be unresectable because of detection of metastatic lesions on laparotomy, which were not detected either by 2D or 3DV preoperative evaluation. The accuracy, false positive and false negative rates of the 2D and the 3DV preoperative assessments in determining tumor resectability were 85.9%, 2.8%, 11.3%, and 97.2% ( $p < 0.05$ ), 2.8%, 0%, respectively. The 3DV and 2D preoperative evaluation revealed 17 and 13 patients with vascular anomalies, respectively. There were 4 patients with major vascular anomalies not detected by 2D evaluation, whose surgical strategies were modified by 3DV evaluation. These results suggested 3DV preoperative assessment could lead to better in evaluating tumor resectability, with potential benefit in the modification of surgical strategy for patients with complex PLC.

**Keywords:** Three-dimensional visualization, complex hepatic cancer, surgical strategy, vascular anomaly

## 1. Introduction

Primary liver cancer (PLC) poses a serious threat to global health (1-3). Partial hepatectomy is still

considered as the curative treatment of choice for PLC in many centers (4). PLC which is close to, or even has invaded the bifurcation of the main portal vein or the hepatico-caval junction, or is centrally located (in liver segments 4, 5, 8) which is associated with major intrahepatic vascular anomalies is defined as complex PLC in this study. It is difficult to treat these lesions with resectional surgery and there is a high inherent risk of postoperative complications (5,6). Accurate preoperative assessment is important for safe surgery in these patients.

The conventional preoperation assessment of tumor resectability is conventionally based on two-

\*Address correspondence to:

Dr. Chihua Fang, Department of Hepatobiliary Surgery, Zhujiang Hospital, Southern Medical University, Guangzhou 510280, China.

E-mail: fangch\_dr@163.com

Dr. Wan Yee Lau, Faculty of Medicine, the Chinese University of Hong Kong, Shatin, New Territories, Hong Kong SAR, China.

E-mail: josephlau@cuhk.edu.hk

dimensional (2D) medical imagings using ultrasound, computed tomography (CT) and magnetic resonance imaging (MRI). These imaging techniques pose difficulty in accurately assessing and planning liver resectional surgery in borderline resectable liver tumors which are commonly found in complex liver tumors (7-9). Three-dimensional visualization (3DV) technology emerged more than 10 years ago, providing an alternative technique for diagnosis and surgical planning of PLC. A number of international groups have successfully developed 3DV technology and applied it in hepatobiliary and pancreatic operations (10-13). A recent report from Japan underlined the practicality of virtual hepatectomy, based on 3D image reconstruction, for surgical planning and performance of living donor liver transplantation and hepatectomy for hepatocellular carcinoma and colorectal liver metastases (14). Our group has also developed a new 3DV abdominal imaging system (software copyright No. 2008SR18798). This system has been used in the preoperative planning for hepatocellular carcinoma (7), intrahepatic calculi (15) and hilar cholangiocarcinoma (16). The present study aimed to discuss the difference between the 3DV and 2D preoperative evaluation and the possible impact of 3DV technology on the surgical strategy for complex PLC.

## 2. Patients and Methods

### 2.1. Study Design

Of 441 patients with complex PLC treated at the Department of Hepatobiliary Surgery of Zhujiang Hospital, Southern Medical University, from January 2008 to January 2017, 335 patients were included in this study. According to the different surgical strategies, patients who underwent laparotomy were selected in the study. The inclusion criteria were *i*) PLC which included hepatocellular carcinoma, intrahepatic cholangiocarcinoma and hepatoblastoma; *ii*) complex liver tumor; *iii*) PLC > 3.0 cm, and any PLC which was not considered to be suitable for radiofrequency ablation in our center; *iv*) no extra-hepatic metastasis; and *v*) preoperative liver function of Child-Pugh Class A or B. The exclusion criteria were: *i*) benign liver tumors; *ii*) metastatic liver cancer; and *iii*) concurrent or history of other malignant tumors.

This study was approved by the Ethics Committee of Zhujiang Hospital, Southern Medical University (No. 2012-GDYK-001).

### 2.2. Preoperative evaluation

#### 2.2.1. Routine investigations

The routine investigations included abdominal CT, complete blood count, liver and renal function tests,

coagulation profile, and tumor markers (AFP, CA 19.9, CEA and CA 125). Magnetic resonance imaging was also carried out in some patients.

#### 2.2.2. 2D preoperative evaluation

For all the patients with a complex hepatic cancer, a 2D preoperative evaluation was performed by a team of hepatic surgeons using patients' clinical data and conventional CT/MRI scan images. A resection line was drawn according to the anatomic marks, such as the hepatic veins, portal veins and gallbladder fossa. The volume of the residual functional liver was calculated manually.

#### 2.2.3. 3D preoperative evaluation

The same team of liver surgeons also went on to do the 3DV reconstruction. 3DV reconstruction: The enhanced thin-slice CT data were collected using a Philips Brilliance 64-multislice spiral CT scanner. The setting of scanning parameters: conventional supine position was chosen for plain scan from head to foot. The range was from the top of diaphragm to the inferior margin of the liver. The scanning condition was 120 kV and 250 mAs. The detector combinations were  $0.625 \times 64$ , the slice thickness was 5mm, the interval was 5mm and the screw pitch was 0.984. The time for one revolution of bulb tube was 0.5 s. The delayed scan of arterial phase was 20-25 s and the delayed scan of portal phase was 50-55 s. These image data were put into CT postprocessing workstation after the scan. Then the CT data were transferred to the 3DV software for 3D reconstruction: *i*) for organ reconstruction; the region-growing method (17) was used to perform a 3D reconstruction of the liver, tumor, pancreas and spleen; *ii*) for vascular reconstruction: the segmentation based on threshold method (18) was used to perform a 3D reconstruction of the portal vein, hepatic artery and hepatic vein. The anatomy and variations of the portal vein, hepatic artery and hepatic vein were classified using Cheng's Standard (19), Michel's Standard (20), and Nakamura's Standard (21), respectively.

Simulated Surgery: Using the information obtained from the 3D reconstruction, which included tumor size, tumor location, proximity and relation of the tumor to its surrounding major blood vessels, and in line with the principle of R0 resection with preservation of adequate non-tumorous liver parenchyma in a cirrhotic patient, the residual liver functional ratio should be greater than 40% (22). After segmentation of the 3DV liver model and simulated surgery were performed using the built-in software, the volumes of the entire liver, tumor, resected liver and residual functional liver were calculated.

### 2.3. Choice of surgical strategy

Patients with complex PLC accepted the operation

according to the comprehensive preoperative assessment and agreement of Multidisciplinary Treatment group of Zhuijiang Hospital. Preoperative assessment included complete blood count, liver and renal function tests, coagulation profile and tumor markers (AFP, CA 19.9, CEA and CA 125). Information of tumor location, size and number obtained from CT or MRI was also important to preoperative assessment. A surgical strategy and a surgical plan were made by the team, based on whether a R0 resection could be carried out safely. The volume of the residual functional liver was calculated and the surgical strategy decision was recorded.

#### 2.4. Statistics

Continuous data were expressed as median and range while categorical data were expressed as numerical numbers or as ratios. Continuous data were evaluated using the Mann-Whitney *U* test, and the categorized data were compared using the Chi square test. All statistical tests were 2-sided. A *p* < 0.05 was considered to be statistically significant. The statistical analysis was performed using SPSS software (version 21.0; SPSS, Chicago, IL).

### 3. Results

#### 3.1. Clinical characteristics of patients who underwent laparotomy

After comprehensive preoperative evaluation, 71 patients underwent laparotomy, and 65 (91.5%) patients were male. Of the 71 patients, 65 (91.5%) patients had hepatitis and 58 (81.7%) patients had liver cirrhosis. The preoperative liver functional status was Child-Pugh grade A (65 patients, 91.5%) and grade B (6 patients, 8.5%). The median size of liver tumors was 8.1cm (range from 4.0 to 17.3 cm). There were 54 (76.1%) patients with a single tumor, while 17 (23.9%) patients had multiple tumors. The pathological results showed 67 patients (94.4%) had hepatocellular carcinoma, 3 patients (3, 4.2%) had intrahepatic cholangiocarcinoma, and 1 patient (1.4%) had hepatoblastoma. Of the 71 patients, 17 patients (23.9%) had vascular anomalies (Table 1).

Two patients were found to have unresectable tumors on laparotomy, as the metastatic lesions were not detected on preoperative CT or MRI. The other 69 patients underwent the following operations successfully: right hemihepatectomy (*n* = 17, 24.6%), resection of segments 6 and 7 + part of segments 5 and 8 (*n* = 9, 13.0%), right hemihepatectomy + resection of segment 1 (*n* = 1, 1.5%), right hemihepatectomy+ partial resection of segment 4 (*n* = 1, 1.5%), resection of segments 4, 5 and 8 (*n* = 2, 2.9%), resection of segments 5, 6 and 7 (*n* = 5, 7.2%), resection of

**Table 1. Clinical characteristics of 71 patients with resectable complex hepatic cancer**

Items	<i>n</i> or median (range)
Age, yrs	44 (13-74)
Sex (Male/Female)	65/6
Hepatitis status	
Hepatitis B	60
Hepatitis C	2
Hepatitis B+C	2
Hepatitis E	1
Negative	6
Cirrhosis	58
Liver functional status	
Child-Pugh Grade A	65
Child-Pugh Grade B	6
AFP > 400 (μg/L, <i>n</i> )	26
AFP < 400 (μg/L, <i>n</i> )	45
HBV-DNA < 500 (copy/mL)	16
HBV-DNA > 500 (copy/mL)	46
Tumor size (cm) <sup>†</sup>	8.1 (4.0-17.3)
Tumor number	
Single	54
Multiple	17
Pathology	
HCC	67
ICC	3
Hepatoblastoma	1
Vascular variation	
PV	6
HA	5
HV	1
PV +HA	3
PV +HA+HV	2

AFP, alpha fetal protein; HA, hepatic artery; HBV, hepatitis B virus; HCC, hepatocellular carcinoma; HV, hepatic vein; ICC, intrahepatic cholangiocarcinoma; PV, portal vein. <sup>†</sup>Tumor size was determined by CT imaging and defined as the largest diameter (in single tumor) and the sum of the largest diameters (in multiple tumors).

segments 5 and 6 (*n* = 4, 5.8%), resection of segments 6 and 7 (*n* = 8, 11.6%), resection of segments 5 and 8 (*n* = 3, 4.4%), resection of segments 6 and 8 (*n* = 1, 1.5%), resection of segments 7 and 8 (*n* = 3, 4.4%), resection of segments 4 and 7 (*n* = 1, 1.5%), resection of segments 2, 3 and 4 (*n* = 4, 5.8%), resection of segments 2, 3, 4, 5 and 8 (*n* = 1, 1.5%), resection of segments 2, 3, 4 and 8 (*n* = 2, 2.9%), resection of segments 2, 3 and 8 (*n* = 1, 1.5%), resection of segments 2 and 5 (*n* = 1, 1.5%), resection of segment 5 (*n* = 1, 1.5%), resection of segment 7 (*n* = 2 cases, 2.9%) and resection of segment 8 (*n* = 2, 2.9%).

#### 3.2. Comparison of preoperative evaluation and the actual surgery in tumor resectability

Of the 71 patients, 2D preoperative evaluation predicted 63 patients to have resectable and 8 patients to have unresectable tumors. The corresponding numbers predicted by 3DV preoperative evaluation were 71 and 0. At the operation, 69 patients underwent R0 resection but 2 patients were found to have unresectable lesions because of detection of metastatic lesions on laparotomy which were not detected either by 2D preoperative

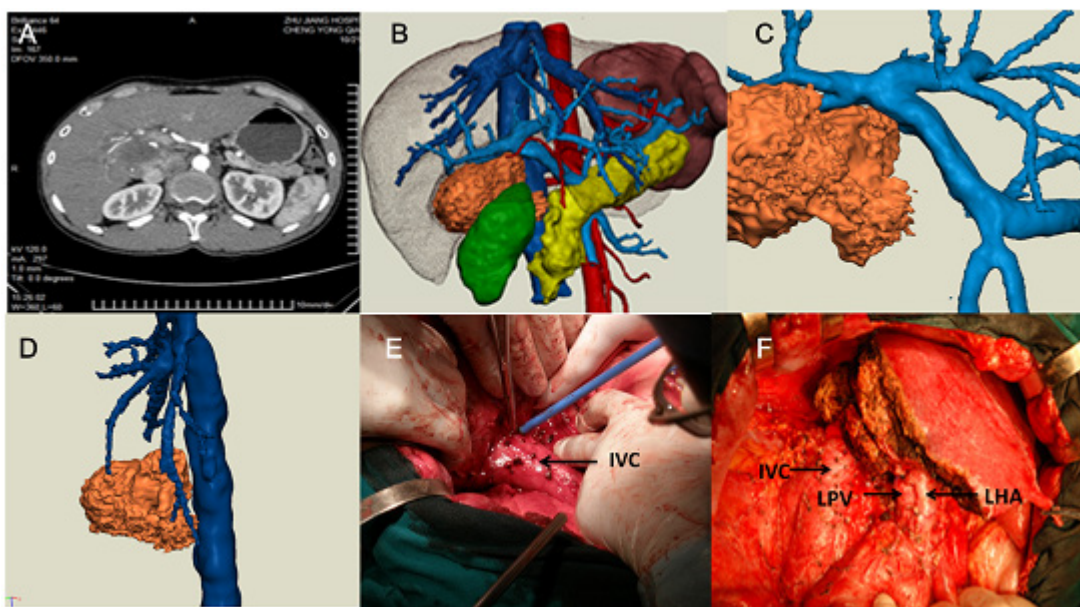


**Figure 1.** A 38-year-old man of HCC with a tumor located in segment 1. (A) CT showed that the tumor had probably invaded the portal vein (PV) and inferior vena cava. TACE was recommended. (B, C, D) 3D reconstruction demonstrated the spatial relationship between the tumor and surrounding tissues, such as the portal vein and inferior vena cava (IVC), without invasion of the PV and IVC. Surgical treatment was recommended as the treatment of choice. (E, F) Right hemihepatectomy and segment 1 resection were successfully performed. (LHA, left hepatic artery; LPV, left portal vein; TACE, transcatheter arterial chemoembolization.)

evaluation or 3DV preoperative evaluation.

Using the intraoperative findings as the gold standard, the accuracy, false positive and false negative rates of the 2D and 3DV preoperative evaluations for tumor resectability were 61/71 (85.9%), 2/71 (2.8%), 8/71 (11.3%), and 69/71 (97.2%), 2/71 (2.8%), 0/71 (0%), respectively. Comparing the 3DV preoperative evaluation with 2D evaluation, there was a significant difference in the accuracy rate (97.2% vs. 85.9%,  $p = 0.016$ ) and the false negative rate (0% versus 11.3%,  $p < 0.001$ ). These results suggested significantly better prediction of the 3DV preoperative assessment in evaluating tumor resectability.

Eight patients who were predicted by 2D preoperative evaluation to have unresectable lesions due to tumor involvement of major vessels were determined to have resectable lesions on 3DV evaluation (Table 2, Figure 1). Of the 63 patients who were predicted by 2D preoperative evaluation to have resectable lesions, 13 cirrhotic patients were preoperatively assessed with future liver remnants to be less than 40% with a high chance of developing postoperative liver failure. After 3DV preoperative evaluation and simulation surgery, the surgical strategy was modified to a lesser extent of anatomical liver resection. These patients did not develop any postoperative liver failure (Table 3). Besides, in 2 patients, the extents of anatomical resection were extended from 2D preoperative evaluation to 3DV preoperative evaluation to allow for a R0 resection with an adequate resection margin. Two operations changed from segments 5 and 7 to resection of segments 5, 6 and 7; and right hemihepatectomy to right hemihepatectomy + segment 4, respectively.

### 3.3. Preoperative evaluation of vascular anomalies and choice of surgical strategy

In the study, 3DV preoperative evaluation revealed 17 patients with vascular anomalies including the portal vein, hepatic artery or hepatic veins, while 2D preoperative evaluation detected 13 patients with vascular anomalies. There were 4 patients with major vascular anomalies who were not detected by 2D evaluation before operation. Figure 2 illustrates a patient with a 13.2 cm complex PLC in liver segments 5, 6, 7, 8 in a cirrhotic patient. The segment 4 portal vein arose from the right anterior sectional portal vein. 2D preoperative evaluation failed to identify this portal vein anomaly and right hemihepatectomy was planned. The future liver remnant was estimated to be 40.8%. Subsequent 3DV preoperative evaluation identified the portal vein anomaly. If right hemihepatectomy were to be carried out, the portal blood supply to segment 4 would have been damaged. Portal ischemia to segment 4 would decrease the actual future liver remnant to 21.4% and the chance of developing postoperative liver failure would be high. The subsequent surgical strategy was modified to extended right posterior sectionectomy (resection of liver segments 6, 7 and part of 5, 8) with preservation of the portal venous branch to liver segment 4. The remaining 3 patients included one patient with Cheng's type III portal vein whose surgical strategy was modified from right hemihepatectomy to resection of liver segments 6 and 7 plus part of segments 5 and 8 (19); one patient with Cheng's type II portal vein whose surgical strategy was modified from right hemihepatectomy to resection of liver segments

**Table 2. The 8 patients of complex PLC performed laparotomy who were predicted to be unresectable by 2D evaluation**

NO.	Sex	Age (years)	Tumor location (segment)	Tumor size(cm)	Hepatic cirrhosis	Major vessels close to tumor	Surgical strategy based on 2D evaluation	Surgical strategy based on 3DV evaluation	Actual surgery
1	Male	29	5/8	12.1	Yes	RHV+MHV+RPV	TACE	Right hemihepatectomy	Right hemihepatectomy
2	Female	50	5,7	7.0	Yes	RHV+RPPV	TACE	Resection of segments 5, 6 and 7	Resection of segments 5, 6 and 7
3	Male	33	8	8.1	Yes	RHV+RPV	TACE	Right hemihepatectomy	Right hemihepatectomy
4	Male	44	5,7	8.1	Yes	RHV+RPPV	TACE	Resection of segments 5, 6 and 7	Resection of segments 5, 6 and 7
5	Male	43	5/8	7.6	Yes	MHV+RPV	TACE	Resection of segments 5 and 8	Resection of segments 5 and 8
6	Male	38	1	8.0	Yes	RPV	TACE	Right hemihepatectomy+ resection of segment 1	Right hemihepatectomy+ resection of segment 1
7	Male	64	5/6/7/8	12.1	Yes	RHV + RPV	TACE	Right hemihepatectomy	Right hemihepatectomy
8	Female	13	6/7	12.6	Yes	RHV+RPV	TACE	Right hemihepatectomy	Right hemihepatectomy

MHV, Middle hepatic vein; RHV, Right hepatic vein; RPPV, Right posterior portal vein; RPV, Right portal vein; TACE: Transcatheter arterial chemoembolization.

**Table 3. Clinical data for the 13 patients in whom the surgical strategy was modified**

NO.	Sex	Age (years)	Tumor location (segment)	Tumor size(cm)	Hepatic cirrhosis	Vascular invasion	Surgical strategy based on 2D evaluation	Surgical strategy based on 3DV evaluation	Actual surgery
1	Male	69	5/8	9.3	Yes	RPV	RT	RH + partial resection of segment 4	RH + partial resection of segment 4
2	Male	28	5/6/7	12.7	Yes	RPPV	RH	Resection of segments 5, 6 and 7	Resection of segments 5, 6 and 7
3	Male	71	5/6/7	6.9	Yes	RPPV	RH	Resection of segments 5,6 and 7	Resection of segments 5,6 and 7
4	Male	39	5/6/7/8	5.4	Yes	RPPV	RH	Resection of segments 6 and 7 + part of segments 5 and 8	Resection of segments 6 and 7 + part of segments 5 and 8
5	Male	37	5/6/7/8	14.6	Yes	RHV	RH	Resection of segments 6 and 7 + part of segments 5 and 8	Resection of segments 6 and 7 + part of segments 5 and 8
6	Male	35	5/6/7/8	12.3	Yes	RHV + RPPV	RH	Resection of segments 6 and 7 + part of segments 5 and 8	Resection of segments 6 and 7 + part of segments 5 and 8
7	Male	43	5/6/7/8	12.3	Yes	RHV + RPPV	RH	Resection of segments 6 and 7 + part of segments 5 and 8	Resection of segments 6 and 7 + part of segments 5 and 8
8	Male	37	6, 8	8.5	Yes	RHV + RPPV	RH	Resection of segments 6 and 7 + part of segments 5 and 8	Resection of segments 6 and 7 + part of segments 5 and 8
9	Male	60	6/7/8	7.9	Yes	RHV + RPPV	RH	Resection of segments 6 and 7 + part of segments 5 and 8	Resection of segments 6 and 7 + part of segments 5 and 8
10	Male	49	7/8	10.4	Yes	RHV	RH	Resection of segments 6 and 7 + part of segments 5 and 8	Resection of segments 6 and 7 + part of segments 5 and 8
11	Male	24	5/6/7	7.3	Yes	RPPV	RH	Resection of segments 6 and 7 + part of segments 5 and 8	Resection of segments 6 and 7 + part of segments 5 and 8
12	Male	35	5/6/7/8	13.2	Yes	RHV + RPPV	RH	Resection of segments 6 and 7 + part of segments 5 and 8	Resection of segments 6 and 7 + part of segments 5 and 8
13	Male	34	6, 8	17.3	Yes	NO	RH	Resection of segments 6 and 8	Resection of segments 6 and 8

RH, Right hemihepatectomy; RHV, Right hepatic vein; RPPV, Right posterior portal vein; RPV, Right portal vein; RT, Right trisegmentectomy.

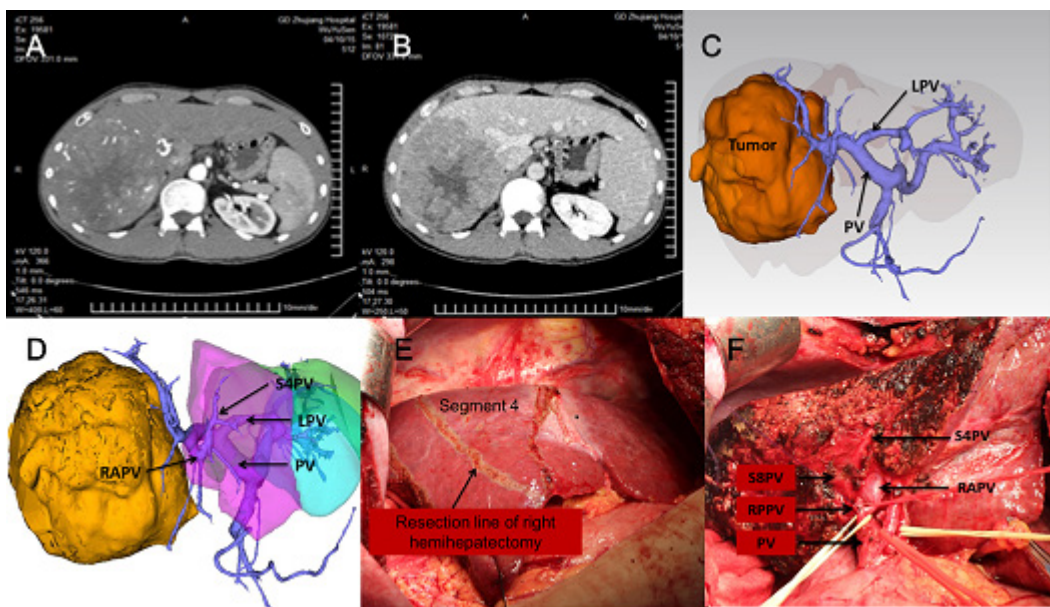


**Figure 2. A 35-year-old man with hepatocellular carcinoma with the tumor located in segments 5/6/7/8.** (A, B) Contrast-enhanced CT indicated that the tumor was close to the right portal vein (RPV) and had invaded the right posterior portal vein (RPPV). Right hemihepatectomy was recommended, and the residual liver volume ratio was 40.8%. (C, D) 3D reconstruction indicated that the tumor had only invaded the right posterior portal vein (RPPV), without invading the right anterior portal vein (RAPV). In addition, a variation of the portal vein of segment 4 (S4PV) was identified, with its origin coming from the RAPV. If the planned right hemihepatectomy was to be performed, according to the 2D CT assessment, the RPV would be ligated and resected, thus decreasing the venous blood supply to segment 4, with resulting ischemia to liver segment 4. The residual liver volume ratio would drop to 21.4% (subtracting the volume of segment 4). Finally, resection of segments 6 and 7 and partial resection of segments 5 and 8 were successfully performed (E, F), with reservation of the portal supply to liver segment 4. (PV, portal vein; S4PV, portal vein of segment 8.)

5,6 and 7; and one patient with hepatic vein anomaly whose surgical strategy was modified from right hemihepatectomy without middle hepatic vein resection to right hemihepatectomy with middle hepatic vein resection.

#### 4. Discussion

Liver resection is still the mainstay of treatment for PLC aiming at cure. The operative risk increases in patients with complex liver cancer which was initially defined by us as liver cancers which were close to, or even had invaded the bifurcation of the main portal vein or the hepatico-caval junction, or centrally located tumors (in liver segments 4, 5, 8) which were associated with major intrahepatic vascular anomalies involving the portal vein, hepatic artery or hepatic vein. 3D technology has been applied in many different fields (7,23,24). For these patients with complex PLC, it is crucial for the surgeons to have a very accurate preoperative assessment of the anatomy, and simulated surgery after 3D reconstruction helps tremendously in the planning of surgical strategies in these patients. Needless to mention that in cirrhotic patients, preoperative assessment and simulated surgery are even more important because the margin of safety in liver resection is low.

Preoperative 2D evaluation based on computed tomography or magnetic resonance is traditionally used by surgeons. This study showed that such an assessment

for complex liver cancer is far from ideal, with an accuracy rate in determining surgical strategy only in 85.9% (61 of 71 patients). Our experience showed that 3DV preoperative evaluation for complex liver cancer allowed a more accurate preoperative evaluation of tumor resectability compared with the 2D preoperative evaluation. More importantly, some patients were assessed by 2D preoperative evaluation to be unresectable, but became resectable after 3D evaluation. Our findings are in agreement with the reports showing 3DV preoperative evaluation to be useful in different types of hepatobiliary surgeries (7,14,16,25).

Preoperative 3DV evaluation enables observation of the spatial relationship between the tumor with its surrounding structures by image amplification, rotation and transparency. It also enables addition or subtraction of the portal venous system, hepatic venous system and hepatic arterial system. Further advantages are its ability to allow segmentation of the liver, calculation of different parts of the liver volumes and simulated operations. It is not surprising that in this study the accuracy rate of the 3DV evaluation for complex liver cancer was 97.2% (69/71) when compared with the gold standard of the actual operations.

Assessment of the volume of the future liver remnant forms an important part of preoperative evaluation in preventing occurrence of postoperative liver failure (26). Mise *et al* suggested that 3DV technology can be used to accurately determine the volumes of all the individual

liver segments and subsegments (27). We agree that not only would the volume of the future liver remnant be determined, but also the volumes of the tumorous and non-tumorous parts of the resected liver. Such an ability enabled us to determine the extent of liver resection in 13 cirrhotic patients with complex hepatic cancer without occurrence of postoperative liver failure (28).

Hepatic vascular anomaly is an important risk factor affecting safety of liver surgical procedures (29). It may be difficult to detect intrahepatic vascular anomalies using the conventional 2D computed tomography or magnetic resonance imaging sometimes. Inadvertent damage to major vascular anomalies can result in adverse consequences to patients (29). In our study, 3DV preoperative evaluation detected 4 patients with major vascular anomalies which were ignored by 2D preoperative evaluation, and according to these vascular anomalies, the surgical strategies determined by 2D preoperative evaluation were modified.

There are limitations of this study. First, the 3DV reconstruction models were based on the data obtained from computed tomography. The quality of the computed tomography would affect the quality of the 3DV reconstruction. Second, any small metastatic tumors which were not detected on computed tomography or magnetic resonance imaging could not be detected by the 3DV reconstruction models. Third, this is a single center study with a relatively small number of patients.

In conclusion, in our study, compared with the 2D preoperative evaluation, the 3DV preoperative assessment could be a better prediction in evaluating tumor resectability, and potential benefit in the modification of surgical strategy for patients with complex PLC.

### Acknowledgements

This study was supported by grants from the National Natural Science Foundation of China under Grant (No.81627805); the National Key Research and Development Program of China (No.2016YFC0106500); the United Fund of National Natural Science Foundation of China and Government of Guangdong Province (No. U1401254); the Science and Technology Plan Project of Guangzhou (No. 201604020144; 201704020141); the National Natural Science Foundation of China (No.81601576); the Science and Technology Plan Project of Guangdong Province (No.2016A020220013); the National High Technology Research and Development Program of China (863 Program) (No.2012AA021105).

### References

- Chen W, Zheng R, Baade PD, Zhang S, Zeng H, Bray F, Jemal A, Yu XQ, He J. Cancer statistics in China, 2015. CA Cancer J Clin. 2016; 66:115-132.
- Torre LA, Bray F, Siegel RL, Ferlay J, Lortet-Tieulent J, Jemal A. Global cancer statistics, 2012. CA Cancer J Clin. 2015; 65:87-108.
- Siegel RL, Miller KD, Jemal A. Cancer statistics, 2018. CA Cancer J Clin. 2018; 68:7-30.
- van Mierlo KM, Schaap FG, Dejong CH, Olde Damink SW. Liver resection for cancer: New developments in prediction, prevention and management of postresectional liver failure. J Hepatol. 2016; 65:1217-1231.
- Sakamoto K, Tamesa T, Yukio T, Tokuhisa Y, Maeda Y, Oka M. Risk factors and managements of bile leakage after hepatectomy. World J Surg. 2016; 40:182-189.
- Schreckenbach T, Liese J, Bechstein WO, Moench C. Posthepatectomy liver failure. Dig Surg. 2012; 29:79-85.
- Fang CH, Tao HS, Yang J, Fang ZS, Cai W, Liu J, Fan YF. Impact of three-dimensional reconstruction technique in the operation planning of centrally located hepatocellular carcinoma. J Am Coll Surg. 2015; 220:28-37.
- Min Hu, Haoyu Hu, Wei Cai, Zhikang Mo, Nan Xiang, Jian Yang, Chihua Fang. The safety and feasibility of three-dimensional visualization technology assisted right posterior lobe allied with part of V and VIII sectionectomy for right hepatic malignancy therapy. J Laparoendosc ADV S. 2018; 28:586-594.
- Wei XB, Xu J, Li N, Yu Y, Shi J, Guo WX, Cheng HY, Wu MC, Lau WY, Cheng SQ. The role of three-dimensional imaging in optimizing diagnosis, classification and surgical treatment of hepatocellular carcinoma with portal vein tumor thrombus. HPB. 2016; 18:287-295.
- Takamoto T, Hashimoto T, Ogata S, Inoue K, Maruyama Y, Miyazaki A, Makuuchi M. Planning of anatomical liver segmentectomy and subsegmentectomy with 3-dimensional simulation software. Am J Surg. 2013; 206:530-538.
- Oshiro Y, Ohkohchi N. Three-dimensional liver surgery simulation: Computer-assisted surgical planning with three-dimensional simulation software and three-dimensional printing. Tissue Eng Part A. 2017; 23:474-480.
- Tani K, Shindoh J, Akamatsu N, Arita J, Kaneko J, Sakamoto Y, Hasegawa K, Kokudo N. Venous drainage map of the liver for complex hepatobiliary surgery and liver transplantation. HPB (Oxford). 2016; 18:1031-1038.
- Schindl MJ, Redhead DN, Fearon KC, Garden OJ, Wigmore SJ, on behalf of the Edinburgh Liver Surgery and Transplantation Experimental Research Group (eLISTER). The value of residual liver volume as a predictor of hepatic dysfunction and infection after major liver resection. Gut. 2005; 54:289-296..
- Mise Y, Hasegawa K, Satou S, Shindoh J, Miki K, Akamatsu N, Arita J, Kaneko J, Sakamoto Y, Kokudo N. How has virtual hepatectomy changed the practice of liver surgery?: Experience of 1194 virtual hepatectomy before liver resection and living donor liver transplantation. Ann Surg. 2018; 268:127-133.
- Fang CH, Xie AW, Chen ML, Huang YP, Lu CM, Li XF, Pan JH, Peng FP. Application of a visible simulation surgery technique in preoperation planning for intrahepatic calculi. World J Surg. 2010; 34:327-335.
- Zeng N, Tao H, Fang C, Fan Y, Xiang N, Yang J, Zhu

- W, Liu J, Guan T, Fang C, Xiang F. Individualized preoperative planning using three-dimensional modeling for Bismuth and Corlette type III hilar cholangiocarcinoma. *World J Surg Oncol.* 2016; 14:44.
17. Dreizin D, Bodanapally UK, Neerchal N, Tirada N, Patlas M, Herskovits E. Volumetric analysis of pelvic hematomas after blunt trauma using semi-automated seeded region growing segmentation: A method validation study. *Abdom Radiol (NY).* 2016; 41:2203-2208.
18. Cunha P, Guevara MA, Messias A, Rocha S, Reis R, Nicolau PM. A method for segmentation of dental implants and crestal bone. *Int J Comput Assist Radiol Surg.* 2013; 8:711-721.
19. Cheng YF, Huang TL, Lee TY, Chen TY, Chen CL. Variation of the intrahepatic portal vein; angiographic demonstration and application in living-related hepatic transplantation. *Transplant Proc.* 1996; 28:1667-1668.
20. Michels NA. Newer anatomy of the liver and its variant blood supply and collateral circulation. *Am J Surg.* 1966; 112:337-347.
21. Nakamura S, Tsuzuki T. Surgical anatomy of the hepatic veins and the inferior vena cava. *Surg Gynecol Obstet.* 1981; 152:43-50.
22. NCCN clinical practice guidelines in oncology: Hepatobiliary cancers. Version 2. 2017. <http://www.lidebiotech.com/nccn/20.pdf> (accessed June 20, 2018).
23. Valls-Ontanon A, Mezquida-Fernandez C, Guijarro-Martinez R, Hernandez-Alfaro F. Three-dimensional surgical planning and simulation to improve surgical accuracy and reduce invasiveness of cranioplasties. *Int J Oral Maxillofac Surg.* 2017; 46:586-589.
24. Li CX. Numerical investigation of a hybrid wave absorption method in 3D numerical wave tank. *CMES.* 2015;107:125-153.
25. Nakayama K, Oshiro Y, Miyamoto R, Kohno K, Fukunaga K, Ohkohchi N. The effect of three-dimensional preoperative simulation on liver surgery. *World J Surg.* 2017; 41:1840-1847.
26. Suzuki K, Kohlbrenner R, Epstein ML, Obajuluwa AM, Xu J, Hori M. Computer-aided measurement of liver volumes in CT by means of geodesic active contour segmentation coupled with level-set algorithms. *Med Phys.* 2010; 37:2159-2166.
27. Mise Y, Satou S, Shindoh J, Conrad C, Aoki T, Hasegawa K, Sugawara Y, Kokudo N. Three-dimensional volumetry in 107 normal livers reveals clinically relevant inter-segment variation in size. *HPB (Oxford).* 2014; 16:439-447.
28. Rahbari NN, Garden OJ, Padbury R, et al. Posthepatectomy liver failure: A definition and grading by the International Study Group of Liver Surgery (ISGLS). *Surgery.* 2011; 149:713-724.
29. Xiang N, Fang C, Fan Y, Yang J, Zeng N, Liu J, Zhu W. Application of liver three-dimensional printing in hepatectomy for complex massive hepatocarcinoma with rare variations of portal vein: Preliminary experience. *Int J Clin Exp Med.* 2015; 8:18873-18878.

(Received August 17, 2018; Revised October 9, 2018;  
Accepted October 31, 2018)

# Total laparoscopic versus robot-assisted laparoscopic pancreaticoduodenectomy

Yuhua Zhang<sup>1,\*</sup>, Defei Hong<sup>2</sup>, Chengwu Zhang<sup>1</sup>, Zhiming Hu<sup>1</sup>

<sup>1</sup> Department of Hepaticobiliarypancreatic and Minimally Invasive Surgery, Zhejiang Provincial People's Hospital, People's hospital of Hangzhou medical college, Hangzhou, China;

<sup>2</sup> Department of General Surgery, Sir Run Run Shaw Hospital, Zhejiang University, Hangzhou, China.

## Summary

In this study, the clinical effectiveness of the robot-assisted laparoscopic pancreaticoduodenectomy (RPD) and Total laparoscopic pancreaticoduodenectomy LPD were retrospectively reviewed. From December 2013 to September 2017, 20 patients underwent robot-assisted laparoscopic pancreaticoduodenectomy and 80 patients underwent Total laparoscopic pancreaticoduodenectomy. The clinical data of the RPDs and the first 20 LPDs were reviewed retrospectively. There is no difference in operative time, estimated blood loss, length of stay, and rates of complications and mortality between the LPD and RPD group. The next 10 cases in the RPD group had shorter operative times ( $p = 0.03$ ) than the first 10 cases. The estimated blood loss and length of stay were also lower in the next 10 cases; however, these results did not reach statistical significance. Our results show that LPD and RPD are technically safe and feasible. Comparable results were demonstrated between the two groups, while the robotic system seemed to shorten the learning curve of minimally invasive pancreaticoduodenectomy (PD).

**Keywords:** Laparoscopic, robotic, pancreaticoduodenectomy, learning curve

## 1. Introduction

Laparoscopic pancreaticoduodenectomy (LPD) was first described by Gagner and Pomp in 1994 (1), and the first robotic-assisted LPD (RPD) was performed by Giulianotti *et al.* in 2001 (2). Minimally invasive pancreaticoduodenectomy (MPD) has gradually gained momentum following 30 years of development of laparoscopic surgical skills, internal closure devices, and energy systems. LPD is a well-established procedure with acceptable morbidity and mortality rates in some specialized high-volume centers (3-8). However, there are intrinsic disadvantages associated with traditional laparoscopy systems, including two-dimensional imaging, poor surgeon ergonomics, and a restricted range of movement up to four degrees of freedom inside the abdominal cavity (9). Application of a robotic surgical system is believed to provide surgeons with

superior magnified high-resolution three-dimensional visualization, enhanced dexterity, greater precision, and greater ergonomic comfort. It enables surgeons to control the surgical instruments with accuracy, flexibility, and a wide range of motion. This is beneficial in procedures that require complicated resection and reconstruction such as prostatectomy, coronary surgery, and pancreaticoduodenectomy (PD). RPD has been proven feasible and safe with the advantage of minimal invasiveness compared with open procedures (10-15). However, robotic systems also have some disadvantages compared with laparoscopic systems, such as their high cost, lack of force feedback, and device-related complications. To the best of our knowledge, no directly comparative data between these two procedures have been reported to date. We herein present a case series with the aim of elucidating the short-term clinical effectiveness between LPD and RPD by direct comparison.

\*Address correspondence to:

Dr. Yuhua Zhang, Department of Hepaticobiliarypancreatic and Minimally Invasive Surgery, Zhejiang Provincial People's Hospital, People's Hospital of Hangzhou Medical College, 158 Shangtang Road, Hangzhou 310014, China.  
E-mail: zhangyuhua1013@126.com

## 2. Materials and Methods

### 2.1. Clinical data

From December 2013 to September 2017, a total of 100

patients with periampullary tumors underwent MPD at Zhejiang Provincial People's Hospital, Hangzhou, China. The indication for MPD was the requirement for PD in the absence of locally advanced malignancy. All patients' general medical conditions were adequate for general anesthesia with pneumoperitoneum. The decision regarding whether to perform LPD or RPD was based on the patient's choice of procedure and the ability to pay for the extra cost associated with robotic surgery. All surgeries were performed by surgeons with experience in open PD and minimally invasive surgery. The clinical data of the first 20 LPDs and RPDs were analyzed to evaluate the LPD and RPD outcomes during the same period of the learning curve. This study was performed with approval of the Zhejiang Provincial People's Hospital review board committee.

The patients' demographic and clinical data were reviewed, including age, sex, body mass index, American Society of Anesthesiologists (ASA) grade (16), operative time, estimated blood loss (EBL), need for blood transfusions, tumor type, margin status, 90-day or in-hospital mortality, length of postoperative hospital stay (LOS), and readmission rate. Postoperative complications were graded using the Clavien–Dindo (CD) classification (17). Pancreatic fistula (18), bile leakage (19), postoperative hemorrhage (20), and delayed gastric emptying (21) were defined according to the established international consensus.

## 2.2. Operative technique

LPD or RPD was performed with the patient in the supine position and secured firmly to the operation table. After establishment of pneumoperitoneum by a closed Veress needle technique, ports were placed as shown (Figure 1).

The operation was started by laparoscopic examination of the entire abdomen. If no contraindications to resection were present, the transverse colon and hepatic flexure were completely mobilized from the head of the pancreas and duodenum. A wide Kocher's maneuver was then performed until the Treitz ligament had been completely mobilized and the right side of the superior mesenteric artery (SMA) had been exposed if possible (Figure 2). Dissection of the hepatoduodenal ligament was started by cystic artery transection and cholecystectomy. The common hepatic duct was divided and temporarily closed by a clip to avoid spillage of bile throughout the procedure if needed. Mobilization of the common bile duct to the superior border of the pancreas was performed with care to prevent injury to the aberrant right hepatic artery arising from the SMA. The underlying portal vein (PV) was identified at the same time. The distal stomach was transected with an endoscopic stapler. The superior border of the pancreas was visualized and the hepatic artery was identified and followed by transection of

the gastroduodenal artery. The superior mesentery vein (SMV) was then dissected at the inferior border of the pancreas, and a retropancreatic tunnel was created if needed. The pancreas was then transected and the pancreatic duct found. The jejunum was pulled to the right upper quadrant under the mesenteric vessels and transected 10 to 15 cm distal to the ligament of Treitz with an endoscopic linear stapler. Dissection of the uncinate process of the pancreas from the right side of SMV and SMA was performed with traction of the uncinate process from the opposite side of the vessels (Figure 3). A Harmonic scalpel and Ligasure were applied in the transection. After this step, the resection part was finished (Figure 4).

Reconstruction was carried out *via* a laparoscopic or robotic system according to the patient's choice. A double-layer duct-to-mucosa pancreaticojejunostomy was carried out using 3-0 Prolene (Ethicon, Somerville, NJ) running sutures for the outside layer and 5-0 Prolene (Ethicon) interrupted sutures for the inner layer (Figure 5). A pancreatic stent was used in all cases. The hepatojejunostomy was performed using a 4-0 polydioxanone (PDS II; Ethicon) in a running fashion. Gastrojejunostomy was performed intracorporeally using 3-0 Stratafix (Ethicon) in both LPD and RPD. The specimen was removed *via* an enlarged periumbilical incision (3-4 cm).

## 2.3. Statistical analysis

Results are presented as mean  $\pm$  standard deviation. Patients who underwent LPD were compared with those who underwent RPD using the chi-square test and Fisher's exact test for categorical variables and the Mann–Whitney *U* test for continuous variables. Differences with *p* values of  $< 0.05$  were considered statistically significant. All analyses were performed using SPSS 13.0 statistical software (SPSS Inc., Chicago, IL).

## 3. Results

Twenty patients underwent a robotic procedure and eighty underwent a laparoscopic technique. Four LPDs were converted to open surgery: one because of intraoperative bleeding and three because the tumors invaded the portal vein or SMV, preventing R0 resection using a minimally invasive procedure. Tumor resection was performed *via* a laparoscopic system in all cases in our group. All four cases that converted to open procedures were at the resection stage with the laparoscopic system, so they were excluded from the analysis.

The demographic and preoperative clinical characteristics of the first 20 RPDs and LPDs are listed in Table 1. There was no significant difference in sex, age, body mass index, or ASA grade between the two



**Figure 1. Trocar positions.** Left picture shows the port positions in LPD procedures and the right one shows the port positions in RPD procedures.

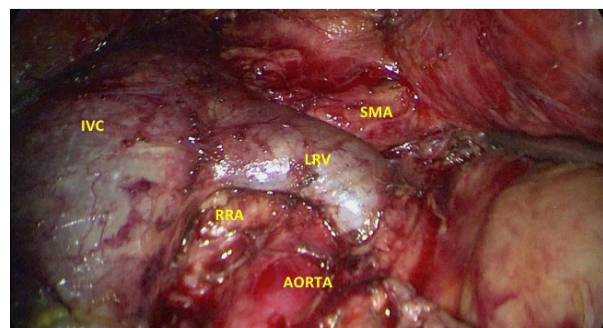


**Figure 2. Right retrospective SMA first approach.** SMA, superior mesentery artery; IVC, inferior vein cava; LRV, left renal vein; RRA, right renal artery.

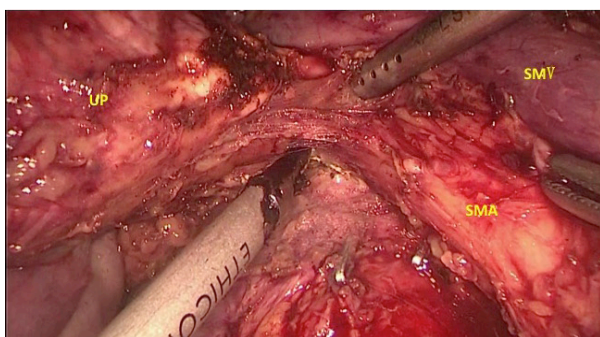


**Figure 3. Dissection of the uncinate process of the pancreas from the right side of SMV and SMA.** UP, uncinate process of the pancreas; SMA, superior mesentery artery; SMV, superior mesentery vein.

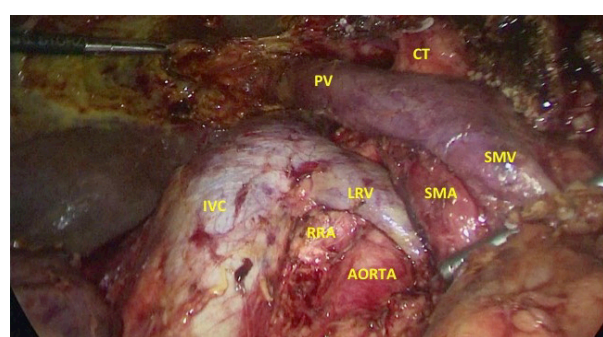


**Figure 4. Complete resection.** CT, celiac truck; PV, portal vein; SMA, superior mesentery artery; SMV, superior mesentery vein; IVC, inferior vein cava; LRV, left renal vein; RRA, right renal artery.

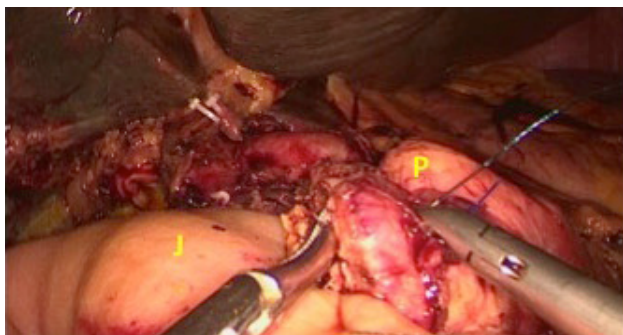


**Figure 5. Pancreaticojejunostomy.** left figure shows laparoscopic pancreaticojejunostomy and right figure shows robotic pancreaticojejunostomy. P, pancreases; J, jejunum.

groups.

The perioperative results are shown in Table 2. The operation time was  $407.0 \pm 91.8$  and  $373.8 \pm 70.2$  minutes in RPD group and LPD group. The estimated blood loss was  $220.5 \pm 165.5$  and  $240.0 \pm 239.5$  ml in RPD group and LPD group, and the LOS was  $14.6 \pm 6.1$  and  $18.1 \pm 11.6$  days in RPD group and LPD group. However, the differences between the two groups did not reach statistical significance. The rates of overall and major complications (CD grade  $\geq II$ ) were similar between the two groups. One patient in the RPD group died of postoperative intra-abdominal active bleeding from the GDA. This patient had embolization of the common hepatic artery and rebleeding after embolization and ultimately died of multiple organ

dysfunction. The occurrence of postoperative pancreatic fistula, delayed gastric emptying, bile leakage, and bleeding were similar in the two groups. There was no significant difference in the reoperation and readmission rates between the two groups.

Because of the limited number of procedures performed, it was impossible to analyze the learning curve of the two procedures. We simply separated each group into two subgroups: the first 10 cases and the last 10 cases. The clinical data between these two subgroups were analyzed. As shown in Table 3, there is no difference between the last 10 cases and the first 10 cases in the LPD group. In the RPD group, the last 10 cases had significantly shorter operative times ( $p = 0.03$ ) than the first 10 cases. The EBL and LOS were

also lower in the last 10 cases; however, these results did not reach statistical significance. More major complications (CD grade  $\geq$  II) occurred in the first than last 10 cases in both groups (LPD, 4 vs. 2; RPD, 3 vs. 2, respectively). The occurrence of postoperative pancreatic fistula was the same between the first and last 10 cases in both groups (LPD, 3 vs. 2; RPD, 2 vs. 1, respectively).

The pathologic results are shown in Table 4. All patients had negative resections, and no difference in the final diagnosis was noted between the two groups.

**Table 1. Patients' demographic and preoperative clinical characteristics**

Items	LPD (20)	RPD (20)	P
Gender	M:F 11:9	M:F 12:8	NS
Age (median)	42-76(64)	50-78(68)	NS
BMI ( $\text{kg}/\text{m}^2$ )	24.0 $\pm$ 3.5	24.8 $\pm$ 2.5	NS
ASA			
II	16	14	NS
III	4	6	
Jaundice (TB $\geq$ 2 mg)	5	7	NS
DM	4	3	NS
Pancreatic duct ( $>$ 3 mm)	13	9	NS

LPD: laparoscopic pancreaticoduodenectomy, RPD: robot-assisted laparoscopic pancreaticoduodenectomy, BMI: body mass index in  $\text{kg}/\text{m}^2$ , ASA: American Society of Anesthesiologists grade, TB: total bilirubin, DM: diabetes mellitus, NS: no significant difference.

**Table 2. Perioperative clinical findings and complications**

Items	LPD (20)	RPD (20)	P
OT (mins)	373.8 $\pm$ 70.2	407.0 $\pm$ 91.8	NS
EBL (ml)	240 $\pm$ 239.5	220.5 $\pm$ 165.5	NS
Mortality	0	1	NS
Morbidity (CD $\geq$ II)	9	8	NS
Pancreatic fistula			NS
A	2	2	
B	1	0	
C	2	1	
Bile leakage	2	1	NS
DGE	1	2	NS
Hemorrhage	3	2	NS
Reoperation	3	3	NS
LOS (days)	18.1 $\pm$ 11.6	14.6 $\pm$ 6.1	NS
Readmission	1	0	NS

LPD: laparoscopic pancreaticoduodenectomy, RPD: robot-assisted laparoscopic pancreaticoduodenectomy, OT: operation time (from cutting of the skin to completion of suturing), EBL: estimated blood loss, LOS: length of postoperative hospital stay, CD: Clavien-Dindo classification, DGE [26]: delayed gastric emptying.

**Table 3. Comparison of the first and last 10 cases**

Items	LPD			RPD		
	LPD (1-10)	LPD (11-20)	P	RPD (1-10)	RPD (11-20)	P
OT (mins)	383.0 $\pm$ 95.8	364.5 $\pm$ 32.1	NS	449 $\pm$ 105.9	365 $\pm$ 51.5	0.03
EBL (mL)	257.0 $\pm$ 288.0	223.0 $\pm$ 193.7	NS	290 $\pm$ 243.6	171 $\pm$ 108.4	NS
LOS (days)	19.4 $\pm$ 14.7	16.7 $\pm$ 8.3	NS	16.5 $\pm$ 8.0	12.7 $\pm$ 3.0	NS

LPD: laparoscopic pancreaticoduodenectomy, RPD: robot-assisted laparoscopic pancreaticoduodenectomy, OT: operation time, EBL, estimated blood loss, LOS: length of postoperative hospital stay.

#### 4. Discussion

After 30 years of development, MPD has been proven safe and has shown some benefits over traditional open procedures, including less pain, less blood loss, better cosmetic outcomes, and faster recovery. However, the complexity of the anatomy during dissection and the need for reconstruction with two challenging anastomoses (pancreatic-enteric and hepato-enteric anastomosis) have made MPD more technically demanding and limited this procedure to a few experienced hands in high-volume centers. Recently reported large series ( $>$  100 cases) of LPD (4,6) have clearly shown that this is a well-established approach. However, LPD has inherent disadvantages such as two-dimensional visualization and a limited degree of freedom due to the straight laparoscopic instruments. These limitations have made some parts of the procedure, such as pancreatic-enteric reconstruction, very technically demanding. Robotic systems have provided surgeons with superior three-dimensional visualization and instrumentation that mimics the surgeon's hand; these instruments have an articulating wrist, are able to achieve seven degrees of freedom, and provide tremor filtration and stable retraction (22). The emergence of robotic systems has captured the attention of many minimally invasive surgeons because it is often believed to overcome the natural limitations of conventional laparoscopy. However, the efficiency of robotic surgery continues to be debated because of its extra cost, lack of force feedback, and device-related complications. Several retrospective reports have compared the safety and feasibility between RPD and open PD (11,14,23) and between LPD and open PD

**Table 4. Pathological results of the two procedures**

Items	LPD (20)	RPD (20)	P
PDAC	8	7	NS
Cholangiocarcinoma	6	4	NS
Ampulla adenocarcinoma	4	5	NS
NET	0	2	NS
IPMN	1	0	NS
Other	1	2	NS

LPD: laparoscopic pancreaticoduodenectomy, RPD: robot-assisted laparoscopic pancreaticoduodenectomy, PDAC: pancreatic duct adenocarcinoma, NET: neuroendocrine tumor, IPMN: intraductal papillary mucinous neoplasm.

(6,10,24,25). The results showed that LPD and RPD had some benefits over open PD. However, whether robot-assisted procedures have advantages over laparoscopic procedures for PD remains unclear.

Our RPD procedures were performed *via* a hybrid laparoscopic-robotic approach (13,26,27). We started with laparoscopic resection followed by reconstruction using a robotic system. We chose this approach to maximize the advantages and bypass the disadvantages of both techniques. The advantages of traditional laparoscopic resection were that it had some force feedback, the ability to change the patient's position during the operation, and the fact that the laparoscopic technique was very well developed. However, the robotic system was proven to be better for procedures performed in small, confined areas and that require superior visualization and a precise technique, such as prostatectomy and coronary artery bypass surgery. For these reasons, we believe that robotic systems are beneficial for challenging reconstructions, including pancreatic-enteric and hepato-enteric anastomosis. However, the current robotic systems also have several disadvantages, including the inability to change the position of the patient after docking, the high cost not covered by health insurance, and incompatibility with current systems. According to these differences between the two systems, we believe that traditional laparoscopy is better than robotic surgery for resection, while robotic surgery is better for reconstruction.

In the present study, we found no significant difference in the operative time or EBL between the two groups. The operative time in the RPD group ( $407.0 \pm 91.8$  min) was longer than that in the LPD group ( $373.8 \pm 70.2$  min). Our operative time was the "skin-to-skin" interval, which included the docking time of the robotic system, which was usually about 40 minutes in the first 10 cases and 20 minutes in the next 10 cases. We also found a greater reduction in the operative time in the RPD group ( $p = 0.03$ ). The operative time was longer in the RPD than LPD group in the first 10 cases ( $449.0 \pm 105.9$  vs.  $383.0 \pm 95.8$  min, respectively) and almost the same in both groups in the next 10 cases ( $364.5 \pm 32.1$  vs.  $365.0 \pm 51.5$  min, respectively). We believe that this reduction was mainly the result of familiarity with the robotic system. Less intraoperative bleeding is widely accepted as one of the major advantages of the minimally invasive approach. The EBL in the present study was similar in the LPD and RPD groups ( $240.0 \pm 239.5$  vs.  $220.5 \pm 165.5$  ml, respectively). This indicates that both minimally invasive approaches effectively reduced bleeding by allowing for precise manipulation and providing magnification.

PD is a complex procedure with a high morbidity rate even in high-volume centers (28). Our results showed that the occurrence of complications was similar in the two groups according to the CD classification system, and the incidence of postoperative

complications (CD grade  $\geq II$ ) in the RPD (40%) and LPD (45%) groups was in accordance with the previously published open PD data (28). This indicates that both of these minimally invasive procedures are as safe as the open approach. The pancreatic fistula continues to be the "Achilles' heel" of PD, and most of the serious complications of PD are associated with POPF. The incidence of pancreatic fistula was 10% to 20% after PD according to the International Study Group of Pancreatic Surgery classification (20,28,29). Some experienced surgeons have tried to improve the anastomosis techniques for PD (30). However, the development of pancreatic fistulas continues to be problematic. In the present study, the incidence of pancreatic fistulas was not significantly different between the two groups (25% vs. 15%) and included a severe (grade C) pancreatic fistula. These findings are similar to those reported in a larger-volume open series (28). The incidence of severe pancreatic fistula was 10% in the LPD group and 5% in the RPD group of the present study; this might have been due to the fact that our series was performed when the surgeon was in the learning stage of both procedures, and the anastomotic technique and peripancreatic drainage were therefore imperfect.

The patients in the LPD group had a longer LOS ( $18.1 \pm 11.6$  days) than those in the RPD group ( $14.6 \pm 6.1$  days), but the difference was not statistically significant. This indicates expedited postoperative recovery in the RPD group. In contrast, a previous review showed that patients who underwent LPD had a shorter LOS than those who underwent RPD ( $11.09 \pm 7.00$  vs.  $13.84 \pm 8.00$  days, respectively) (31). However, they compared data from different institutions located on different continents with different health insurance systems. We believe that the patients who underwent RPD in the present study had an expedited postoperative recovery. The lack of statistical significance might have been due to the insufficient statistical power.

The number of cases in our series was small, so it is difficult to quantify the learning curve. We compared the clinical data of the first and next 10 cases in each group. Several interesting findings emerged from this comparison. Limited improvement in the measured parameters was achieved in the LPD group. However, improvements were detected in the RPD group. A significant decrease in the operative time in the next 10 cases was found in the RPD group ( $p = 0.03$ ). The EBL and LOS were decreased in next 10 cases, although the difference did not reach statistical significance because of the small number of cases. In our opinion, the main reason is the difference in the surgeon's skill level between the two systems. The surgeon who performed the operations was a well-trained laparoscopic surgeon. Therefore, the surgeon's laparoscopic technique was fully developed when LPD was started. Because the robotic system was new and high-cost, there was limited

opportunity to train the surgeon in simple procedures such as cholecystectomy before we start RPD. We believe that this was the main reason for this difference. From another point of view, the robotic system has great potential for improved performance in the future. Furthermore, our data demonstrated that RPD might be associated with a shorter learning curve than LPD.

There was no difference in the final pathological results between the two groups. All patients had a negative resection margin, and the lymph nodes harvested were the same in all patients with pancreatic cancer (data not shown). Because of the limited number of cases, the survival benefit could not be determined.

In conclusion, LPD and RPD had comparable short-term results. Both approaches were technically feasible with acceptable short-term outcomes in experienced hands. There was a steep learning curve for both LPD and RPD; however, RPD seems to have a shorter learning curve for this complex procedure. A further large-volume study should be performed to compare the long-term outcomes between LPD and RPD.

### Acknowledgement

This work was supported by the Natural Science Foundation of Zhejiang Province, China (LY15H160054).

### References

- Gagner M, Pomp A. Laparoscopic pylorus-preserving pancreateoduodenectomy. *Surg Endosc*. 1994; 8:408-410.
- Giulianotti PC, Coratti A, Angelini M, Sbrana F, Cecconi S, Balestracci T, Caravaglios G. Robotics in general surgery: personal experience in a large community hospital. *Arch Surg*. 2003; 138:777-784.
- Dulucq JL, Wintringer P, Mahajna A. Laparoscopic pancreaticoduodenectomy for benign and malignant diseases. *Surg Endosc*. 2006; 20:1045-1050.
- Croome KP, Farnell MB, Que FG, Reid-Lombardo KM, Truty MJ, Nagorney DM, Kendrick ML. Total laparoscopic pancreaticoduodenectomy for pancreatic ductal adenocarcinoma: oncologic advantages over open approaches? *Ann Surg*. 2014; 260:633-638; Discussion 638-640.
- Palanivelu C, Rajan PS, Rangarajan M, Vaithiswaran V, Senthilnathan P, Parthasarathi R, Praveen Raj P. Evolution in techniques of laparoscopic pancreaticoduodenectomy: A decade long experience from a tertiary center. *J Hepatobiliary Pancreat Surg*. 2009; 16:731-740.
- Song KB, Kim SC, Hwang DW, Lee JH, Lee DJ, Lee JW, Park KM, Lee YJ. Matched Case-Control Analysis Comparing Laparoscopic and Open Pylorus-preserving Pancreaticoduodenectomy in Patients With Periampullary Tumors. *Ann Surg*. 2015; 262:146-155.
- Corcione F, Pirozzi F, Cuccurullo D, Piccolboni D, Caracino V, Galante F, Cusano D, Sciuto A. Laparoscopic pancreaticoduodenectomy: experience of 22 cases. *Surg Endosc*. 2013; 27:2131-2136.
- Wang M, Zhang H, Wu Z, Zhang Z, Peng B. Laparoscopic pancreaticoduodenectomy: single-surgeon experience. *Surg Endosc*. 2015; 29:3783-3794.
- Smith CD, Farrell TM, McNatt SS, Metreveli RE. Assessing laparoscopic manipulative skills. *Am J Surg*. 2001; 181:547-550.
- Baker EH, Ross SW, Seshadri R, Swan RZ, Iannitti DA, Vrochides D, Martinie JB. Robotic pancreaticoduodenectomy: Comparison of complications and cost to the open approach. *Int J Med Robot*. 2016; 12:554-560.
- Buchs NC, Addeo P, Bianco FM, Ayloo S, Benedetti E, Giulianotti PC. Robotic versus open pancreaticoduodenectomy: a comparative study at a single institution. *World J Surg*. 2011; 35:2739-2746.
- Chalikonda S, Aguilar-Saavedra JR, Walsh RM. Laparoscopic robotic-assisted pancreaticoduodenectomy: A case-matched comparison with open resection. *Surg Endosc*. 2012; 26:2397-2402.
- Narula VK, Mikami DJ, Melvin WS. Robotic and laparoscopic pancreaticoduodenectomy: A hybrid approach. *Pancreas*. 2010; 39:160-164.
- Chen S, Chen JZ, Zhan Q, Deng XX, Shen BY, Peng CH, Li HW. Robot-assisted laparoscopic versus open pancreaticoduodenectomy: a prospective, matched, mid-term follow-up study. *Surg Endosc*. 2015; 29:3698-3711.
- Giulianotti PC, Sbrana F, Bianco FM, Elli EF, Shah G, Addeo P, Caravaglios G, Coratti A. Robot-assisted laparoscopic pancreatic surgery: single-surgeon experience. *Surg Endosc*. 2010; 24:1646-1657.
- Rozner MA. The American Society of Anesthesiologists physical status score and risk of perioperative infection. *JAMA*. 1996; 275:154 4.
- Dindo D, Demartines N, Clavien PA. Classification of surgical complications: a new proposal with evaluation in a cohort of 6336 patients and results of a survey. *Ann Surg*. 2004; 240:205-213.
- Bassi C, Dervenis C, Butturini G, Fingerhut A, Yeo C, Izicki J, Neoptolemos J, Sarr M, Traverso W, Buchler M, International Study Group on Pancreatic Fistula D. Postoperative pancreatic fistula: an international study group (ISGPF) definition. *Surgery*. 2005; 138:8-13.
- Koch M, Garden OJ, Padbury R, et al. Bile leakage after hepatobiliary and pancreatic surgery: A definition and grading of severity by the International Study Group of Liver Surgery. *Surgery*. 2011; 149:680-688.
- Wente MN, Veit JA, Bassi C, Dervenis C, Fingerhut A, Gouma DJ, Izicki JR, Neoptolemos JP, Padbury RT, Sarr MG, Yeo CJ, Buchler MW. Postpancreatectomy hemorrhage (PPH): An International Study Group of Pancreatic Surgery (ISGPS) definition. *Surgery*. 2007; 142:20-25.
- Wente MN, Bassi C, Dervenis C, Fingerhut A, Gouma DJ, Izicki JR, Neoptolemos JP, Padbury RT, Sarr MG, Traverso LW, Yeo CJ, Buchler MW. Delayed gastric emptying (DGE) after pancreatic surgery: A suggested definition by the International Study Group of Pancreatic Surgery (ISGPS). *Surgery*. 2007; 142:761-768.
- Memon S, Heriot AG, Murphy DG, Bressel M, Lynch AC. Robotic versus laparoscopic proctectomy for rectal cancer: A meta-analysis. *Ann Surg Oncol*. 2012; 19:2095-2101.
- Lai EC, Yang GP, Tang CN. Robot-assisted laparoscopic pancreaticoduodenectomy versus open pancreaticoduodenectomy – a comparative study. *Int J Surg*. 2012; 10:475-479.
- Croome KP, Farnell MB, Que FG, Reid-Lombardo KM, Truty MJ, Nagorney DM, Kendrick ML.

- Pancreaticoduodenectomy with major vascular resection: a comparison of laparoscopic versus open approaches. *J Gastrointest Surg.* 2015; 19:189-194; Discussion 194.
- 25. Langan RC, Graham JA, Chin AB, et al. Laparoscopic-assisted versus open pancreaticoduodenectomy: early favorable physical quality-of-life measures. *Surgery.* 2014; 156:379-384.
  - 26. Ji W, Ding K, Kao X, He C, Li N, Li J. Robotic and laparoscopic hybrid pancreaticoduodenectomy: surgical techniques and early outcomes. *Chin Med J (Engl).* 2014; 127:3027-3029.
  - 27. Zureikat AH, Nguyen KT, Bartlett DL, Zeh HJ, Moser AJ. Robotic-assisted major pancreatic resection and reconstruction. *Archives of surgery.* 2011; 146:256-261.
  - 28. Cameron JL, Riall TS, Coleman J, Belcher KA. One thousand consecutive pancreaticoduodenectomies. *Ann Surg.* 2006; 244:10-15.
  - 29. Dong X, Zhang B, Kang MX, Chen Y, Guo QQ, Wu YL. Analysis of pancreatic fistula according to the International Study Group on Pancreatic Fistula classification scheme for 294 patients who underwent pancreaticoduodenectomy in a single center. *Pancreas.* 2011; 40:222-228.
  - 30. Cho A, Yamamoto H, Kainuma O, Muto Y, Park S, Arimitsu H, Sato M, Souda H, Ikeda A, Nabeya Y, Takiguchi N, Nagata M. Performing simple and safe dunking pancreaticojejunostomy using mattress sutures in pure laparoscopic pancreaticoduodenectomy. *Surg Endosc.* 2014; 28:315-318.
  - 31. Orti-Rodriguez RJ, Rahman SH. A comparative review between laparoscopic and robotic pancreaticoduodenectomies. *Surg Laparosc Endosc Percutan Tech.* 2014; 24:103-108.

(Received September 28, 2018; Revised October 19, 2018;  
Accepted October 25, 2018)

# Bao Yuan decoction and Tao Hong Si Wu decoction improve lung structural remodeling in a rat model of myocardial infarction: Possible involvement of suppression of inflammation and fibrosis and regulation of the TGF- $\beta$ 1/Smad3 and NF- $\kappa$ B pathways

Guozhen Yuan<sup>1,§</sup>, Anbang Han<sup>1,§</sup>, Jing Wu<sup>1</sup>, Yingdong Lu<sup>1</sup>, Dandan Zhang<sup>1</sup>, Yuxiu Sun<sup>1</sup>, Jian Zhang<sup>2</sup>, Mingjing Zhao<sup>3</sup>, Bingbing Zhang<sup>1</sup>, Xiangning Cui<sup>1,\*</sup>

<sup>1</sup> Department of Cardiology, Guang'anmen Hospital, China Academy of Chinese Medical Sciences, Beijing, China;

<sup>2</sup> Naton Medical Group, Haidian District, Beijing, China;

<sup>3</sup> The Key Laboratory of Chinese Internal Medicine of the Ministry of Education, Dongzhimen Hospital, Beijing University of Chinese Medicine, Beijing, China.

## Summary

Chronic heart failure (CHF) leads to pulmonary structural remodeling, which may be a key factor for poor clinical outcomes in patients with end-stage heart failure, and few effective therapeutic options are presently available. The aim of the current study was to explore the mechanism of action and pulmonary-protective effects of treatment with Bao Yuan decoction combined with Tao Hong Si Wu decoction (BYTH) on lung structural remodeling in rats with ischemic heart failure. In a model of myocardial infarction (MI) induced by ligation of the left anterior descending (LAD) artery, rats were treated with BYTH. Heart function and morphometry were measured followed by echocardiography, histological staining, and immunohistochemical analysis of lung sections. The levels of transforming growth factor- $\beta$ 1 (TGF- $\beta$ 1), type I collagen, phosphorylated-Smad3 (p-Smad3), tumor necrosis factor- $\alpha$  (TNF- $\alpha$ ), toll-like receptor 4 (TLR4), active nuclear factor  $\kappa$ B (NF- $\kappa$ B) and alpha smooth muscle actin ( $\alpha$ -SMA) were detected using Western blotting. Lung weight increased after an infarct with no evidence of pulmonary edema and returned to normal as a result of BYTH. In addition, BYTH treatment reduced levels of type I collagen, TGF- $\beta$ 1, and  $\alpha$ -SMA expression and decreased the phosphorylation of Smad3 in the lungs of rats after MI. BYTH treatment also reduced the elevated levels of lung inflammatory mediators such as TNF- $\alpha$ , TLR4, and NF- $\kappa$ B. Results suggested that BYTH could effectively improve lung structural remodeling after MI because of its anti-inflammatory and anti-fibrotic action, which may be mediated by suppression of the TGF- $\beta$ 1/Smad3 and NF- $\kappa$ B signaling pathways.

**Keywords:** Lung remodeling, BYTH, TGF- $\beta$ 1/Smad3, NF- $\kappa$ B, myocardial infarction

## 1. Introduction

Chronic heart failure (CHF) has been singled out as an emerging epidemic, which could be the result of increased incidence and/or increased survival leading to increased prevalence (1). In 60 to 80% of patients, congestive heart failure is complicated by pulmonary

hypertension (PH) (2,3). PH secondary to chronic left ventricular (LV) failure reduces exercise capacity and represents an important independent prognostic factor in sufferers, especially when associated with right ventricular (RV) dysfunction (4,5). However, the lungs are generally neglected by clinicians as therapeutic targets in CHF, except for symptomatic treatment of pulmonary edema. Accordingly, the mechanisms causing PH associated with CHF need to be explored and therapeutic strategies to effectively inhibit that PH need to be devised.

The mechanisms responsible for the pathobiology of PH secondary to chronic LV failure involve both

<sup>§</sup>These authors contributed equally to this work.

\*Address correspondence to:

Dr. Xiangning Cui, Department of Cardiology, Guang'anmen Hospital, China Academy of Chinese Medical Sciences, North Line 5, Xicheng District, Beijing 100053, China.  
E-mail: cuixiangning@126.com

pulmonary vascular and alveolar septa structural remodeling, which characterized by thickening of the capillary endothelial and alveolar epithelial cell basement membranes with abundant proliferation of myofibroblasts (MFs) and excess deposition of collagen with reticulin (6-9). When CHF develops, the pulmonary alveolar-capillary barrier is subjected to repeated cycles of injury and repair leading to lung parenchymal remodeling, which consists of cellular proliferation and fibrosis leading to the thickening of the inter-alveolar septa (10-12). Lung fibrosis and remodeling are initially adaptive and protect against the development of pulmonary edema, but maladaptive fibrosis and remodeling can have a negative impact on prognosis and contribute to the development of PH. Therefore, novel therapies specifically targeting lung structural remodeling may become available in the future.

Fibrosis and an inflammatory response are typical characteristics of lung structural remodeling following CHF. Transforming growth factor  $\beta$ 1 (TGF- $\beta$ 1) is a locally generated cytokine that has been implicated as a major contributor to fibroblast proliferation and lung fibrosis. The current authors and other researchers have found that lung TGF- $\beta$ 1 mRNA and protein levels increase in animal models of heart failure. TGF- $\beta$ 1 acts by binding to the membrane-bound TGF- $\beta$ 1 type II receptor (T $\beta$ RII), which activates T $\beta$ RI kinase, resulting in the phosphorylation and activation of Smad2/3. Activated Smad2/3 proteins form oligomeric complexes with Smad4 proteins and translocate into the nucleus, where they induce the expression of target genes, including extracellular matrix (ECM) proteins, and thus contribute to the development of lung fibrosis (13,14). The down-regulation of TGF- $\beta$  expression and modulation of TGF- $\beta$ /Smad signaling may be effective in preventing lung fibrosis. Animal experiments have also indicated that lung injury associated with CHF is characterized by excessive collagen deposition in the alveoli, inside the vessels, and in the vascular walls of large vessels. This is accompanied by the accumulation of leukocytes and macrophages and increased levels of tumor necrosis factor- $\alpha$  (TNF- $\alpha$ ), and Toll-like receptor-4 (TLR4) mRNA or protein in the lungs, suggesting that inflammation also plays an important role in lung structural remodeling (15). Among a variety of transcription regulators, nuclear factor  $\kappa$ B (NF- $\kappa$ B) has been found to play a critical role in regulating the expression of large numbers of genes encoding inflammatory mediators. In viral induced acute respiratory distress syndrome, treatment with curcumin was found to inhibit the inflammatory response and subsequent pulmonary fibrosis by inhibiting NF- $\kappa$ B activation and fibroblast differentiation (16). In an animal model of pulmonary fibrosis, administration of NF- $\kappa$ B pathway inhibitors dramatically inhibited pulmonary fibrogenesis (17-19). Therefore, novel

therapies specifically targeting TGF- $\beta$ 1 and NF- $\kappa$ B pathways would be of great potential therapeutic benefit in inhibiting progressive pulmonary remodeling in CHF.

In traditional Chinese medicine, a qi deficiency and blood stasis are the main causes of heart failure. The approach of supplementing qi and increasing blood circulation, or Yiqi Huoxue, is widely used in clinical practice. BaoYuan decoction (BYD) is a typical Chinese medicine to supplement qi and Tao Hong Si Wu decoction (THSWD) is a typical Chinese medicine to increase blood circulation. Both are widely used to treat patients with CHF of any etiology, including coronary heart disease, and chronic obstructive pulmonary disease. BYD was first mentioned in a famous medical text, *Jing Yue Quan Shu*, by Zhang Jingyue in 1624 (during China's Ming Dynasty). THSWD was first described in a well-known medical text, *Yi Zong Jin Jian*, in 1742 (during China's Qing Dynasty). In accordance with Yiqi Huoxue, the traditional Chinese medicines THSWD and BYD were reported to markedly improve heart function in patients with congestive heart failure in conjunction with conventional therapy (20,21). Experimental studies confirmed that THSWD can inhibit proliferation of myocardium interstitial collagenous fibers and expression of collagen protein after acute myocardial infarction (MI) in rats (22), decrease hepatic necroinflammatory disease and fibrosis in an animal model of chronic liver disease (23), and inhibit inflammatory responses by decreasing the expression of TNF- $\alpha$  in cerebral ischemia (24). Both Zhang *et al.* and Du *et al.* found that cardioprotection conferred by BYD was related to attenuation of oxidative stress and inflammatory cell infiltration in CHF post-MI induced by ligation of the left anterior descending (LAD) artery (25,26). In another study, BYD markedly prevented collagen fiber deposition, thus alleviating cardiac fibrosis in cardiac hypertrophy (27). Moreover, the use of BYD (28) in patients with chronic obstructive pulmonary disease had a positive effect on pulmonary function by improving gas diffusion and exercise capacity, suggesting that THSWD and BYD could also have beneficial effects on lung fibrosis and inflammation in CHF. The current study used a post-MI heart failure model to determine whether BYD combined with THSWD (BYTH) improved lung structural remodeling associated with CHF by inhibiting lung inflammation and fibrosis. This study also examined the possible mechanisms for the antifibrotic action of BYTH. The effects of BYTH were compared to those of valsartan. An angiotensin II receptor antagonist commonly used in clinical practice, valsartan is known to protect the heart and lungs during the treatment of CHF (6).

## 2. Materials and Methods

### 2.1. Drug preparation

All herbs in BYTH were supplied by traditional

**Table 1. Composition of Bao Yuan Tao Hong (BYTH)**

Chinese name	Botanical name	Part used	Weight (g)
Ren Shen	<i>Panax ginseng</i> C. A. Meyer	Root	9
Huang Qi	<i>Astragalus membranaceus</i> (Fisch.) Bge.	Root	27
Rou Gui	<i>Cinnamomum cassia</i> Presl.	Bark	4.5
Zhi Gan Cao	<i>Glycyrrhiza uralensis</i> Fisch.	Root and rhizome	9
Shu Di Huang	<i>Rehmannia glutinosa</i> Libosch.	Root tuber	12
Dang Gui	<i>Angelica sinensis</i> (Oliv.) Diels	Root	9
Bai Shao	<i>Paeonia lactiflora</i> Pall.	Root	9
Chuan Xiong	<i>Ligusticum chuanxiong</i> Hort.	Rhizome	6
Tao Ren	<i>Prunus persica</i> (L.) Batsch	Seed	9
Hong Hua	<i>Carthamus tinctorius</i> L.	Flower	9

Chinese medicine pharmacy of Guang'anmen Hospital, China Academy of Chinese Medical Sciences. Species were carefully examined by professional traditional Chinese pharmacists at Guang'anmen Hospital, and the composition and dose are listed in Table 1. The herb mixtures were soaked in 10 volumes (v/w) of distilled water for 90 min and then boiled for 60 min (single decoction of *Panax ginseng*). The decoction was poured into a container. The dregs in the original container were added to 8 volumes (v/w) of distilled water and boiled again for 60 min. The two decoctions were mixed together and filtered repeatedly through a 100-mesh sieve to yield a concentration of 1 g of crude drug/mL. The pre-prepared decoction was poured in a centrifuge tube and stored at 4°C before use. BYTH was administered by oral gavage at a dose of 15 g/kg/day in this study. Valsartan (batch number X1428), manufactured by Beijing Novartis Pharmaceutical Co. Ltd., was dissolved in sterile water.

## 2.2. Animal model and administration

Male Sprague-Dawley (SD) rats (220-250 g) were donated by Beijing Vital River Laboratory Animal Technology Co. Ltd. (animal license number: SCXK (Beijing) 2012-0001). All animal experimental procedures and protocols were approved by the Institutional Animal Care and Use Committee of Guang'anmen Hospital, China Academy of Chinese Medical Sciences. A rat model of CHF was created by inducing MI following ligation of the LAD artery (25,26,29-32). Briefly, rats were intra-peritoneally anaesthetized with 1% sodium pentobarbital solution (50 mg/kg), intubated, and placed on a rodent ventilator (Huaihe Apparatus, Shanghai). A left-sided thoracotomy was performed in order to expose the heart, and the proximal left anterior descending coronary artery was ligated. The sham group underwent the same procedure with the exception of ligation of the artery. A 12-lead ECG was recorded before and after surgery. Rats after MI were fed normally for 4 weeks. Based on the results of transthoracic echocardiography (Table 2), the surviving rats were randomly assigned to the following groups: a CHF group ( $n = 12$ ), a sham group ( $n = 10$ ), a BYTH

**Table 2. Echocardiographic ejection fraction levels in the study groups before treatment with BYTH ( $\bar{x} \pm s$ )**

Group	n	EF (%)
Sham	10	$84.490 \pm 7.3354$
CHF	12	$44.708 \pm 8.4369^*$
BYTH	10	$46.863 \pm 9.0312^*$
Valsartan	9	$47.911 \pm 9.1068^*$

\*:  $p > 0.05$  vs. the sham group

group ( $n = 10$ ), and a valsartan group ( $n = 9$ ). BYTH (15 g/kg) and valsartan (10 mg/kg) were administered by gavage once a day for 4 weeks. An equal volume of distilled water was administered to the CHF and sham groups.

## 2.3. Transthoracic echocardiography

Rats in each group were examined to evaluate the morphology and function of the left ventricle using noninvasive transthoracic echocardiography. Short-axis images were obtained at the papillary muscle level and 2-D-guided M-mode tracings were recorded at a speed of 200 mm/s. Anterior and posterior end-diastolic wall thickness and LV internal dimensions were measured and the percent fractional shortening (FS%) was calculated. Left atrial (LA) volume, LV end-diastolic volume (EDV), LV end-systolic volume (ESV), LV ejection fraction (EF), LV end-diastolic dimension (LVIDd), and LV end-systolic dimension (LVIDs) were measured and calculated from apical views.

## 2.4. Sample preparation

At the end of 4 weeks, the rats were sacrificed by removing the heart, lung, and other major organs under abundant anesthesia, and the organs were immediately weighed. Lung tissue was dried at 58°C to a constant weight. The relative water content in lung tissue was calculated. The left lung and left ventricle were snap frozen in liquid nitrogen pending biochemical analysis. The airway of the upper right lobe and the heart were subsequently fixed in 4% paraformaldehyde and embedded in paraffin for histological analysis.

## 2.5. Hematoxylin and eosin (HE) and Masson staining

Rat lungs and hearts were fixed in formalin for 48 h, embedded in paraffin, and sectioned into 4-mm thick slices for HE staining or Masson staining. After slides with stained tissue slices were sealed with neutral gum, they were microscopically examined at the appropriate magnification. Color images of five randomly chosen microscopic fields were obtained from each slice. Medical imaging software (NIH image, Bethesda, MD) was used to semi-quantitatively determine the area density (AD) *i.e.* the area of collagen fibers with respect to the area of the lung.

## 2.6. Immunohistochemical staining

Immunohistochemical staining for smooth muscle  $\alpha$ -actin ( $\alpha$ -SMA) was used to identify smooth muscle cells or myofibroblasts (using a mouse monoclonal anti- $\alpha$  smooth muscle actin antibody, Abcam, Inc.), and staining for NF- $\kappa$ B was performed on 4- $\mu$ m sections of tissue deparaffinized using xylene. Endogenous peroxidase was quenched with 3% H<sub>2</sub>O<sub>2</sub> for 10 min. The antigen was recovered in Tris-EDTA buffer (pH = 9.0) for 2 min and 30 s at 140°C and then washed in phosphate-buffered saline (PBS). The sections were incubated with monoclonal anti  $\alpha$ -SMA antibody (1:200, Abcam, Inc.) or rabbit anti-NF- $\kappa$ B p65 (1:200; Santa Cruz, Inc.) at 37°C for 1 h followed by biotinylated secondary antibody for 20 min. The sections were stained with diaminobenzidine chromogen and counterstained with hematoxylin.

## 2.7. Western blot analysis

Total protein was obtained from heart and lung tissues by sonication, centrifugation, and heat denaturation. The protein lysates were electrophoresed and separated on 10% sodium dodecyl sulfate-polyacrylamide gels and then transferred onto nitrocellulose membranes (Millipore, Inc, USA). The membranes were blocked with 5% skim milk at room temperature for 1 h and then incubated overnight at 4°C with primary antibodies, including rabbit polyclonal Anti-Collagen I (1:800, ABcam, Inc.), mouse monoclonal anti-TGF- $\beta$ 1 (1:500, Abcam, Inc.), rabbit monoclonal anti-Smad3 (phosphor C25A9) (1:500, Cell Signaling Technology, Inc.), rabbit polyclonal anti-TNF- $\alpha$  (1:1000, Abcam, Inc.), mouse monoclonal anti-TLR4 (1:2000, Abcam, Inc.), and rabbit anti-NF- $\kappa$ B p65 (1:800; Santa Cruz, Inc.). The membranes were then incubated with the secondary antibody (1:2000) at room temperature for 2 h. Electrochemiluminescence was induced and the Gene Gnome Gel Imaging System (Syngene Co.) was used to capture the resulting images. Image J (NIH image, Bethesda, MD) was used to analyze the gel images. The results were expressed as density values normalized to GAPDH.

## 2.8. Statistical analysis

Data were expressed as the mean  $\pm$  standard deviation. The statistical significance of differences between mean values was determined using one-way analysis of variance (ANOVA), and a *p* value of less than 0.05 was considered significant. Statistical calculations were performed using the software SPSS verion19.0.

## 3. Results

### 3.1. Effects of BYTH on LV function and LV remodeling

LV echocardiographic parameters are shown in Figure 1. The ejection fraction and fractional shortening measurements were greater in the BYTH group and the valsartan group than those in the CHF group (*p* < 0.05) (Figure 1B and 1C), while the end-systolic volume and LV end-systolic dimension measurements were smaller (*p* < 0.05) (Figure 1D and 1E). Although the EDV and LVIDd tended to decrease in both the BYTH and the valsartan groups versus those in the CHF group, the difference was not statistically significant (*p* > 0.05) (Figure 1F and 1G). EF and FS measurements in the CHF group, the BYTH group, and the valsartan group were smaller than those in the sham group (*p* < 0.05) (Figure 1B and 1C), while the ESV and LVIDs increased (*p* < 0.05) (Figure 1D and 1E). Histological study revealed that the fractional area of collagen in the LV (Figure 2A and 2B) increased markedly in the CHF group in comparison to that in the sham group (*p* < 0.05), and that area decreased as a result of BYTH and valsartan treatment. The parameters of LV remodeling and dysfunction were significantly altered by BYTH treatment.

### 3.2. Effects of BYTH on pulmonary structural remolding

As shown in Figure 3, the wet lung/body weight ratio increased after MI (*p* < 0.05) and BYTH and valsartan markedly improved this ratio (*p* < 0.05) (Figure 3A). Similarly, the dry lung/body weight ratio increased after MI (*p* < 0.05), providing evidence of substantial pulmonary remodeling; treatment with BYTH and valsartan reversed the increase in this ratio (*p* < 0.05) (Figure 3B). The dry/wet lung weight ratio was comparable among all groups, suggesting that no significant edema occurred (Figure 3C).

HE staining revealed intact and clear alveoli, normal interstitium, and few inflammatory cells in the lungs of the sham group. However, the CHF group had LV dysfunction caused by progressive lung injury, as evinced by destruction of lung alveoli, inflammatory cell infiltration, and thickening of the lung interstitium. BYTH or valsartan treatment prevented these changes in the lungs of rats after MI. Interestingly, the CHF group had prominent pulmonary vascular and perivascular

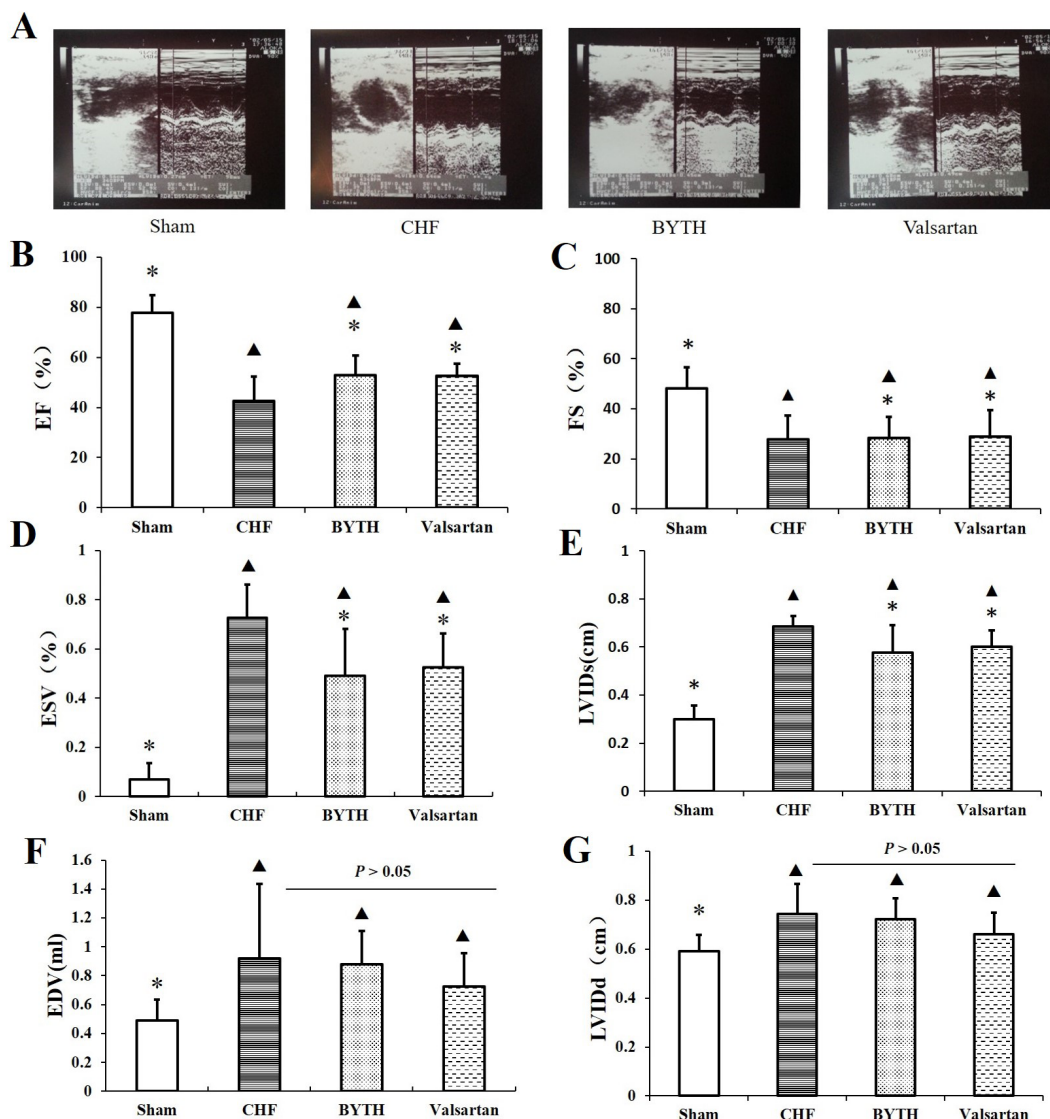


**Figure 1.** Effects of BYTH on echocardiographic left ventricular (LV) function in rats with CHF. **(A)** Typical echocardiography images; **(B)** LV ejection fraction (EF); **(C)** LV fractional shortening (FS); **(D)** LV end-systolic volume (ESV); **(E)** LV end-systolic dimensions (LVIDs); **(F)** LV end-diastolic volume (EDV) and **(G)** LV end-diastolic dimension (LVIDd) ( $\blacktriangle p < 0.05$  vs. the sham group,  $*$  $p < 0.05$  vs. the CHF group).

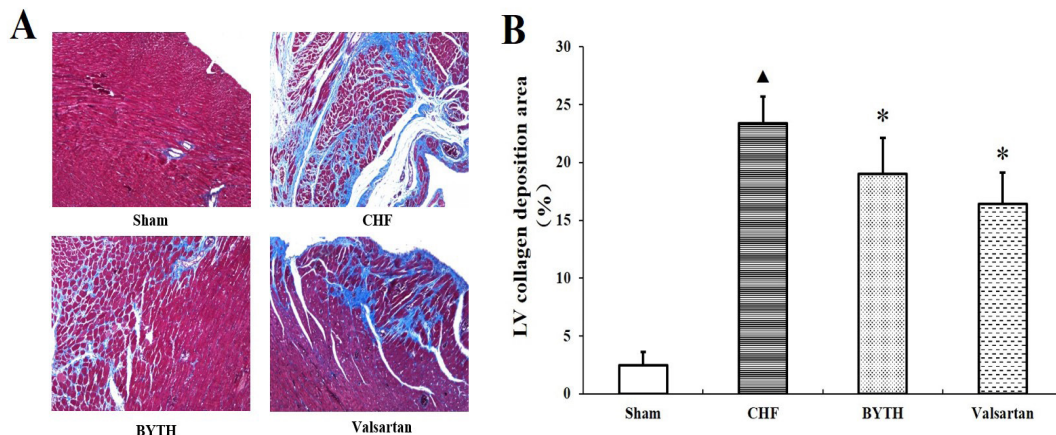


**Figure 2.** Effects of BYTH on myocardial fibrosis in rats with CHF. **(A)** Representative Masson Trichrome-stained LV areas are shown and blue areas indicate fibrotic staining ( $\times 10$ ); **(B)** Fibrosis was measured in the whole LV section, and 5 sections were calculated for each heart ( $\blacktriangle p < 0.05$  vs. the sham group,  $*$  $p < 0.05$  vs. the CHF group).

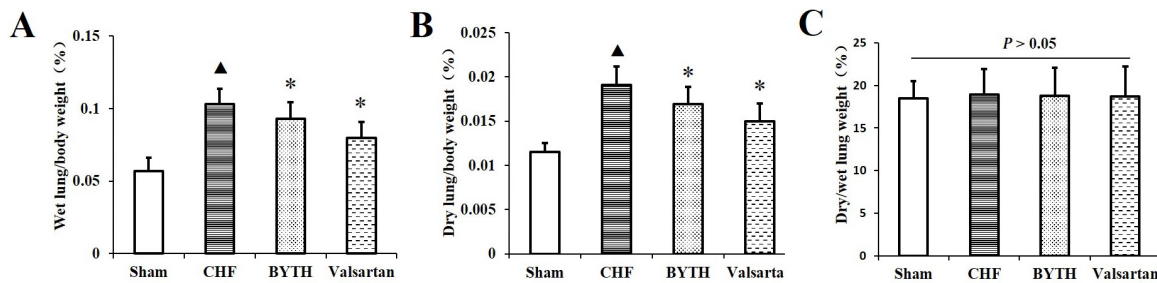


**Figure 3. Effect of BYTH on lung weight in rats with CHF. (A)** Wet lung/body weight; **(B)** Dry lung/body weight; **(C)** Ratio of dry/wet lung weight. (<sup>▲</sup> $p < 0.05$  vs. the sham group, \* $p < 0.05$  vs. the CHF group).

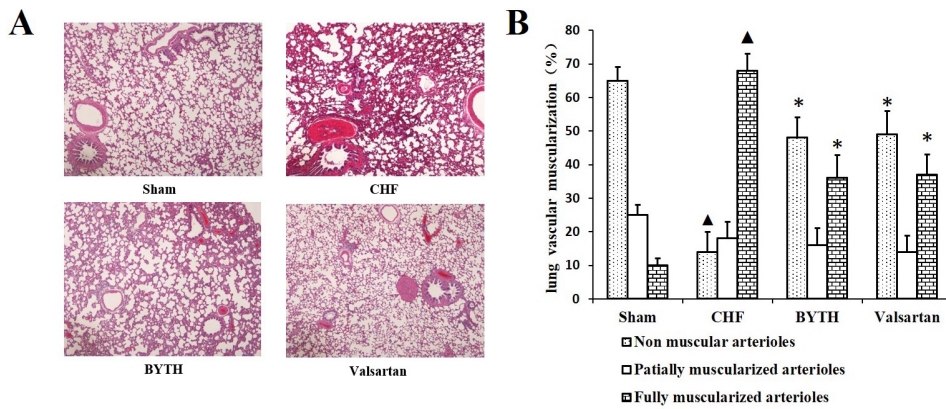


**Figure 4. Effects of BYTH on lung vascular masculinization in rats with CHF. (A)** Histological lung section with hematoxylin and eosin staining ( $\times 40$ ); **(B)** Quantitative analysis of the distribution of non-muscular, partially muscular, and fully muscularized small arteries (<sup>▲</sup> $p < 0.05$  vs. the sham group, \* $p < 0.05$  vs. the CHF group).

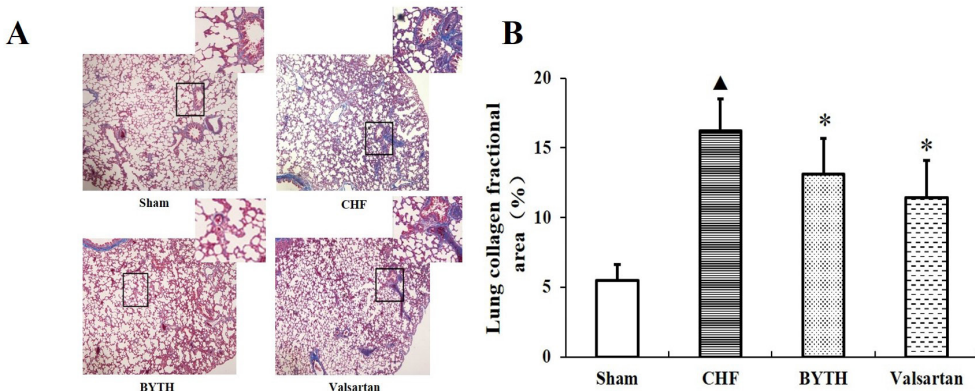


**Figure 5. Effects of BYTH on pulmonary structural remodeling in rats with CHF. (A)** Masson's trichrome staining for collagen in blue ( $\times 40$ ); **(B)** Quantitative analysis of lung collagen deposition (<sup>▲</sup> $p < 0.05$  vs. the sham group, \* $p < 0.05$  vs. the CHF group).

remodeling. LV dysfunction also caused an increase in fully muscularized (FM) small arteries, but there were significantly fewer FM small arteries in rats in the BYTH and valsartan groups compared to the number in the CHF group. Similarly, the BYTH treatment group had significantly more non-muscularized (NM) small arteries compared to the CHF group (Figure 4), indicating that BYTH and valsartan significantly improved lung vascular remodeling induced by ligation

of the LAD artery. Masson trichrome staining also revealed intact alveoli and normal interstitium in the lungs of rats in the sham group. Ligation of the LAD artery resulted in greater destruction of lung alveoli, thickening of interstitium, and fibroblast diffusion in rat lungs, and BYTH or valsartan treatment significantly halted these changes in rat lungs after MI (Figure 5).  $\alpha$ -SMA expression has been extensively used as a marker of fibroblast differentiation into its activated state, the

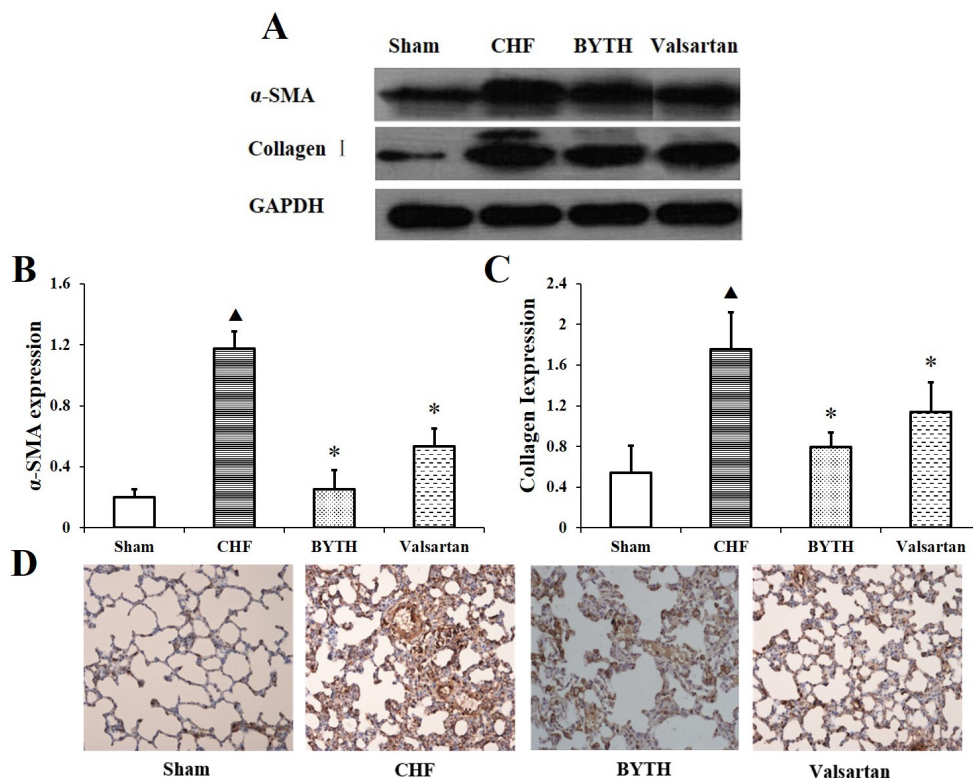


**Figure 6. Effects of BYTH on expression of proteins related to lung fibrosis in rats with CHF. (A)** and (B) Expression of  $\alpha$ -SMA; (A) and (C) Expression of type I collagen; (D) Immunohistochemistry for  $\alpha$ -SMA; original magnification  $\times 100$  ( $\blacktriangle p < 0.05$  vs. the sham group,  $*p < 0.05$  vs. the CHF group).

myofibroblast. Expression of  $\alpha$ -SMA increased in the interalveolar septa of animals after MI compared to its expression in the sham group; however, BYTH and valsartan treatment significantly reduced that expression (Figure 6).

$\alpha$ -SMA-positive MFs actively synthesize ECM components. Type I collagen, the main collagen isoform produced by fibroblasts in many fibrotic processes, was measured in the current study. Western blotting revealed that type I collagen deposition was significantly greater in rats in the CHF group compared to that in the sham group; however, BYTH significantly decreased the expression of type I collagen protein in the lungs (Figure 6). Together, these findings indicate that the parameters of lung tissue fibrotic remodeling were significantly reversed by BYTH and valsartan treatment.

### 3.3. Effects of BYTH on the TGF- $\beta$ 1/Smad3 signaling pathway in rat lungs after CHF

CHF markedly increased the level of TGF- $\beta$ 1 protein in treated rat compared to that in the sham group at the endpoint of 4 weeks; however, BYTH and valsartan treatment significantly reduced the level of TGF- $\beta$ 1 expression compared to that in the CHF group (Figure 7). Similarly, CHF markedly increased the level of p-Smad3 protein in the lungs of treated rats compared to that in the sham group, and BYTH and valsartan treatment

significantly reduced p-Smad3 expression compared to that in the CHF group (Figure 7).

### 3.4. Effects of BYTH on the NF- $\kappa$ B signaling pathway in rat lungs after CHF

As shown in Figure 8, results indicated that the CHF group had increased expression of lung TNF- $\alpha$ , TIR4, and NF- $\kappa$ B p65 protein compared to expression in the sham group. After 4 weeks of treatment, BYTH significantly reversed those changes (Figure 8).

## 4. Discussion

The current results indicated that treatment with BYTH protects the pulmonary structure and cardiac function in rats after MI. After MI, rats developed CHF with major lung structural remodeling characterized by alveolar wall collagen deposition, a dramatic increase in the percentage of FM lung vessels, and an increase in expression of inflammatory cytokines in lung tissues. Treatment with BYTH and valsartan reduced lung and vascular fibrosis, fibroblast proliferation, and proinflammatory cytokine expression. The mechanism for this action may involve suppression of TGF- $\beta$ 1/Smad3 and NF- $\kappa$ B signaling. The current results suggest that BYTH has some direct beneficial effects on pulmonary fibrosis and the inflammatory response following CHF.

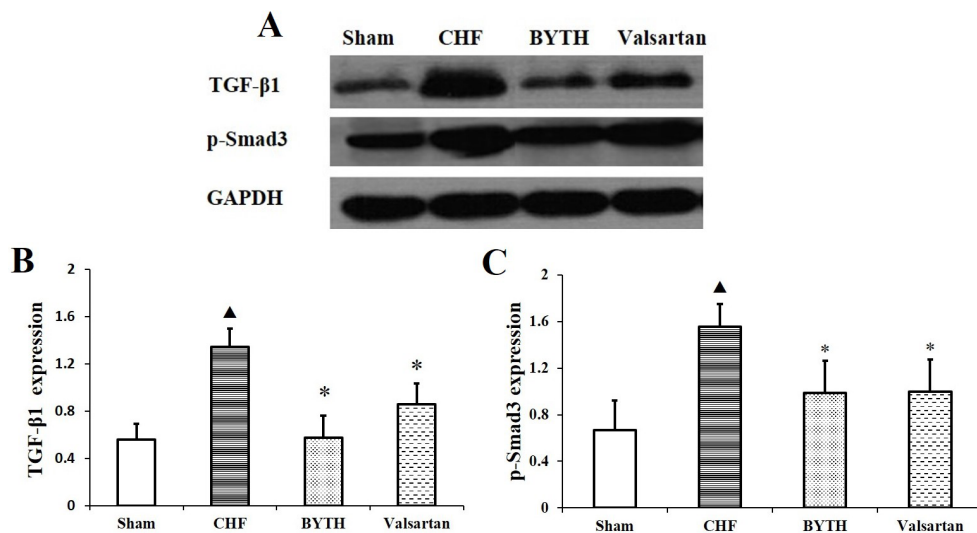


**Figure 7. Effects of BYTH on lung TGF- $\beta$ 1/Smad3 signaling pathway expression in rats with CHF.** (A) Expression of transforming growth factor TGF- $\beta$ 1; (B) and (C) Expression of p-Smad3 ( $\blacktriangle p < 0.05$  vs. the sham group,  $*$  $p < 0.05$  vs. the CHF group).

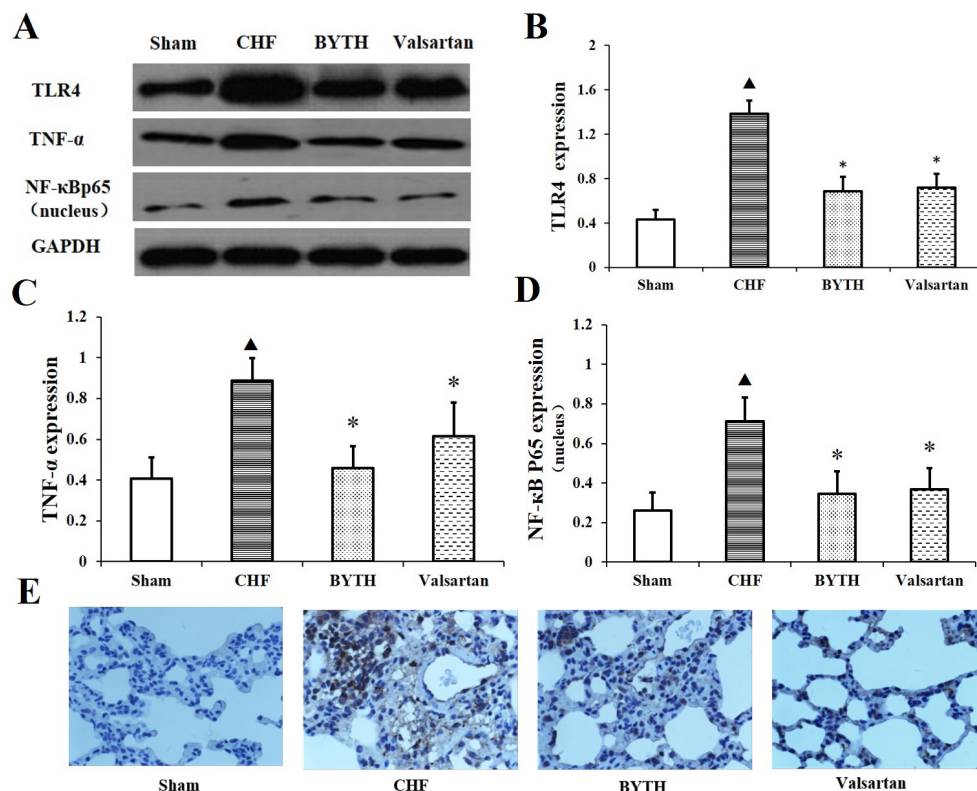


**Figure 8. Effects of BYTH on expression of protein related to lung inflammation in rats with CHF.** (A) and (B) Expression of TLR4; (A) and (C) Expression of TNF- $\alpha$ ; (A) and (D) The activation of NF- $\kappa$ B; (E) Immunohistochemistry for NF- $\kappa$ B; Original magnification  $\times 100$  ( $\blacktriangle p < 0.05$  vs. the sham group,  $*$  $p < 0.05$  vs. the CHF group).

The lungs are the organs most affected by CHF. In patients with CHF, an elevation in the LV filling pressure results in a passive increase in pulmonary venous pressure and pulmonary alveolar-capillary stress failure, resulting in cycles of alveolar wall injury and repair. Consequently, pathological morphological changes occur in small pulmonary arteries as well as in the alveolar-

epithelial units and the ECM (8,33-36). This reparative "scarring" process causes a restrictive lung syndrome characterized by impaired gas exchange (37), a reduction in lung volume, and decreased lung compliance. This pathological process may also contribute to type 2 PH (PH secondary to chronic LV failure), further increase the RV afterload and RV dysfunction, and ultimately

cause heart failure. Lung structural remodeling may be a key factor for poor clinical outcomes in patients with end-stage heart failure. Thus, the effective treatment of LV end-stage heart failure may require additional action to reduce lung fibrosis.

The current results revealed that the total lung weight in the CHF group increased while water content in the lungs decreased. This indicates that, in CHF models, the pulmonary weight increase is due to structural remodeling with abundant proliferation of MFs and excess collagen, elastin, and reticulin deposition (ECM deposition) rather than edema. MFs have been found to play a key role in animal as well as human pulmonary fibrotic disorders (38). MFs are characterized by the expression of  $\alpha$ -SMA, as well as excessive production of collagenous ECM after tissue injury. The current study found that excessive collagen deposition and upregulated  $\alpha$ -SMA protein expression in lungs after MI were both reversed by BYTH treatment, suggesting that BYTH may have anti-fibrotic action by inhibiting MF proliferation and collagen production.

From the perspective of traditional Chinese medicine, the fundamental problem in heart failure post-MI is the prolonged deficiency of qi in the heart, which causes the heart to become too weak to move blood and transport fluid, leading to blood "stasis" and phlegm "stagnation," resulting in accumulation in the heart and lungs. These concepts are consistent with the pathological changes of collagen deposition and interstitial fibrosis. The heart and lungs are closely related, and the approach of supplementing qi and increasing blood circulation, or Yiqi Huoxue, is widely used in the treatment of cardiac and pulmonary diseases. BYD is a typical Chinese medicine to supplement qi and THSWD is a typical Chinese medicine to increase blood circulation. BYTH consists of BYD and THSWD, which include 10 Chinese herbs. The main active ingredients of those medicines are Astragalus membranaceus and Panax ginseng, which invigorate qi in the heart and lungs. Peach pits, Carthamus tinctorius, Ligusticum chuanxiong, and Radix angelicae sinensis increase blood circulation and eliminate the stasis of blood, water, and phlegm. Modern pharmacological research has indicated that ginseng, one of the main components of BYTH, has cardiovascular benefits and is therefore usually used to treat heart disease (39). Emerging evidence also suggests that ginseng attenuates myocardial hypertrophy, thus blunting the processes of remodeling and heart failure (40). Astragalus injections can enhance myocardial contractility, improve circulation, protect myocardial cells, and regulate immunity (41). The current study found that BYTH protects from cardiac and pulmonary injury induced by MI in rats.

TGF- $\beta$ 1 is a locally generated cytokine that has been implicated as a major contributor to fibroblast proliferation and tissue fibrosis in various organ systems. Increased lung TGF- $\beta$ 1 mRNA and protein levels

in mice with heart failure suggest that the TGF- $\beta$ 1 signaling pathway might contribute to the development of lung fibrosis and remodeling in this model (42). As a main downstream signal transducer of TGF- $\beta$ 1, Smad3 can be phosphorylated by an activated type I receptor of TGF- $\beta$ 1. It then forms a complex with Smad4 and translocates into the nucleus, where it acts as a transcription factor and it promotes the expression of target genes including type I and type III collagen. The current study indicated that lung TGF- $\beta$ 1 protein expression increased in rats with heart failure following MI, and the level of p-Smad3 also increased markedly; both were reversed by BYTH. These results suggest that the significant activation of the TGF- $\beta$ 1/Smad3 signaling pathway in lung tissues after CHF can lead to fibroblast proliferation and a marked upregulation of type I collagen expression. BYTH may disrupt the TGF- $\beta$ 1/Smad3 signaling pathway, which may be why it attenuates lung fibrosis in CHF.

Inflammation is an integral part of the healing response to lung injury induced by CHF. While inflammation may be beneficial in the short term (for example, by inducing immune responses that lead to the eradication of pathogens), chronic inflammation and the associated regenerative wound healing response are closely linked to the development of fibrosis. In the inflammatory cascade, NF- $\kappa$ B is a predominant regulator of inflammatory cytokines. Activated NF- $\kappa$ B increases the expression of TGF- $\beta$ 1, TNF- $\alpha$ , and IL-1 $\beta$ , which subsequently activate collagen deposition and fibrosis that lead to lung structural remodeling. Inhibition of the NF- $\kappa$ B pathway can ameliorate pulmonary inflammation and fibrosis. Thus, NF- $\kappa$ B signaling plays an important role in both fibrosis and an inflammatory response. An inflammatory response is usually associated with the activation of innate immunity. Recent studies have suggested that lung TLR4 expression both at the mRNA and protein level increased in mice with heart failure (15). TLR4-mediated pathways played a key role in triggering the lung inflammatory response by activating the NF- $\kappa$ B system. The current study revealed increased expression of lung TLR4, NF- $\kappa$ B, and TNF- $\alpha$  following the induction of MI, and treatment with BYTH significantly decreased the expression of those inflammatory markers. The pulmonary protective effects of BYTH may be because it suppresses the TLR4/NF- $\kappa$ B signaling pathway.

In conclusion, the current study revealed that treatment with BYTH has notable benefits in terms of preventing lung structural remodeling following MI. The potential mechanisms of that action may be associated with the anti-fibrotic and anti-inflammatory action of BYTH on lung issue. Based on the current results, BYTH has anti-fibrotic action mainly by suppressing the TGF- $\beta$ 1/Smad3 signaling pathway, which might contribute to its attenuation of myofibroblast proliferation and collagen deposition. The possible mechanisms may

also involve inhibition of the excessive expression of the TLR4-NF- $\kappa$ B pathway.

### Acknowledgements

This work was supported by a grant from the National Natural Science Foundation of China (Grant No. 81273945).

### References

1. Roger VL. The heart failure epidemic. *Int J Environ Res Public Health.* 2010; 7:1807-1830.
2. Ghio S, Gavazzi A, Campana C, Inserra C, Klersy C, Sebastiani R, Arbustini E, Recusani F, Tavazzi L. Independent and additive prognostic value of right ventricular systolic function and pulmonary artery pressure in patients with chronic heart failure. *J Am Coll Cardiol.* 2001; 37:183-188.
3. Lam CS, Roger VL, Rodeheffer RJ, Borlaug BA, Enders FT, Redfield MM. Pulmonary hypertension in heart failure with preserved ejection fraction: A community-based study. *J Am Coll Cardiol.* 2009; 53:1119-1126.
4. Abramson SV, Burke JF, Kelly JJ, Kitchen JG, Dougherty MJ, Yih DF, McGeehin FC, Shuck JW, Phiambolis TP. Pulmonary hypertension predicts mortality and morbidity in patients with dilated cardiomyopathy. *Ann Intern Med.* 1992; 116:888-895.
5. Butler J, Chomsky DB, Wilson JR. Pulmonary hypertension and exercise intolerance in patients with heart failure. *J Am Coll Cardiol.* 1999; 34:1802-1806.
6. Huang W, Kingsbury MP, Turner MA, Donnelly JL, Flores NA, Sheridan DJ. Capillary filtration is reduced in lungs adapted to chronic heart failure: morphological and haemodynamic correlates. *Cardiovasc Res.* 2001; 49:207-217.
7. Jasmin JF, Calderone A, Leung TK, Villeneuve L, Dupuis J. Lung structural remodeling and pulmonary hypertension after myocardial infarction: Complete reversal with irbesartan. *Cardiovasc Res.* 2003; 58:621-631.
8. Kingsbury MP, Huang W, Donnelly JL, Jackson E, Needham E, Turner MA, Sheridan DJ. Structural remodelling of lungs in chronic heart failure. *Basic Res Cardiol.* 2003; 98:295-303.
9. Gehlbach BK, Geppert E. The pulmonary manifestations of left heart failure. *Chest.* 2004; 125:669-682.
10. West JB, Mathieu-Costello O. Vulnerability of pulmonary capillaries in heart disease. *Circulation.* 1995; 92:622-631.
11. Townsley MI, Fu Z, Mathieu-Costello O, West JB. Pulmonary microvascular permeability. Responses to high vascular pressure after induction of pacing-induced heart failure in dogs. *Circ Res.* 1995; 77:317-325.
12. Guazzi M. Alveolar-capillary membrane dysfunction in heart failure: Evidence of a pathophysiologic role. *Chest.* 2003; 124:1090-1102.
13. Mackinnon AC, Gibbons MA, Farnworth SL, Leffler H, Nilsson UJ, Delaine T, Simpson AJ, Forbes SJ, Hirani N, Gauldie J. Regulation of transforming growth factor- $\beta$ 1-driven lung fibrosis by galectin-3. *Am J Respir Crit Care Med.* 2012; 185:537-546.
14. Chen T, Nie H, Gao X, Yang J, Pu J, Chen Z, Cui X, Wang Y, Wang H, Jia G. Epithelial-mesenchymal transition involved in pulmonary fibrosis induced by multi-walled carbon nanotubes via TGF-beta/Smad signaling pathway. *Toxicol Lett.* 2014; 226:150-162.
15. Chen Y, Guo H, Xu D, Xu X, Wang H, Hu X, Lu Z, Kwak D, Xu Y, Gunther R, Huo Y, Weir EK. Left ventricular failure produces profound lung remodeling and pulmonary hypertension in mice heart failure causes severe lung disease. *Hypertension.* 2012; 59:1170-1178.
16. Avasarala S, Zhang F, Liu G, Wang R, London SD, London L. Curcumin modulates the inflammatory response and inhibits subsequent fibrosis in a mouse model of viral-induced acute respiratory distress syndrome. *PLoS One.* 2012; 8:e57285.
17. Cao H, Zhou X, Zhang J, Huang X, Zhai Y, Zhang X, Chu L. Hydrogen sulfide protects against bleomycin-induced pulmonary fibrosis in rats by inhibiting NF- $\kappa$ B expression and regulating Th1/Th2 balance. *Toxicol Lett.* 2013; 224:387-394.
18. Chitra P, Saiprasad G, Manikandan R, Sudhandiran G. Berberine attenuates bleomycin induced pulmonary toxicity and fibrosis via suppressing NF- $\kappa$ B dependant TGF- $\beta$  activation: A biphasic experimental study. *Toxicol Lett.* 2013; 219: 178-193.
19. El-Khouly D, El-Bakly WM, Awad AS, El-Mesallamy HO, El-Demerdash E. Thymoquinone blocks lung injury and fibrosis by attenuating bleomycin-induced oxidative stress and activation of nuclear factor Kappa-B in rats. *Toxicology.* 2012; 302:106-113.
20. Li DP, Chen Q, Yi L. Effects of yiqi huoxue method on cardiac function in patients with congestive heart failure. *Zhongguo Zhong Xi Yi Jie He Za Zhi.* 2006; 26:552-554. (in Chinese)
21. Sun CC, Gao SS. Clinical observation on treating heart failure with Baoyuan decoction and Taohong Siwu decoction. *Clinical Journal of Chinese Medicine.* 2014; 6:62-63. (in Chinese)
22. Zhou YC, Liu B, Wang J, Sun XG, Huang GQ, Zeng YJ, Chen J. Influence of Taohong Siwu decoction on myocardium interstitial collagen reconstitution after acute myocardial infarction in rats. *Chinese Journal of Experimental Traditional Medical Formulae.* 2011; 17:152-155. (in Chinese)
23. Xi S, Shi M, Jiang X, Minuk GY, Cheng Y, Peng Y, Gong Y, Xu Y, Wang X, Yang J, Yue L, Wang Y. The effects of Tao-Hong-Si-Wu on hepatic necroinflammatory activity and fibrosis in a murine model of chronic liver disease. *J Ethnopharmacol.* 2016; 180:28-36.
24. Yen TL, Ong ET, Lin KH, Chang CC, Jayakumar T, Lin SC, Fong TH, Sheu JR. Potential advantages of Chinese medicine Taohong Siwu Decoction () combined with tissue-plasminogen activator for alleviating middle cerebral artery occlusion-induced embolic stroke in rats. *Chin J Integr Med.* 2014;1-9.
25. Zhang Y, Li C, Meng H, Guo D, Zhang Q, Lu W, Wang Q, Wang Y, Tu P. BYD ameliorates oxidative stress-induced myocardial apoptosis in heart failure post-acute myocardial infarction via the P38 MAPK-CRYAB signaling pathway. *Front Physiol.* 2018; 9:505.
26. Du Z, Shu Z, Lei W, Li C, Zeng K, Guo X, Zhao M, Tu P, Jiang Y. Integration of metabolomics and transcriptomics reveals the therapeutic effects and mechanisms of Baoyuan decoction for myocardial ischemia. *Front Pharmacol.* 2018; 9:514.
27. Du Z, Wen R, Liu Q, Wang J, Lu Y, Zhao M, Guo X,

- Tu P, Jiang Y.  $^1\text{H}$  NMR-based dynamic metabolomics delineates the therapeutic effects of Baoyuan decoction on isoproterenol-induced cardiac hypertrophy. *J Pharm Biomed Anal.* 2018; 163:64-77.
28. Wu CJ, Xie XM. Thirty cases with chronic obstructive pulmonary disease at acute and aggravated stage treated with Original Qi Preserving decoction. *Henan Traditional Chinese Medicine.* 2015; 35:2167-2168. (in Chinese)
29. Samsamshariat SA, Samsamshariat ZA, Movahed MR. A novel method for safe and accurate left anterior descending coronary artery ligation for research in rats. *Cardiovasc Revasc Med.* 2005; 6:121-123.
30. Muthuramu I, Lox M, Jacobs F, De Geest B. Permanent ligation of the left anterior descending coronary artery in mice: A model of post-myocardial infarction remodelling and heart failure. *J Vis Exp.* 2014; 2: e52206.
31. Liang T, Zhang Y, Yin S, Gan T, An T, Zhang R, Wang Y, Huang Y, Zhou Q, Zhang J. Cardio-protecteffect of qiliqiangxin capsule on left ventricular remodeling, dysfunction and apoptosis in heart failure rats after chronic myocardial infarction. *Am J Transl Res.* 2016; 8:2047-2058.
32. Luo J, Chen X, Luo C, Lu G, Peng L, Gao X, Zuo Z. Hydrochlorothiazide modulates ischemic heart failure-induced cardiac remodeling via inhibiting angiotensin II type 1 receptor pathway in rats. *Cardiovasc Ther.* 2017; 35: e12246.
33. Delgado JF, Conde E, Sánchez V, López-Ríos F, Gómez-Sánchez MA, Escribano P, Sotelo T, Gómez de la Cámara A, Cortina J, de la Calzada CS. Pulmonary vascular remodeling in pulmonary hypertension due to chronic heart failure. *Eur J Heart Fail.* 2005; 7:1011-1016.
34. Townsley M, Snell KS, Ivey CL, Culberson DE, Liu DC, Reed RK, Mathieu-Costello O. Remodeling of lung interstitium but not resistance vessels in canine pacing-induced heart failure. *J Appl Physiol (1985).* 1999; 87:1823-1830.
35. Ahmed MS, Øie E, Vinge LE, von Lueder TG, Attramadal T, Attramadal H. Induction of pulmonary connective tissue growth factor in heart failure is associated with pulmonary parenchymal and vascular remodeling. *Cardiovasc Res.* 2007; 74:323-333.
36. Jiang BH, Tardif JC, Sauvageau S, Ducharme A, Shi Y, Martin JG, Dupuis J. Beneficial effects of atorvastatin on lung structural remodeling and function in ischemic heart failure. *J Card Fail.* 2010; 16:679-688.
37. Cahalin LP, Chase P, Arena R, Myers J, Bensimhon D, Peberdy MA, Ashley E, West E, Forman DE, Pinkstaff S, Lavie CJ, Guazzi M. A meta-analysis of the prognostic significance of cardiopulmonary exercise testing in patients with heart failure. *Heart Fail Rev.* 2013; 18:79-94.
38. Zhang K, Rekhter MD, Gordon D, Phan SH. Myofibroblasts and their role in lung collagen gene expression during pulmonary fibrosis. A combined immunohistochemical and *in situ* hybridization study. *Am Journal Pathol.* 1994; 145:114-125.
39. Zheng SD, Wu HJ, Wu DL. Roles and mechanisms of ginseng in protecting heart. *Chin J Integr Med.* 2012; 18:548-555.
40. Karmazyn M, Moey M, Gan XT. Therapeutic potential of ginseng in the management of cardiovascular disorders. *Drugs.* 2011; 71:1989-2008.
41. Zhang JG, Gao DS, Wei GH. Clinical study on effect of Astragalus injection on left ventricular remodeling and left ventricular function in patients with acute myocardial infarction. *Zhongguo Zhong Xi Yi Jie He Za Zhi.* 2002; 22:346-348. (in Chinese)
42. Ikeuchi M, Tsutsui H, Shiomi T, Matsusaka H, Matsushima S, Wen J, Kubota T, Takeshita A. Inhibition of TGF-beta signaling exacerbates early cardiac dysfunction but prevents late remodeling after infarction. *Cardiovasc Res.* 2004; 64:526-535.

(Received October 8, 2018; Revised October 27, 2018;  
Accepted October 29, 2018)

## Novel compound heterozygous mutations in *SLC26A4* gene in a Chinese family with enlarged vestibular aqueduct

Xuelei Zhao, Xiaohua Cheng, Lihui Huang\*, Xianlei Wang, Cheng Wen, Xueyao Wang

Beijing Tongren Hospital, Capital Medical University; Beijing Institute of Otolaryngology; Key Laboratory of Otolaryngology, Head and Neck Surgery, Ministry of Education, Beijing, China.

### Summary

In order to investigate the genetic causes of hearing loss in a Chinese proband with nonsyndromic hearing loss and enlarged vestibular aqueduct (EVA), we conducted clinical and genetic evaluations in a deaf proband and her parents with normal hearing. 20 exons and flanking splice sites of the *SLC26A4* gene were screened for pathogenic mutations by PCR amplification and bidirectional sequencing. As a control, a group of 400 healthy newborns from the same ethnic background were subjected to *SLC26A4* gene screening using the same method. The proband harbored two mutations in the *SLC26A4* gene in the form of compound heterozygosity. She was found to be heterozygous for a novel mutation c.574delC (p.Leu192Ter) in exon 5 and for the known mutation c.919-2A>G(c.IVS7-2A>G). Her mother was a heterozygous carrier of the c.919-2A>G mutation, and her father was a heterozygous carrier of the c.574delC and therefore co-segregated with the genetic disease. The c.574delC mutation was absent in 400 healthy newborns. The frameshift mutation causes the leucine (Leu) at amino acid position 192 to become a termination codon, leading to termination of protein sequence coding. This study demonstrates that the novel frameshift mutation c.574delC (p.Leu192Ter) in compound heterozygosity with c.919-2A>G in the *SLC26A4* gene is the main cause of deafness in a family. Our study will expand the spectrum of known *SLC26A4* mutations in the Chinese population, providing more information on genetic counseling, and diagnosis in hearing loss with EVA.

**Keywords:** *SLC26A4*, novel mutation, enlarged vestibular aqueduct

### 1. Introduction

*SLC26A4* (OMIM 605646, also named PDS gene, NM\_000441.1) maps on 7q22-31(DFNB4 locus) (1). Domestic epidemiological data shows that *SLC26A4* is the second most common gene that causes nonsyndromic hearing loss (NSHL), accounting for 14.5% (2), which encodes a 780-amino-acid protein called pendrin, a member of the solute carrier 26 protein family that functions as a chloride iodide transporter in cell expression systems (3). There are two clinical phenotypes from mutations in the *SLC26A4* gene: (1) the syndromic

form, called Pendred Syndrome (PS) (OMIM 274600), characterized by hearing loss, goiter and eventually hypothyroidism, with/without EVA or other inner ear malformations; (2) the nonsyndromic form, called DFNB4 or non syndromic EVA (OMIM 600791) (when EVA is present), characterized by hearing loss with/without EVA or other inner ear malformations (4-6). The common mutations of the *SLC26A4* gene show regional and ethnic diversity. To date, about 539 mutations have been identified. (<http://www.hgmd.cf.ac.uk/ac/gene.php?gene=SLC26A4>)

Enlarged vestibular aqueduct (EVA) is known as an inner ear malformation of the temporal bone that predisposes patients to hearing loss from childhood as well as vestibular symptoms. It is a congenital abnormality that can be diagnosed radiographically in the hearing loss population. Nonsyndromic hearing loss (NSHL) with EVA is typically characterized by congenital, bilateral sensorineural hearing loss (SNHL),

\*Address correspondence to:

Dr. Lihui Huang, Beijing Tongren Hospital, Capital Medical University; Beijing Institute of Otolaryngology; Key Laboratory of Otolaryngology, Head and Neck Surgery, Ministry of Education, No.17 Houguo Lane, Chongnei Street, Beijing 100005, China.

E-mail: huangpub@126.com

which can be progressive and usually ranges from severe to profound (7). It is believed that *SLC26A4* gene mutations may cause NSHL associated with EVA, with hearing loss found at birth or during early childhood. According to domestic studies, about 62%-88.4% of patients with EVA can be due to bi-allelic mutations (including homozygous mutations and compound heterozygous mutations). Among those mono-allelic mutations of *SLC26A4* accounts for about 7.4%-24% (8,9).

In this study, we investigated the *SLC26A4* gene in 3 members of a Chinese family associated with EVA. As a result, novel compound heterozygous mutations of *SLC26A4* were identified. This will expand the spectrum of *SLC26A4* mutations in the Chinese population.

## 2. Materials and Methods

Written informed consent was obtained from parents. The protocol was approved by the Declaration of Helsinki principles and Ethics Committee of Beijing Tongren Hospital, Capital Medical University.

### 2.1. Subjects and clinical evaluation

A Chinese family associated with EVA was recruited from the Department of Otolaryngology, Head and Neck Surgery, Beijing Tongren Hospital (Beijing, China). The proband performed with c.919-2A>G single-allele mutation detected by deafness genetic screening (9 variants in 4 genes, including *GJB2* c.235delC, c.299delAT, c.176delI6, and c.35delG; *GJB3* c.538C>T; *SLC26A4* c.919-2A>G and c.2168A>G; and Mt 12SrRNA m.1555A>G and m.1494C>T). Clinical evaluation was conducted including description of family history and detailed medical history, and a physical examination, including thyroid sonography, and a high-resolution computed tomography (CT) scan of the temporal bone. Four hundred unrelated Chinese newborns with normal hearing were recruited as normal controls.

### 2.2. Mutational analysis

Genomic DNA was extracted from 2 ml of whole blood from each patient, using the Blood DNA kit (Tiangen Biotech, Beijing, China). 20 exons and flanking splice sites of the *SLC26A4* gene were screened for mutations by PCR amplification and bidirectional sequencing. ACMG guidelines were used for variant interpretations (10).

### 2.3. Bioinformatics and validation of the variants

Sequence data were analyzed by alignment with the National Center for Biotechnology Information (NCBI) reference sequence of *SLC26A4* (NT\_007933) with

the assistance of DNA Star 5.0 software. The 1000 Genomes Project database (<http://www.1000genomes.org/>), ClinVar (<https://www.ncbi.nlm.nih.gov/clinvar/>) dbSNP database of NCBI(<http://www.ncbi.nlm.nih.gov/>), and the Deafness Variation Database(<http://deafnessvariationdatabase.org/>)were used as references to assess the novelty of mutations found in this study.

### 2.4. Auditory evaluation

The subject underwent universal newborn hearing screening and had specific results. Comprehensive audiological evaluation included pure tone audiometry (PTA), auditory brainstem response (ABR), 40Hz auditory event-related potential, distortion product otoacoustic emission (DPOAE), auditory steady-state response (ASSR), acoustic immittance, and pediatric behavioral audiometry. The hearing threshold was calculated as the average hearing level at 0.5, 1.0, 2.0, and 4.0 k Hz according to the 1997 World Health Organization standard. The severity of hearing impairment was defined as mild (26-40 dB), moderate (41-60 dB), severe (61-80 dB), or profound (> 80 dB). Owing to the subjects' young age, the ABR threshold and/or ASSR were recorded, and mean thresholds at frequencies in the 0.5-4 k Hz range were averaged to obtain an approximation for directional conditioned reflex (11,12).

## 3. Results and Discussion

All the members were negative for systemic and thyroid disease, and physical examination and otoscopy were also normal. There was one subject aged nine months old with hearing loss in this family (II-1), and pure-tone audiometry revealed normal hearing in two family members (I-1, I-2). The proband (II-1) referred UNHS with two ears and then was diagnosed with bilateral profound SNHL when first seen by a doctor in our hospital at three months old. The air-conduction and bone-conduction of ABR of the proband showed both sides were not elicited as a reproducible wave at 100 dB nHL and 50 dB nHL, respectively. The proband had a tympanogram result of "A", and the bilateral acoustic stapedial reflex was not elicited. DPOAE showed no response from the patient in both ears. A temporal bone CT scan of the proband showed bilateral EVA with the width of the vestibular aqueduct greater than 1.5 mm and she was diagnosed with bilateral large vestibular aqueduct syndrome at seven months old (Figure 1C). The results of pediatric behavioral audiometry in the proband and PTA in her parents are demonstrated in Figure 1B

The sequence analysis of *SLC26A4* indicated that the proband presented compound heterozygosity of a c.919-2A>G (IVS7-2A>G) (rs111033313) mutation in intron7 and a c.574delC (p.Leu192Ter) frameshift mutation in exon 5. Additionally, the mother was a

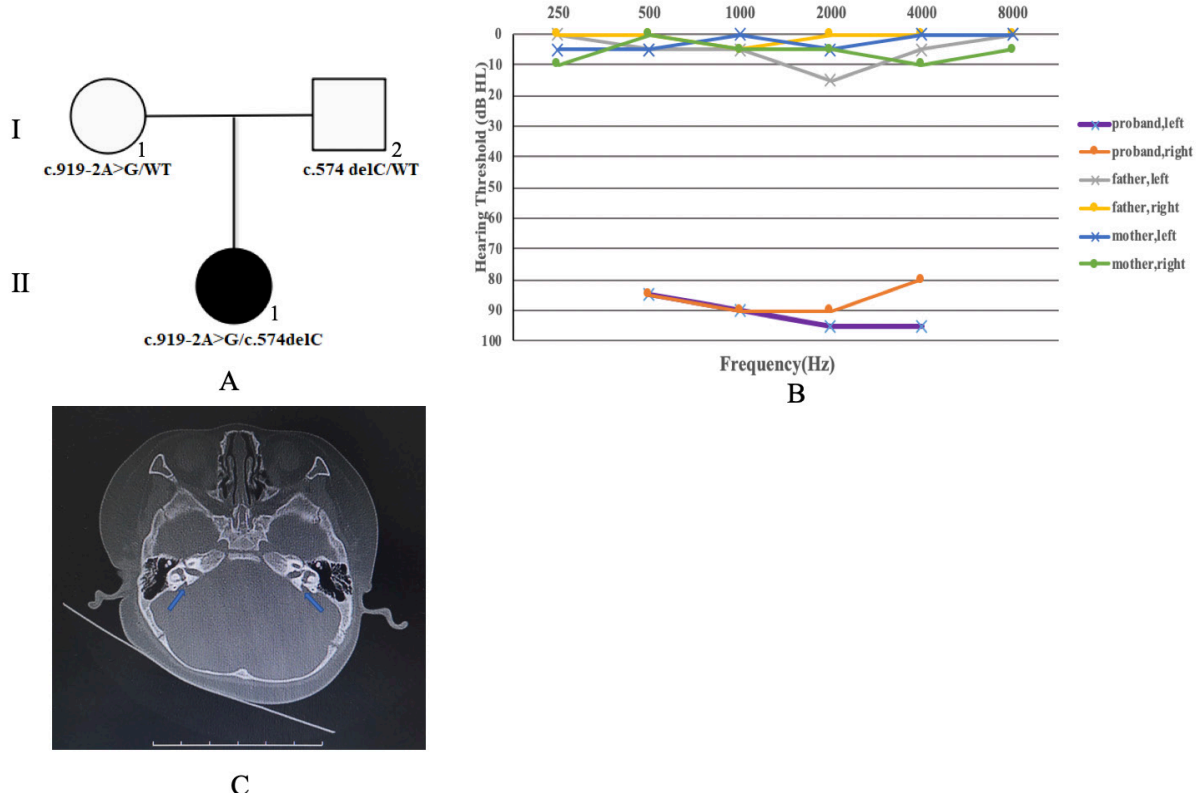


**Figure 1. Genotypes and clinical phenotype presentations of the pedigree.** (A) Pedigree map of the three families. Squares and circles denote male and female patients, respectively. Abbreviations: WT, wild type. (B) The audiograms of pediatric behavioral audiology in the proband and PTA in her parents. Frequency in hertz (Hz) is plotted on the x-axis and the hearing level in decibels (dB HL) on the y-axis. (C) The temporal bone CT scan of the proband shows the bilateral enlarged vestibular aqueduct (arrows).

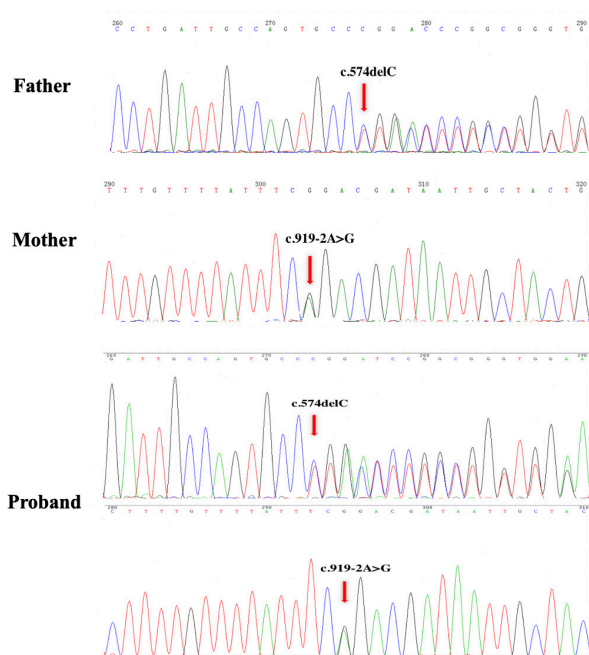


**Figure 2. Sequence electropherograms of abnormal sequences from three members of this family.**

heterozygous carrier of the c.919-2A>G mutation, and the father was a heterozygous carrier of the c.574delC (p.Leu192Ter) mutation. Figure 1A and Figure 2

demonstrate a pedigree map of the three families and sequence electropherograms of abnormal sequences from three members of this family, respectively. The variant c.574delC (p.Leu192Ter) was not reported in ClinVar, Pubmed, Deafness Variation Database, dbSNP, the 1000 Genomes Project database and HGMD, and has never been described in a clinical report. The novel mutation was not found in 400 healthy newborns. The part of *SLC26A4* amino acid sequence alignment demonstrated that the encoded amino acid sequence of c.574delC is only the part before the asterisk, the theoretical amino acid sequence is given from the missing position (arrow), shown in Figure 3. The frameshift mutation causes the leucine (Leu) at amino acid position 192 to become a termination codon, leading to termination of protein sequence coding.

EVA is a genetically autosomal recessive disorder. Subjects with bi-allelic mutations have earlier age of onset, more severe deafness, more fluctuating hearing loss, and larger vestibular aqueduct size than those without mutations (13,14). It is currently known that EVA is closely linked to the *SLC26A4* mutations and the variants have high heterogeneity and ethnic differences. p.V138F (c.412G>T) is the most common mutation in the Czech population (15). p.L236P (c.707T>C), p.T416P(c.1246A>C), and IVS8+1G>A(c.1001+1G>A) are mainly detected in Caucasian (16), and p.H72R

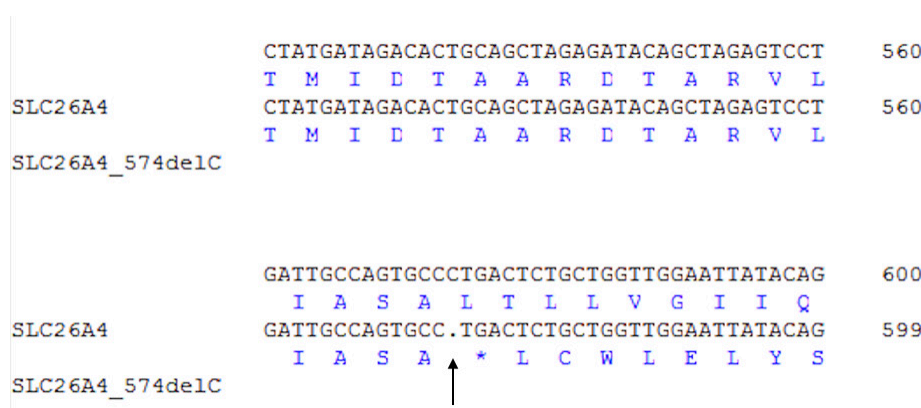


**Figure 3.** *SLC26A4* amino acid sequence alignment between normal and c.574delC (Part), Asterisk: termination codon.

(c.2168A>G) in Korean (17). The deaf population in South America and North America is dominated by p.V609G (c.1826T>G) mutation and IVS8+1G>A (c.1001+1G>A) mutation, respectively (18). Along with increasing research related to genes, more and more novel mutations have been reported in Chinese patients. c.919-2A>G(IVS7-2A>G) and p.H723R (c.2168A>G) account for the majority of mutations in China (19).

In this study, we found the proband's father and mother(the heterozygous carrier of c.574delC and c.919-2A>G mutation, respectively) both demonstrate normal hearing, while the proband with compound heterozygous mutations c.919-2A>G and c.574delC has profound SNHL, as well as EVA. Therefore, gene mutations transmitted from the parents to offspring indicate the segregation of genotype and phenotype. The splice-site mutation of c.919-2A>G mentioned above is the most prevalent pathogenic mutation of *SLC26A4* in China. Another mutation, c.574delC (p.Leu192Ter), has not been reported in other countries and ethnicities, which causes the leucine (Leu) at amino acid position 192 to become a termination codon, leading to termination of protein sequence coding and therefore, leads to early translational termination at amino acid position 515 in the sulfate transporter and anti-sigma factor antagonist (STAS) domain. Meanwhile, SLC26 STAS domain amino acid position 673 indicates human disease associated with a frameshift (20). However, the STAS domain included in members of the SLC26A family regulates the stability, trafficking, and anion transport function of SLC26A family proteins (20). The structural significance of this domain has been substantiated by the disease-causing nature of mutations among SLC26A family proteins (21). Therefore, it is possible that the novel mutation discovered in our study is closely related to hearing loss. Meanwhile, according to ACMG guidelines, c.574delC is pathogenic.

#### 4. Conclusions

This study demonstrates that the novel frameshift mutation c.574delC (p.Leu192Ter) in compound

heterozygosity with the c.919-2A>G in *SLC26A4* gene is the main cause of deafness in a family. Our study will expand the spectrum of known *SLC26A4* mutations in the Chinese population, providing more information on genetic counseling, and diagnosis of hearing loss with EVA.

#### Acknowledgements

The authors thank the patients and their family members for their participation in this study. This research was supported by the National Natural Science Foundation of China [grant number 81870730], the National Key R&D Program of China [grant number 2018YFC1002204] and The priming scientific research foundation for the senior researcher in Beijing Tongren Hospital, Capital Medical University [grant number 2016-YJJ-GGL-018]

#### References

1. Everett LA, Glaser B, Beck JC, Idol JR, Buchs A, Heyman M, Adawi F, Hazani E, Nassir E, Baxevanis AD, Sheffield VC, Green ED. Pendred syndrome is caused by mutations in a putative sulphate transporter gene (PDS). *Nat Genet.* 1997; 17:411–422.
2. Azaiez H, Yang T, Prasad S, Sorensen JL, Nishimura CJ, Kimberling WJ, Smith RJ. Genotype–phenotype correlations for *SLC26A4*-related deafness. *Hum Genet.* 2007; 122:451–457.
3. Scott DA, Karniski LP. Human pendrin expressed in *Xenopus laevis* oocytes Mediates chloride/format exchange. *Am J Physiol Cell Physiol.* 2000; 278:07-11.
4. Martini A, Calzolari F, Sensi A. Genetic syndromes involving hearing. *Int J Pediatr Otorhinolaryngol.* 2009; 73:S2–S12.
5. Li X, Everett LA, Lalwani AK, Desmukh D, Friedman TB, Green ED, Wilcox ER. A mutation in PDS causes non-syndromic recessive deafness. *Nat. Genet.* 1998; 18:215–217.
6. Royaux IE, Belyantseva IA, Wu T, Kachar B, Everett LA, Marcus DC, Green ED, Localization and functional studies of pendrin in the mouse inner ear provide insight about the etiology of deafness in pendred syndrome. *J Assoc Res Otolaryngol.* 2003; 4:394-404.

7. Valvassori GE, Clemis JD. The large vestibular aqueduct syndrome. *Laryngoscop e.* 1978; 88:723-728.
8. Wu C, Lu Y. Phenotypic analyses and mutation screening of the SLC26A4 and FOXI1 genes in 101 Taiwanese families with bilateral nonsyndromic enlarged vestibular aqueduct (DFNB4) or Pendred syndrome. *Audiology & neuro-otology.* 2010; 15:57-66.
9. Zhao J, Yuan Y, Jing C, Huang S, Wang G, Han D, Dai P. SLC26A4 gene copy number variations in Chinese patients with non-syndromic enlarged vestibular aqueduct. *Journal of Translational Medicine.* 2012; 10:1051.
10. Sue R, Nazneen A, Sherri B, David B, Soma D, Julie GF, Wayne WG, Madhuri H, Elaine L, Elaine S, Karl V, Heidi LR. Standards and guidelines for the interpretation of sequence variants: A joint consensus recommendation of the American College of medical genetics and genomics and the association for molecular pathology. *Genet Med.* 2015; 17:405.
11. Kim SY, Park G, Han K, Kim A, Koo JW, Chang SO, Oh SH, Park WY, Choi BY. Prevalence of p.V37I variant of *GJB2* in mild or moderate hearing loss in a pediatric population and the interpretation of its pathogenicity. *PLoS ONE.* 2013; 8:e61592.
12. Liu J, Huang L, Fu X, Liu H, Yang Y, Cheng X, Ni T. The audiological characteristics of large vestibular aqueduct syndrome in infants and young children. *J Clin Otorhinolaryngol Head Neck Surg (China).* 2016; 30:1702-1709. (in Chinese)
13. Albert S, Blons H, Jonard L, et al. *SLC26A4* gene is frequently involved in nonsyndromic hearing impairment with enlarged vestibular aqueduct in Caucasian populations. *Eur J Hum Genet.* 2006; 14:773-779.
14. Zhao F, Lan L, Wang D, Han B, Qi Y, Zhao Y, Zong L, Li Q, Wang Q. Correlation analysis of genotypes, auditory function, and vestibular size in Chinese children with enlarged vestibular aqueduct syndrome. *Acta Otolaryngol.* 2013; 133:1242-1249.
15. Pourová R, Janousek P, Jurovcík M, Dvoráková M, Malíková M, Rasková D, Bendová O, Leonardi E, Murgia A, Kabelka Z, Astl J, Seeman P. Spectrum and frequency of SLC26A4 mutations among Czech patients with early hearing loss with and without enlarged vestibular aqueduct(EVA). *Ann Hum Genet.* 2010; 74:299-307.
16. Campbell C, Cucci RA, Prasad S, Green GE, Edeal JB, Galer CE, Karniski LP, Sheffield VC, Smith RG. Pendred syndrome, DFNB4, and PDS/SLC26A4 identification of eight novel mutations and possible genotype–phenotype correlations. *Hum Mutat.* 2001; 17:403–411.
17. Park HJ, Lee SJ, Jin HS, Lee JO, Go SH, Jang HS, Moon SK, Lee SC, Chun YM, Lee HK, Jung SC, Griffith AJ, Koo SK. Genetic basis of hearing loss associated with enlarged vestibular aqueducts in Koreans. *Clin Genet.* 2005; 67:160-165.
18. Lin Z, Lu Y, Qian X, Yao J, Wei Q, Cao X. Study on molecular structure and racial difference of high frequency pathological SLC26A4mutations in hearing loss. *J Nanjing Medical University.* 2015; 09:1185-1194. (in Chinese)
19. Yuan Y, Huang S, Wang G, Kang D, Han D, Huang D, Dai P. Sequencing analysis of entire *SLC26A4* gene with focus on IVS7- 2A>G mutation in 2352 patients with moderate to profound SNHL in China. *Chin J Otology.* 2011; 09:17-23. (in Chinese)
20. Sharma AK, Rigby AC, Alper SL. Stas domain structure and function. *Cell Physiol Biochem Int J Exp Cell physiol Biochem Pharmacol.* 2011; 28:407.
21. Sharma AK, Ye L, Baer CE, Shanmugasundaram K, Alber T, Alper SL, Rigby AC. Solution Structure of the Guanine Nucleotide-binding STAS Domain of SLC2 6-related SulP Protein Rv1739c from Mycobacterium tuberculosis. *J Biol Chem.* 2011; 286:8534-8544.

(Received October 2, 2018 Revised October 26, 2018;  
Accepted October 29, 2018)

# HIV/AIDS responses in China should focus on the impact of global integration

Qi Tang<sup>1,2</sup>, Hongzhou Lu<sup>1,2,3,\*</sup>

<sup>1</sup> Scientific Research Center, Shanghai Public Health Clinical Center, Fudan University, Shanghai, China;

<sup>2</sup> Department of Infectious Diseases, Shanghai Public Health Clinical Center, Fudan University, Shanghai, China;

<sup>3</sup> Department of Infectious Disease, Huashan Hospital Affiliated to Fudan University, Shanghai, China.

## Summary

China has made substantial progress in tackling its Human immunodeficiency virus (HIV) epidemic, however, the number of people living with HIV / acquired immunodeficiency syndrome (AIDS) continues to increase, with the number of all-cause deaths rising. There are a total 75.6 million people living with HIV and 2.39 million people newly infected with HIV as of December 31, 2017 in China. Besides, while the number of new HIV infections continued to decline in 2017 globally, the data from Chinese Center for Disease Control and Prevention (CCDC) show steady increases in new HIV infections in China. The compound annual growth rate (CAGR) of new HIV infections in China from 2012 to 2017 was 10.29%, and the CAGR of AIDS-related deaths was 5.92%. Moreover, there was a sudden increase in new HIV infections in China from January 2018, showing the compound monthly growth rate (CMGR) of 2018 increased by 9.92% compared to 2017. Given the advance of globalization, it is increasingly important to focus on the impact of global integration for HIV/AIDS responses, facing the increasing challenge of key affected populations such as men who have sex with men (MSM), young people and older people. Certainly, comprehensive strategies for prevention, drug treatment, and even functional cure will also be crucial for curbing the HIV epidemic in China in the new era.

**Keywords:** HIV/AIDS response, globalization, growth trend, key population

Human immunodeficiency virus (HIV)/acquired immunodeficiency syndrome (AIDS) continue to be a major global public health issue, having claimed more than 35 million lives so far (1). Although new HIV infections fell by 36% and HIV-related deaths fell by 38% between 2000 and 2017, people living with HIV increased by 14% between 2010 and 2017, indicating the HIV/AIDS epidemic is still on the rise (2). With the advance of globalization, it is increasingly important to focus on the impact of global integration for HIV/AIDS responses.

## 1. New HIV infections in China increased rapidly since 2018

China has made substantial progress in HIV/AIDS

response in the last decade and increased national measures have stemmed its epidemic across the country as well as improving the quality of life for people living with HIV.

Despite these efforts, the number of people living with HIV/AIDS continues to increase, with the number of all-cause deaths rising (Figure 1) (3-8). There are a total 75.6 million people living with HIV and 2.39 million people newly infected with HIV as of December 31, 2017 in China. Besides, the data from Chinese Center for Disease Control and Prevention (CCDC) show steady increases in new HIV infections in China, while the number of new HIV infections globally continued to decline in 2017 (Figure 2) (3-8). The compound annual growth rate (CAGR) of new HIV infections in China from 2012 to 2017 was 10.29%, and the CAGR of AIDS-related deaths was 5.92%. Moreover, there was a sudden increase in new HIV infections in China from January 2018. Figure 3 shows the compound monthly growth rate (CMGR) of 2018 increased by 9.92% compared to 2017 (3-9). By July of this year, the number of new HIV

\*Address correspondence to:

Dr. Hongzhou Lu, Shanghai Public Health Clinical Center, Fudan University, No.2901, Caolang Road, Jinshan District, Shanghai 201508, China.

E-mail: luhongzhou@fudan.edu.cn

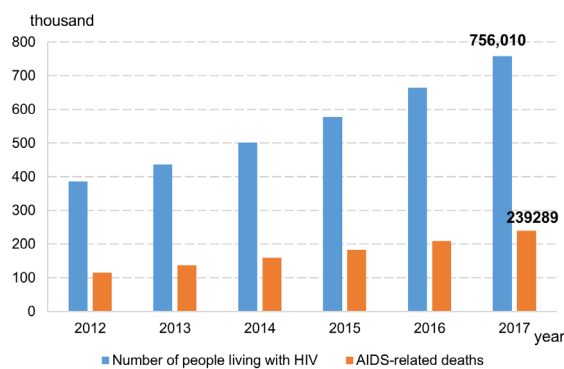


**Figure 1. HIV/AIDS epidemic in China in 2012-2017.** There are a total 75.6 million people living with HIV and 2.39 million people newly infected with HIV as of December 31, 2017 in China.

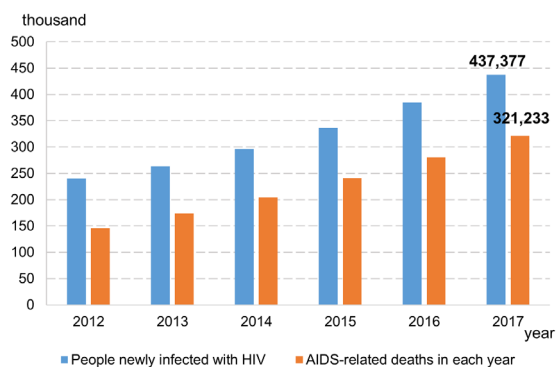


**Figure 2. HIV/AIDS epidemic in China annually from 2012 to 2017.** A total of 437,377 people with HIV/AIDS and 321,233 people with AIDS-related deaths in 2017 in China, showing steady increases in new HIV infections in China in recent years. The compound annual growth rate (CAGR) of new HIV infections in China from 2012 to 2017 was 10.29%, and the CAGR of AIDS-related deaths was 5.92%.

infections has reached 91,301, with sexual transmission accounting for 91.76% (9).

The development of globalization affects the HIV epidemic at this stage, so that we should pay more attention to the impact of the process of global integration development in the process of HIV/AIDS responses.

## 2. Impact of global integration needs to be taken seriously for HIV/AIDS responses

China has a relatively low national HIV prevalence rate, but with higher-prevalence in some groups. Given global integration, China is also faced with the increasing challenge of key affected populations such as men who have sex with men (MSM), young people and older people.

**MSM.** HIV prevalence among MSM has been rising in China in this day and age. The data from the 5th National Conference on HIV/AIDS showed the average prevalence of HIV infection to be 7.3% in the MSM group (10). It is clear that the HIV epidemic among men

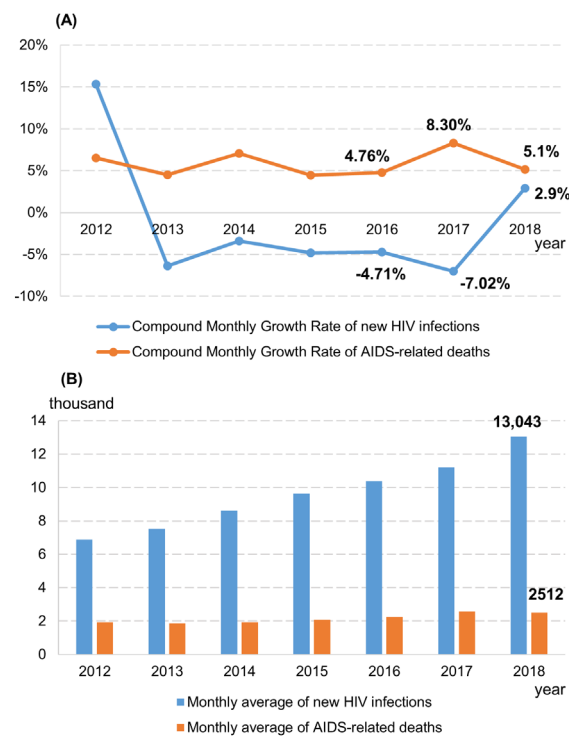


**Figure 3. HIV/AIDS epidemic in China monthly from 2012 to 2018.** There was a sudden increase in new HIV infections in China from January 2018, showing compound monthly growth rate (CMGR) of 2018 increased by 9.92% compared to 2017.

who have sex with men is a concern in China so that a more effective response that meets this group's needs should be conducted.

**Young people.** One of the growing key affected populations in China is young people who are more likely to accept the impact of new things. CCDC reports the proportion of new infections among people aged 15 to 24 has increased by 13.1% from 2008 to 2017, and 81.8% of young students have been among young men who have sex with men in 2017 (10). It is therefore vital that HIV services and education are tailored to the key affected groups within this younger population.

**Older people.** Given population aging in the world, elderly HIV infections are gradually increasing. Sex demand and openness are the major factors in the rising HIV epidemic among HIV-infected people among the elderly age 60 or over whose prevalence rate increased from 7.4% to 14.7% in 2010-2017 (10). Elderly people HIV/AIDS policy in China is limited, and the design and formulation of HIV/AIDS policies and programs will be important in tackling the epidemic among this population in China.

## 3. Expectations for HIV/AIDS responses in a globalized world

It is clear that China's epidemic significantly affects key populations around the country in such a globalized world, including MSM, young people and older people.

Greater effort, including large-scale publicity campaigns, health education activities, condom promotion, HIV testing and counselling, *etc.*, will be required for providing more targeted interventions that adequately and effectively support these groups.

Therefore, comprehensive strategies for prevention, drug treatment, and even functional cure will also be crucial for curbing the HIV epidemic in China in the new era. Certainly, China's comprehensive approach to HIV can provide important data and lessons for many countries in Asia and the Pacific and beyond.

### Acknowledgements

This research was funded by the 13th Five-Year National Science and Technology Major Project from Ministry of Science and Technology of the People's Republic of China (Grant No.: 2017ZX09304027).

### References

1. The Joint United Nations Programme on HIV and AIDS. Ending AIDS: progress towards the 90–90–90 targets. [http://www.unaids.org/en/resources/documents/2017/20170720\\_Global\\_AIDS\\_update\\_2017](http://www.unaids.org/en/resources/documents/2017/20170720_Global_AIDS_update_2017) (accessed October 16, 2018)
2. The Joint United Nations Programme on HIV and AIDS. UNAIDS DATA 2018. <http://www.unaids.org/en/resources/documents/2018/unaids-data-2018> (accessed October 16, 2018)
3. Chinese Center for Disease Control and Prevention. The national epidemic of AIDS and STDs with the main prevention and treatment progress in 2012. Chinese Journal of AIDS & STD. 2013; 19:85. (in Chinese)
4. Chinese Center for Disease Control and Prevention. The national epidemic of AIDS and STDs with the main prevention and treatment progress in 2013. Chinese Journal of AIDS & STD. 2014; 20:75. (in Chinese)
5. Chinese Center for Disease Control and Prevention. The national epidemic of AIDS and STDs with the main prevention and treatment progress in 2014. Chinese Journal of AIDS & STD. 2015; 21:87. (in Chinese)
6. Chinese Center for Disease Control and Prevention. The national epidemic of AIDS and STDs with the main prevention and treatment progress in 2015. Chinese Journal of AIDS & STD. 2016; 22:69. (in Chinese)
7. Chinese Center for Disease Control and Prevention. The national epidemic of AIDS and STDs in 2016. Chinese Journal of AIDS & STD. 2017; 23:93. (in Chinese)
8. Chinese Center for Disease Control and Prevention. The national epidemic of AIDS and STDs in July 2017. Chinese Journal of AIDS & STD. 2018; 24:865. (in Chinese)
9. Chinese Center for Disease Control and Prevention. The national epidemic of AIDS and STDs in 2017. Chinese Journal of AIDS & STD. 2018; 24:111. (in Chinese)
10. Chinese Center for Disease Control and Prevention. The 5th National Conference on HIV/AIDS. 2018. Kunming, China. <http://2018aids.medmeeting.org/cn> (accessed October 16, 2018)

(Received October 3, 2018; Revised October 26, 2018;  
Accepted October 29, 2018)

# Considerations on PCR-based methods for malaria diagnosis in China malaria diagnosis reference laboratory network

Jianhai Yin\*, Mei Li, He Yan, Shuisen Zhou\*

National Institute of Parasitic Diseases, Chinese Center for Disease Control and Prevention, Chinese Center for Tropical Diseases Research, WHO Collaborating Centre for Tropical Diseases, National Center for International Research on Tropical Diseases, Ministry of Science and Technology, Key Laboratory of Parasite and Vector Biology, Ministry of Health, Shanghai 200025, China.

**Summary** Precise diagnosis is a key measurement for malaria control and elimination, traditional microscopy and rapid diagnostic tests cannot satisfy the requirements especially in the low transmission endemic areas or in the malaria elimination phase. Polymerase chain reaction (PCR) with high sensitivity and specificity can be considered as a diagnostic standard while no uniform PCR assay was established due to variations in their performance and lack of formal external quality assurance programs for validation for PCR assays in use. Here, 24 articles including 43 paired comparative evaluations limited to paired comparison of diagnostic performance between real-time PCR and conventional PCR to detect plasmodium in blood samples of human subjects from clinics or the field are systematically summarized. And according to the Landis and Koch classification, nineteen pairs showed almost perfect agreement, followed by 8 pairs of moderate agreement and 4 pairs of good agreement, while the kappa values of 12 pairs couldn't be examined. Moreover, the performance of 14 pairs were completely the same and 8 pairs had no differences, but 14 pairs were significant different including 8 pairs of real-time PCR with better performance than conventional PCR. Therefore, it is still an outstanding issue to choose PCR methods, and more work such as the standardization of materials and methods in use and their availability are needed to settle priority to better promote the role of malaria diagnosis reference laboratories.

**Keywords:** *Plasmodium species*, real-time PCR, conventional PCR, reference laboratory, quality assurance

## 1. Introduction

One of the strategies to control and eliminate malaria is the precise laboratorial diagnosis in order to recognize infection promptly and treat positive cases appropriately. A variety of diagnostic methods are used for plasmodium parasites identification and speciation.

Malaria microscopy on Giemsa-stained thick and thin blood smears is still the gold standard method for malaria diagnosis, clinical trials efficacy evaluation and epidemiological surveys. However, it has many

limitations such as low sensitivity detection limit, poor specificity due to morphological changes that are enhanced by the staining and the similarities between several parasites, and operator dependence that even highly qualified microscopists can make an incorrect or incomplete assessment of the *Plasmodium* species (1).

Alternatively, a variety of rapid diagnostic tests (RDT) for plasmodium antigen detection have been developed for use with sensitivity above 90% if > 100 parasites/ $\mu$ L, and a result can be obtained within half an hour by nonskilled technicians (2). But, there is low sensitivity if < 100 parasites/ $\mu$ L, and false positives particularly after treatment, and limitations for *Plasmodium* species speciation and case review.

Nucleic acid tests based on polymerase chain reactions (PCR) have high sensitivity and specificity to detect and identify pathogens. This is primarily useful for epidemiological investigations of malaria because the

\*Address correspondence to:

Dr. Jianhai Yin and Shuisen Zhou, National Institute of Parasitic Diseases, Chinese Center for Disease Control and Prevention, No. 207 Ruijin Er Lu, Shanghai 200025, China.  
E-mail: chart2543@163.com (Yin J), zss163@hotmail.com (Zhou S)

infections are frequently associated with asymptomatic and/or microscopically sub-patent parasite levels and various mixed infections. Numerous PCR assays have been developed for the laboratory diagnosis of malaria, including conventional and real-time PCR techniques, that allow the differentiation of all five species of human *Plasmodium* with as few as five parasites per microliter of blood and even probably as low as 0.002 parasites/ $\mu\text{L}$  (3,4). Moreover, the nested PCR developed by Snounou *et al.* (5) has been widely used and considered as the molecular gold standard for malaria parasites detection due to its good performance (6) and it also was recommended as the confirmatory test documented in the manual of China Malaria Diagnosis Reference Laboratory Network (7). Meanwhile, malaria case diagnosis according to the laboratorial detection based on nucleic acids of plasmodium parasites was firstly documented in the new version of 'Diagnosis of malaria (WS 259-2015)' in China (8), although no detailed protocol was mentioned. Additionally, the use of malaria real-time or quantitative PCR as a confirmatory endpoint assay in field research has increased exponentially. Several provincial malaria diagnosis reference laboratories recommended the application of real-time PCR for malaria cases confirmation and quality assurance of malaria diagnosis in the network due to its convenience and time saving. Therefore, the issue is not which PCR method should be adopted but whether PCR be the accepted gold standard, and it is necessary to compare the benefits of different PCR methods, optimize the protocol, and train staff in the reference laboratory network.

## 2. Comparison of Real-time PCR and Conventional PCR Assays for malaria diagnosis

A total of 24 articles about 14 clinical studies and 10 field studies related to pair comparison of real-time PCR and conventional PCR to detect samples of human subjects from clinics or the field rather than model organisms for malaria parasites were enrolled (Supplementary Table 1, <http://www.biosciencetrends.com/action/getSupplementalData.php?ID=29>) (9-32), and agreement of paired methods was determined by calculating Kappa Statistics. The kappa values ( $\kappa$ ) were interpreted with the Landis and Koch classification (33):  $\kappa < 0$ , poor agreement;  $\kappa = 0.01-0.20$ , slight agreement;  $\kappa = 0.21-0.40$ , fair agreement;  $\kappa = 0.41-0.60$ , moderate agreement;  $\kappa = 0.61-0.80$ , good agreement; and  $\kappa = 0.81-1.00$ , almost perfect agreement, respectively. Moreover, the differences of the detection levels of compared PCR assays were analyzed by the  $\chi^2$  test or Fisher exact test,  $p < 0.05$  was considered statistically significant.

### 2.1. PCR assays for malaria parasites detection

Six fluorescence-reporting systems (TaqMan

[13/24], SYBR green [6/24], Photo-induced electron transfer fluorogenic primer (PET) [2/24], molecular beacon probes [1/24], LightCycler probes [1/24] and Fluorescence resonance energy transfer (FRET) [1/24]) were used. 14 different real-time PCR methods were used in the 14 studies, and another two methods were used in two studies each respectively.

In respect to conventional PCR assays, nested PCR was the most selected method (18/24) used. Moreover, five and six studies applied multiplex PCR and simple PCR respectively. In addition, two classical nested PCR assays developed by Snounou *et al.* (11/24) (5) and Singh *et al.* (3/24) (34) were used extensively.

### 2.2. Target molecules

*Plasmodium* 18S rRNA gene was used most frequently in both real-time PCR assays (21/24) and conventional PCR assays (21/24), and the *Plasmodium falciparum*-specific cytochrome c oxidase subunit 1 (Cox1) gene was used in two studies of real-time PCR, and the *Plasmodium* cytochrome B gene, *Plasmodium ovale*-specific reticulocyte-binding protein 2 (Porbp2) gene and mitochondrial cytochrome C oxidase gene for *Plasmodium falciparum* and *Plasmodium vivax* were used in one paper each by real-time PCR (Supplementary Table 1, <http://www.biosciencetrends.com/action/getSupplementalData.php?ID=29>). Meanwhile, merozoite surface protein 2 (MSP2) gene, cytochrome B gene, *Plasmodium ovale* tryptophan-rich antigen (*Potra*) gene and mitochondrial cytochrome C oxidase gene were selected in conventional PCR assays (Supplementary Table 1, <http://www.biosciencetrends.com/action/getSupplementalData.php?ID=29>).

### 2.3. Agreement analysis

IA total of 43 paired comparative evaluations performed in the 24 enrolled studies, and 19 pairs showed almost perfect agreement, followed by 8 pairs of moderate agreement and 4 pairs of good agreement, while the kappa values of 12 pairs couldn't be examined directly or calculated using the data provided, partly due to the fact that the identification of *Plasmodium* spp were not identical although the number of positive and negative samples were the same detected by both real-time PCR and conventional PCR assays.

### 2.4. Differences in detection performance

The results of 14 paired comparisons (14/43) were completely the same in respect to the composition of positive and negative samples, and 8 pairs were between real-time PCR and nested PCR. Moreover, there were 8 paired analyses that showed no differences in detection capacity between real-time PCR and conventional PCR (including 4 nested PCR, 2 simple

PCR and multiplex PCR each) ( $p > 0.05$ ), but 14 pairs were significantly different including 8 pairs of real-time PCR with better performance than conventional PCR (including 4 nested PCR, 2 simple PCR and multiplex PCR each) ( $p < 0.05$ ). In addition, detection capacity can't be compared in several studies because not all of the samples were tested by the comparative assays due to insufficient sample volumes.

### 3. Challenges and prospects

Precise diagnosis and confirmatory identification of malaria infection is crucially important, especially in low-density parasitaemia or sub-microscopic infections, which is an important reservoir of malaria parasites and a big challenge for malaria elimination and prevention of re-introduction. Quality assurance performed by reference laboratories is a key tool to guarantee and maintain the performances of diagnostic assays. PCR with much more sensitivity and specificity than microscopy and RDT is a useful tool for confirmatory identification of *Plasmodium* spp, and it could be used in a quality assurance scheme to provide an excellent quality control for results obtained by conventional microscopy and other diagnostic methods to ensure that results are reliable and comparable.

Unlike in routine clinical practice for malaria diagnosis, the time lag between sample collection, transportation and processing, and dissemination of results (35) is less important than the precise result in quality assurance which is a key role of the reference laboratory. Factors such as limited financial resources and inadequate laboratory infrastructures hindered the application of PCR assays previously has been improved significantly in the China Malaria Diagnosis Reference Laboratory Network. Additionally, nucleic acids detection based on PCR for malaria parasites has been recommended as the confirmatory test documented in the manual of China malaria diagnosis reference laboratory network and the diagnosis standard of 'Diagnosis of malaria (WS 259-2015)' in China. Nevertheless, a uniform PCR method considered as the gold standard to formalize and extend the exercise couldn't be determined due to a wide variation in the performance of the numerous PCR methods.

In view of the summary of agreement analysis and performances in detecting clinical and field samples from 43 comparative evaluations between real-time PCR and conventional PCR (including nested PCR, multiplex PCR and simple PCR) provided in the 24 articles above, it is still difficult to select the best PCR assay used as standard protocol for malaria diagnosis, although real-time PCR seems better than conventional PCR. Moreover, the standardization of PCR templates including positive as well as negative ones for controls in reference laboratories should be a priority. It will help researchers in different conditions to ensure

that the nucleic acid amplification protocols they use provide the requisite level of sensitivity, and permit comparison between sites and the efficacy of various PCR protocols. Only *Plasmodium falciparum* DNA standard material was established, but it is not widely available, and no application was found in these 24 articles. Moreover, the standardization of materials and source material in use are also important to ensure the compatibility of tests, because of the differences in the target molecules, space, time, reagents or enzymes, the type of thermocycler used, and/or subtle variations, and even data interpretations, and much more, can cause variations.

Although no significant differences were found in the performance between real-time PCR and conventional PCR for malaria diagnosis above, and nested PCR represents the most appropriate techniques for detecting malaria parasites, but the advantages of quantification of parasite densities, a less laborious workflow, rapidity, lower contamination and more possibility for the diagnosis of low-level parasitaemia, contribute to real-time PCR to be an appropriate method used in reference laboratory and routine malaria diagnosis, especially for asymptomatic infections. Furthermore, very few quality control programs for PCR protocols about malaria diagnosis were published (7,36,37), and it is time to develop a formal external quality assurance scheme to provide validation for PCR assays in use, and ensure accurate diagnosis (38). In addition, differences in protocols of sample collection, storage, and DNA extraction etc. can influence the specificity and sensitivity of PCR amplification.

In conclusion, PCR assays should be considered to be the gold standard for malaria diagnosis, but more work should be needed to settle the issue of which PCR method is adopted. Moreover, the standardization of materials and methods in use and their availability must be given priority in the process of the development to better promote the role of malaria diagnosis reference laboratorys.

### Acknowledgements

The authors would like to thank financial support from the Youth Program of Shanghai Municipal Commission of Health and Family Planning (20164Y0216).

### References

1. Gautret P, Legros F, Koulmann P, Rodier MH, Jacquemin JL. Imported *Plasmodium vivax* malaria in France: Geographical origin and report of an atypical case acquired in Central or Western Africa. *Acta Trop.* 2001; 78:177-181.
2. Mills CD, Burgess DC, Taylor HJ, Kain KC. Evaluation of a rapid and inexpensive dipstick assay for the diagnosis of *Plasmodium falciparum* malaria. *Bull World Health Organ.* 1999; 77:553-559.

3. Berry A, Benoit-Vical F, Fabre R, Cassaing S, Magnaval JF. PCR-based methods to the diagnosis of imported malaria. *Parasite*. 2008; 15:484-488.
4. Kamau E, Tolbert LS, Kortepeter L, Pratt M, Nyakoe N, Muringo L, Ongutu B, Waitumbi JN, Ockenhouse CF. Development of a highly sensitive genus-specific quantitative reverse transcriptase real-time PCR assay for detection and quantitation of plasmodium by amplifying RNA and DNA of the 18S rRNA genes. *J Clin Microbiol*. 2011; 49:2946-2953.
5. Snounou G, Viriyakosol S, Jarra W, Thaithong S, Brown KN. Identification of the four human malaria parasite species in field samples by the polymerase chain reaction and detection of a high prevalence of mixed infections. *Mol Biochem Parasitol*. 1993; 58:283-292.
6. Johnston SP, Pieniazek NJ, Xayavong MV, Slemenda SB, Wilkins PP, da Silva AJ. PCR as a confirmatory technique for laboratory diagnosis of malaria. *J Clin Microbiol*. 2006; 44:1087-1089.
7. Yin JH, Yan H, Huang F, Li M, Xiao HH, Zhou SS, Xia ZG. Establishing a China malaria diagnosis reference laboratory network for malaria elimination. *Malar J*. 2015; 14:40.
8. China NHFPC. Diagnosis of malaria (WS 259-2015). 2015. (in Chinese)
9. Hwang SY, Kim SH, Lee GY, Hang VT, Moon CS, Shin JH, Koo WL, Kim SY, Park HJ, Park HO, Kho WG. A novel real-time PCR assay for the detection of *Plasmodium falciparum* and *Plasmodium vivax* malaria in low parasitized individuals. *Acta Trop*. 2011; 120:40-45.
10. Fabre R, Berry A, Morasson B, Magnaval JF. Comparative assessment of conventional PCR with multiplex real-time PCR using SYBR Green I detection for the molecular diagnosis of imported malaria. *Parasitology*. 2004; 128:15-21.
11. Mwingira F, Genton B, Kabanywanyi AN, Felger I. Comparison of detection methods to estimate asexual *Plasmodium falciparum* parasite prevalence and gametocyte carriage in a community survey in Tanzania. *Malar J*. 2014; 13:433.
12. Rosanas-Urgell A, Mueller D, Betuela I, Barnadas C, Iga J, Zimmerman PA, del Portillo HA, Siba P, Mueller I, Felger I. Comparison of diagnostic methods for the detection and quantification of the four sympatric *Plasmodium* species in field samples from Papua New Guinea. *Malar J*. 2010; 9:361.
13. Wang B, Han SS, Cho C, Han JH, Cheng Y, Lee SK, Galappaththy GN, Thimasarn K, Soe MT, Oo HW, Kyaw MP, Han ET. Comparison of microscopy, nested-PCR, and Real-Time-PCR assays using high-throughput screening of pooled samples for diagnosis of malaria in asymptomatic carriers from areas of endemicity in Myanmar. *J Clin Microbiol*. 2014; 52:1838-1845.
14. Lau YL, Lai MY, Anthony CN, Chang PY, Palaeaya V, Fong MY, Mahmud R. Comparison of three molecular methods for the detection and speciation of five human *Plasmodium* species. *Am J Trop Med Hyg*. 2015; 92:28-33.
15. Boonma P, Christensen PR, Suwanarusk R, Price RN, Russell B, Lek-Uthai U. Comparison of three molecular methods for the detection and speciation of *Plasmodium vivax* and *Plasmodium falciparum*. *Malar J*. 2007; 6:124.
16. Genc A, Eroglu F, Koltas IS. Detection of *Plasmodium vivax* by nested PCR and real-time PCR. *Korean J Parasitol*. 2010; 48:99-103.
17. Kim JY, Goo YK, Ji SY, Shin HI, Han ET, Hong Y, Chung DI, Cho SH, Lee WJ. Development and efficacy of real-time PCR in the diagnosis of vivax malaria using field samples in the Republic of Korea. *PloS one*. 2014; 9:e105871.
18. Perandin F, Manca N, Calderaro A, Piccolo G, Galati L, Ricci L, Medici MC, Arcangeletti MC, Snounou G, Dettori G, Chezzi C. Development of a real-time PCR assay for detection of *Plasmodium falciparum*, *Plasmodium vivax*, and *Plasmodium ovale* for routine clinical diagnosis. *J Clin Microbiol*. 2004; 42:1214-1219.
19. Safeukui I, Millet P, Boucher S, Melinard L, Fregeville F, Receveur MC, Pistone T, Fialon P, Vincendeau P, Fleury H, Malvy D. Evaluation of FRET real-time PCR assay for rapid detection and differentiation of *Plasmodium* species in returning travellers and migrants. *Malar J*. 2008; 7:70.
20. Farcas GA, Zhong KJ, Mazzulli T, Kain KC. Evaluation of the RealArt Malaria LC real-time PCR assay for malaria diagnosis. *J Clin Microbiol*. 2004; 42:636-638.
21. Talundzic E, Maganga M, Masanja IM, Peterson DS, Udhayakumar V, Lucchi NW. Field evaluation of the photo-induced electron transfer fluorogenic primers (PET) real-time PCR for the detection of *Plasmodium falciparum* in Tanzania. *Malar J*. 2014; 13:31.
22. Lima GF, Levi JE, Geraldi MP, Sanchez MC, Segurado AA, Hristov AD, Inoue J, Costa-Nascimento Mde J, Di Santi SM. Malaria diagnosis from pooled blood samples: comparative analysis of real-time PCR, nested PCR and immunoassay as a platform for the molecular and serological diagnosis of malaria on a large-scale. *Mem Inst Oswaldo Cruz*. 2011; 106:691-700.
23. Lee PC, Chong ET, Anderios F, Al Lim Y, Chew CH, Chua KH. Molecular detection of human *Plasmodium* species in Sabah using PlasmoNex multiplex PCR and hydrolysis probes real-time PCR. *Malar J*. 2015; 14:28.
24. Lucchi NW, Narayanan J, Karell MA, Xayavong M, Kariuki S, DaSilva AJ, Hill V, Udhayakumar V. Molecular diagnosis of malaria by photo-induced electron transfer fluorogenic primers: PET-PCR. *PloS one*. 2013; 8:e56677.
25. Veron V, Simon S, Carme B. Multiplex real-time PCR detection of *P. falciparum*, *P. vivax* and *P. malariae* in human blood samples. *Exp Parasitol*. 2009; 121:346-351.
26. Costa DC, Madureira AP, Amaral LC, Sanchez BA, Gomes LT, Fontes CJ, Limongi JE, Brito CF, Carvalho LH. Submicroscopic malaria parasite carriage: how reproducible are polymerase chain reaction-based methods? *Mem Inst Oswaldo Cruz*. 2014; 109:21-28.
27. Xu W, Morris U, Aydin-Schmidt B, Msellemi MI, Shakely D, Petzold M, Bjorkman A, Martensson A. SYBR Green real-time PCR-RFLP assay targeting the *plasmodium* cytochrome B gene--a highly sensitive molecular tool for malaria parasite detection and species determination. *PloS one*. 2015; 10:e0120210.
28. Elsayed S, Plewes K, Church D, Chow B, Zhang K. Use of molecular beacon probes for real-time PCR detection of *Plasmodium falciparum* and other *plasmodium* species in peripheral blood specimens. *J Clin Microbiol*. 2006; 44:622-624.
29. Gama BE, Silva-Pires Fdo E, Lopes MN, Cardoso MA, Britto C, Torres KL, de Mendonca Lima L, de Souza JM, Daniel-Ribeiro CT, Ferreira-da-Cruz M. Real-time PCR versus conventional PCR for malaria parasite detection in low-grade parasitemia. *Exp Parasitol*. 2007; 116:427-432.
30. Malhotra I, Dent A, Mungai P, Muchiri E, King CL.

- Real-time quantitative PCR for determining the burden of *Plasmodium falciparum* parasites during pregnancy and infancy. *J Clin Microbiol.* 2005; 43:3630-3635.
31. Oguike MC, Betson M, Burke M, Nolder D, Stothard JR, Kleinschmidt I, Proietti C, Bousema T, Ndounga M, Tanabe K, Ntege E, Culleton R, Sutherland CJ. *Plasmodium ovale curtisi* and *Plasmodium ovale wallikeri* circulate simultaneously in African communities. *Int J Parasitol.* 2011; 41:677-683.
32. Souza CR, Carvalho TA, Amaral RC, Cunha LS, Cunha MG, Guerreiro JF. Prevalence of *Plasmodium falciparum* and *P. vivax* in an area of transmission located in Para State, Brazil, determined by amplification of mtDNA using a real-time PCR assay. *Genet Mol Res.* 2012; 11:3409-3413.
33. Landis JR, Koch GG. The measurement of observer agreement for categorical data. *Biometrics.* 1977; 33:159-174.
34. Singh B, Bobogare A, Cox-Singh J, Snounou G, Abdullah MS, Rahman HA. A genus- and species-specific nested polymerase chain reaction malaria detection assay for epidemiologic studies. *Am J Trop Med Hyg.* 1999; 60:687-692.
35. Hanscheid T, Grobusch MP. How useful is PCR in the diagnosis of malaria? *Trends Parasitol.* 2002; 18:395-398.
36. Taylor SM, Mayor A, Mombo-Ngoma G, et al. A quality control program within a clinical trial Consortium for PCR protocols to detect *Plasmodium* species. *J Clin Microbiol.* 2014; 52:2144-2149.
37. Murphy SC, Hermsen CC, Douglas AD, et al. External quality assurance of malaria nucleic acid testing for clinical trials and eradication surveillance. *PloS one.* 2014; 9:e97398.
38. WHO. A WHO external quality assurance scheme for malaria nucleic acid amplification testing. World Health Organization, 20 Avenue Appia, 1211 Geneva 27, Switzerland, 2015.

(Received August 22, 2018; Revised October 10, 2018;  
Accepted October 16, 2018)

## The importance of non-tuberculous mycobacteria identification in Chinese patients infected with HIV

Li Liu<sup>1</sup>, Renfang Zhang<sup>1</sup>, Yang Tang<sup>1</sup>, Tangkai Qi<sup>1</sup>, Wei Song<sup>1</sup>, Zhenyan Wang<sup>1</sup>, Yinzhou Shen<sup>1</sup>, Hongzhou Lu<sup>1,2,\*</sup>

<sup>1</sup> Department of Infectious Disease, Shanghai Public Health Clinical Center, Fudan University, Shanghai, China;

<sup>2</sup> Department of Infectious Disease, Huashan Hospital Affiliated to Fudan University, Shanghai, China.

### Summary

The increased co-incidence of tuberculosis (TB) and AIDS is compounded by the emergence of opportunistic infections with non-tuberculous mycobacteria (NTM) in patients with HIV/AIDS, and the treatment for these infections differs from that for TB. The high frequency of NTM strains found in patients infected with HIV raises concerns about accurate species identification before deciding proper treatment. A total of 101 isolates from 2014, 137 from 2015, and 162 from 2016 were subjected to 16S rDNA sequencing to identify the species. Forty-one (41/101, 40.6%) were identified as NTM in 2014, 64 (64/137, 46.7%) were identified as NTM in 2015, and 72 (72/162, 44.4%) were identified as NTM in 2016 in Chinese patients infected with HIV. The species of *Mycobacteria* isolates needs to be rapidly and accurately identified to determine appropriate antibiotic therapy, and this is especially true for patients infected with HIV.

**Keywords:** Non-tuberculous mycobacteria, tuberculosis (TB), HIV, identification

People living with human immunodeficiency virus (HIV) are approximately 30 times more likely to develop tuberculosis (TB) than individuals without HIV. TB is the most common presenting illness among people living with HIV, including those receiving antiretroviral treatment, and the major cause of HIV-related death (1). The TB-HIV/AIDS epidemic is compounded by the emergence of opportunistic infections with non-tuberculous mycobacteria (NTM) in patients with HIV/AIDS patients, and the treatment for these infections differs from that for TB. In patients with AIDS, the clinical and radiological features of infections with NTM and tuberculous mycobacteria (MTB) are more complex and usually involve different disease patterns and atypical clinical findings, thus limiting the diagnosis of mycobacterial infections in patients infected with HIV (2-3). Given the high prevalence of HIV infection in China, there is a growing concern that NTM and other infections could be misdiagnosed as MTB in people infected with

HIV. A recent report from Guangxi, China indicated that M. tuberculosis was found in 117 patients infected with HIV (53%) while NTM was found in 102 (47%) (4). The current study has determined the frequency with which MTB and NTM strains were isolated from patients infected with HIV in Shanghai from 2014 to 2016 and the genotype of NTM in this population.

A total of 101 isolates from 2014, 137 from 2015, and 162 from 2016 were subjected to 16S rDNA sequencing to identify the species. Forty-one (41/101, 40.6%) were identified as NTM in 2014, 64 (64/137, 46.7%) were identified as NTM in 2015, and 72 (72/162, 44.4%) were identified as NTM in 2016 (Figure 1). A total of 7 NTM species or complexes were identified from the NTM isolates (Table 1). The organism detected most frequently was M. avium complex (MAC), followed by M. gordonae and M. kansasii.

The high frequency of NTM strains found in patients infected with HIV raises concerns about accurate species identification before deciding proper treatment (5). Failure to characterize acid-fast bacilli (AFB)-positive lung infections caused by NTM has led to the misdiagnosis of these infections and mistreatment for pulmonary TB in developing countries such as China. Treatment is limited because of the difficulty in

\*Address correspondence to:

Dr. Hongzhou Lu, Shanghai Public Health Clinical Center, Fudan University, No.2901, Caolang Road, Jinshan District, Shanghai 201508, China.  
E-mail: luhongzhou@fudan.edu.cn

**Table 1. Identification of the species of NTM isolates**

Year	2014	2015	2016
M. avium complex (MAC)	17 (17/41, 41.5%)	26 (26/64, 40.6%)	32 (32/72, 44.4%)
M. gordonae	10 (10/41, 24.3%)	20 (20/64, 31.3%)	19 (19/72, 26.4%)
M. kansasii	11 (11/41, 26.8%)	15 (15/64, 23.4%)	18 (18/72, 25%)
M. fortuitum	2 (2/41, 4.9%)	0	0
M. abscessus	0	0	1 (1/72, 1.4%)
M. xenopi	0	3 (3/64, 4.7%)	2 (2/72, 2.8%)
M. szulgai	1 (1/41, 2.4%)	0	0

M: mycobacteria.

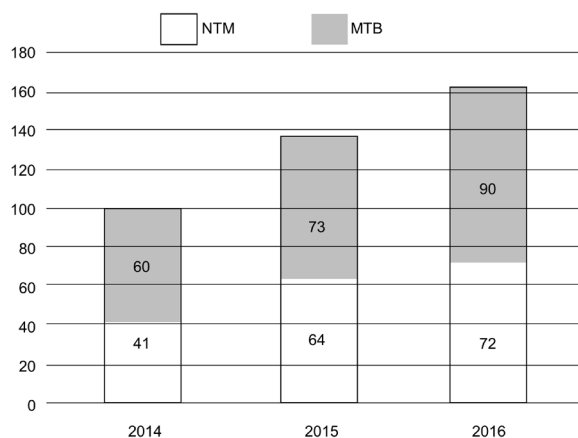


**Figure 1. Mycobacterium tuberculosis and non-tuberculous mycobacteria isolates from patients infected with HIV from 2014-2016 in Shanghai, China.** A total of 101,137 M. tuberculosis isolates and 162 non-tuberculous mycobacterium (NTM) isolates were subjected to 16S rDNA sequencing to identify the species. Forty-one samples (41/101, 40.6%) were identified as NTM in 2014, 64 (64/137, 46.7%) were identified as NTM in 2015, and 72 (72/162, 44.4%) were identified as NTM in 2016.

identifying the species of pathogen up and the resistance of most strains of NTM to conventional anti-MTB drugs (6). When treated empirically, some NTM infections are misdiagnosed as non-responsive or drug-resistant MTB cases, and this can result in poor outcomes for those patients (7). Overall, the species of Mycobacteria isolates needs to be rapidly and accurately identified to determine appropriate antibiotic therapy, and this is especially true for patients infected with HIV (8). However, many clinical laboratories in designated HIV/AIDS care units do not have proper facilities and experienced technicians, thus hampering the accurate diagnosis of mycobacterial infections in HIV/AIDS patients in China. All positive mycobacterial isolates need to be sent to an authorized lab for further identification. Conventional biochemical tests are time-consuming and their results are not reproducible, while novel molecular biology techniques and high-performance liquid chromatographic analysis of mycolic acid can be performed accurately and rapidly.

## Acknowledgements

This research was funded by a grant from the Shanghai Municipal Commission of Health and Family Planning (grant no. 15GWZK0103 ).

## References

1. Abubakar I, Gupta RK1, Rangaka MX, Lipman M. Update in tuberculosis and nontuberculous mycobacteria 2017. Am J Respir Crit Care Med. 2018; 197:1248-1253.
2. Nyamogoba HD, Mbuthia G, Mining S, Kikuvi G, Biegton R, Mpoke S, Menya D, Waiyaki PG. HIV co-infection with tuberculous and non-tuberculous mycobacteria in western Kenya: Challenges in the diagnosis and management. Afr Health Sci. 2012; 12:305-311.
3. Brode S.K, Daley C.L, Marras T.K. The epidemiologic relationship between tuberculosis and nontuberculous mycobacterial disease: A systematic review. Int J Tuberc Lung Dis. 2014; 18:1370-1377
4. Lan R, Yang C, Lan L, Ou J, Qiao K, Liu F, Gao Q. Mycobacterium tuberculosis and non-tuberculous mycobacteria isolates from HIV-infected patients in Guangxi, China. Int J Tuberc Lung Dis. 2011; 15:1669-1675.
5. Henkle E, Winthrop KL. Nontuberculous mycobacteria infections in immunosuppressed hosts. Clin Chest Med. 2015; 36:91-99.
6. Hoza AS, Mfinanga SG, Rodloff AC, Moser I, König B. Increased isolation of nontuberculous mycobacteria among TB suspects in Northeastern, Tanzania: Public health and diagnostic implications for control programmes. BMC Res Notes. 2016; 9:109.
7. Bjerrum S, Oliver-Commeij J, Kenu E, Lartey M, Newman MJ, Addo KK, Hilleman D, Andersen AB, Johansen IS. Tuberculosis and non-tuberculous mycobacteria among HIV-infected individuals in Ghana. Trop Med Int Health. 2016; 21:1181-1190.
8. Kobayashi T, Nishijima T, Teruya K, Aoki T, Kikuchi Y, Oka S, Gatanaga H. High mortality of disseminated non-tuberculous mycobacterial infection in HIV-infected patients in the antiretroviral therapy era. PLoS One. 2016; 11:e0151682.

(Received October 19, 2018; Accepted October 25, 2018)

## Correlation between the use of antibiotics and development of a resistant bacterial infection in patients in the ICU

Yingxia Li<sup>1</sup>, Xiyan Xia<sup>2</sup>, Xiaohui Li<sup>3</sup>, Ke Xiao<sup>3</sup>, Xuewei Zhuang<sup>3,\*</sup>

<sup>1</sup> General Surgery, Qilu Hospital Affiliated with Shandong University, Ji'nan, China;

<sup>2</sup> Department of Immunology, Jinan Vocational College of Nursing, Ji'nan, China;

<sup>3</sup> Clinical Laboratory, Qilu Hospital Affiliated with Shandong University, Ji'nan, China.

### Summary

The current study analyzed the correlation between the use of antibiotics and development of a resistant bacterial infection in 454 patients in intensive care units (ICUs), and this study also examined factors related to development of an infection in order to facilitate more rational use of antibiotics and to reduce the incidence of resistant bacterial infections. Potential subjects were patients who were admitted to the ICU in 2016, and 454 such patients were selected using cluster sampling. Patient information was documented using an original questionnaire. Patients in the ICU with a Resistant Bacterial Infection. The correlation between use of an antibiotic and development of a resistant bacterial infection was examined. The rate of infection significantly increased over time and with receipt of various antibiotics. The development of a resistant bacterial infection was found to correlate with the use of antibiotics. Antibiotics should be used more carefully to reduce the incidence of resistant bacterial infections

**Keywords:** Patients in the ICU, antibiotics, resistant bacterial infection

Antibiotic resistance due to the severe overuse of antibiotics has become a worldwide problem. The global increase in infections with resistant bacteria is a cause for concern because these highly resistant bacteria are associated with higher patient morbidity and because these bacteria are susceptible to few or no antimicrobials (1-3). The Chinese Ministry of Health's Department of Medical Administration has conducted several trials to reduce the overuse of antibiotics, but more than 20% inpatients still develop a resistant bacterial infection. This has a serious impact on infection control efforts due to the lack of effective antibiotics, and especially in intensive care units (ICUs) (4). The current study examined the correlation between the use of antibiotics and development of a resistant bacterial infection and related factors in order to promote more rational use of antibiotics to reduce the development of resistant bacterial infections.

Potential subjects were patients age 18 or over who

were admitted to the ICU at this Hospital no more than 48 h prior in 2016. Subjects were 454 such patients who were selected using cluster sampling. All subjects provided written informed consent prior to participation in this study, and this study was approved by the ethics committee at this hospital. Basic patient information was documented using an original questionnaire. Infection surveillance was achieved using a nosocomial infection surveillance system (NISS) and a hospital information system (HIS) as well as a point-of-care investigation. Data were analyzed using the statistical software SPSS 19.0. Basic information is expressed as the mean  $\pm$  standard deviation, the rate, the percentage, etc. Continuous variables were compared using the Student *t* test and categorical variables were compared using the chi-square test. A difference of  $p < 0.05$  was considered statistically significant.

Of the 454 patients, 427 received an antibiotic during hospitalization. One hundred and thirty of the 427 patients (30.44%) who received an antibiotic developed a resistant bacterial infection while 1 of the 27 patients (3.70%) who did not receive antibiotics developed a resistant bacterial infection. The rate of infection differed significantly between the two groups ( $p = 0.003$ ) (Table 1).

\*Address correspondence to:

Dr. Xuewei Zhuang, Clinical Laboratory Medicine, Qilu Hospital Affiliated with Shandong University, 107 Wenhua West Road, Ji'nan, Shandong 250012, China.  
E-mail: zhuangxuewei@sdu.edu.cn

**Table 1. Infection with a resistant bacterium and use of an antibiotic**

Antibiotics used	Developed a resistant bacterial infection (n)		Total	Rate of infection (%)	$\chi^2$	p
	Yes	No				
No	1	26	27	3.70	8.846	0.003*
Yes	130	297	427	30.44		

**Table 2. Number of antibiotics and development of a resistant bacterial infection**

Number of antibiotics	Developed a resistant bacterial infection (n)		Total	Rate of infection (%)	$\chi^2$	p
	Yes	No				
One	12	165	177	6.78	152.779	0.000
Two	38	100	138	27.54		
Three	31	27	58	53.45		
Four or more	48	5	53	90.57		

The rate of infection with a resistant bacterium differed significantly in patients who had received one, two, three, or four or more antibiotics, indicating that the rate of infection increased significantly when patients received a combination of antibiotics (Table 2).

Of the 454 patients, 298 patients had previously received an antibiotic before admission to the ICU. One hundred and twelve of those 298 patients (37.58%) subsequently developed a resistant bacterial infection. Only 18 of the 156 remaining patients (11.54%) developed a resistant bacterial infection. The rate of infection in those two groups different significantly ( $p < 0.001$ ). Patients who received an antibiotic before admission to the ICU developed a resistant bacterial infection at a rate of 37.58%, which was significantly higher than the rate in patients who had not received an antibiotic ( $p < 0.001$ ). Fifty-four of the 454 patients died, and 34 of those patients had a resistant bacterial infection. Only 97 of the 400 surviving patients had a resistant bacterial infection. The rate of infection in patients who died was 62.96%, which was significantly higher than the rate in patients who survived ( $p < 0.001$ ).

Infections are effectively regulated as a result of the large-scale use of antibiotics. However, the overuse of antibiotics has led to strains developing antibiotic resistance and even causing reinfection. Moreover, infections rage out of control and mortality increases when host bacterial homeostasis *in vivo* is disrupted (3). Patients with an infection have more severe subsequent complications and a higher mortality, and unwarranted use of antibiotics results in a vicious circle of resistant bacterial infections (5,6). Hence, antibiotic resistance has garnered attention around the world. The current study examined the correlation between use of an antibiotic and development of a resistant bacterial infection in detail. Patients who had previously received an antibiotic developed a resistant bacterial infection at a higher rate than patients who had not received antibiotics. The rate of infection increased over time

and with previous receipt of an antibiotic. Patients in the ICU who had previously received an antibiotic had a significantly higher rate of infection than patients who had not received antibiotics. The incidence of a resistant bacterial infection was correlated with the receipt of an antibiotic, and especially a broad-spectrum antibiotic. Infection with an antibiotic-resistant bacterium is one of the leading causes of mortality (7).

In summary, the current study found that development of a resistant bacterial infection correlated with the use of antibiotics. Antibiotics should be used more carefully to reduce the incidence of resistant bacterial infections. Medical personnel should adopt certain principles to reduce resistant bacterial infections as much as possible, such as rational prescribing based on a drug's properties, combating infections based on a drug sensitivity test, proper dosage over the required period, careful attention to normal bacteria, use of certain routes of medications, and avoiding blind usage and frequent alternations in medication (8).

### Acknowledgements

This study was supported in part by grants from the Shandong Provincial Key Research Program (2016GSF201169), the Shandong Provincial Nature Science Foundation (2015ZRE2757), the Shandong Provincial Medicine and Health Development Plan (QW019), and the Shandong Provincial Population and Family Development Plan (200910).

### References

1. Haverkate MR, Derde LP, Brun-Buisson C, Bonten MJ, Bootsma MC. Duration of colonization with antimicrobial-resistant bacteria after ICU discharge. *Intensive Care Med.* 2014; 40:564-571.
2. Magiorakos AP, Burns K, Rodríguez Baño J, Borg M, Daikos G, Dumpis U, Lucet JC, Moro ML, Tacconelli E, Simonsen GS, Szilágyi E, Voss A, Weber JT.

- Infection prevention and control measures and tools for the prevention of entry of carbapenem-resistant *Enterobacteriaceae* into healthcare settings: Guidance from the European Centre for Disease Prevention and Control. *Antimicrob Resist Infect Control*. 2017; 6:113.
3. Martin-Loeches I, Torres A, Rinaudo M, Terraneo S, de Rosa F, Ramirez P, Diaz E, Fernández-Barat L, Li Bassi GL, Ferrer M. Resistance patterns and outcomes in intensive care unit (ICU)-acquired pneumonia. Validation of European Centre for Disease Prevention and Control (ECDC) and the Centers for Disease Control and Prevention (CDC) classification of multidrug resistant organisms. *J Infect*. 2015; 70:213-222.
  4. Hanberger H, Walther S, Leone M, Barie PS, Rello J, Lipman J, Marshall JC, Anzueto A, Sakr Y, Pickkers P, Felleiter P, Engoren M, Vincent JL; EPIC II Group of Investigators. Increased mortality associated with methicillin-resistant *Staphylococcus aureus* (MRSA) infection in the intensive care unit: Results from the EPIC II study. *Int J Antimicrob Agents*. 2011; 38:331-335.
  5. Harris AD, Pineles L, Belton B, et al. Universal glove and gown use and acquisition of antibiotic-resistant bacteria in the ICU: A randomized trial. *JAMA*. 2013; 310:1571-1580.
  6. Derde LP, Dautzenberg MJ, Bonten MJ. Chlorhexidine body washing to control antimicrobial-resistant bacteria in intensive care units: A systematic review. *Intensive Care Med*. 2012; 38:931-939.
  7. Shafi S, Collinsworth AW, Richter KM, et al. Bundles of care for resuscitation from hemorrhagic shock and severe brain injury in trauma patients-translating knowledge into practice. *J Trauma Acute Care Surg*. 2016; 81:780-794.
  8. Yang A, Tang WS, Si T, Tang JX. Influence of physical effects on the swarming motility of *Pseudomonas aeruginosa*. *Biophys J*. 2017; 112:1462-1471.

(Received June 12, 2018; Revised September 3, 2018;  
Accepted October 6, 2018)

## The relation between social cohesion and the care burden of family healthcare providers

**Yuki Naganuma<sup>1</sup>, Sumiko Kihara<sup>2</sup>, Yasuhiko Fujita<sup>2</sup>, Kazue Yamaoka<sup>3</sup>, Kenzo Takahashi<sup>3,\*</sup>**

<sup>1</sup> Department of Nursing, Tokyo Ariake University of Medical and Health Sciences, Tokyo, Japan;

<sup>2</sup> Tokunoshima Tokushukai Hospital, Tokunoshima, Japan;

<sup>3</sup> Teikyo University Graduate School of Public Health, Tokyo, Japan.

### Summary

This study aimed to clarify the relationship between social cohesion and family care burden. The social capital indicators of Kondo *et al.* and the short version of the Zarit Care Burden Interview Scale in Japanese (J-ZBI\_8) were used. Data were analyzed by multiple regression models. Seventy-one caregivers responded. Factors showing statistical significance in the multiple regression analysis included "receipt of emotional support" ( $p = 0.009$ ) and "instrumental support provided" ( $p = 0.010$ ). Social support was suggested to have a possible effect on the care burden of the main caregivers to relate to less burden. The gap between the original ideal loss and the social role caused by providing nursing care is likely to increase the degree of care burden.

**Keywords:** Care burden, family caregivers, home care, social cohesion, Zarit Care Burden Interview Scale

The aging population in Japan is expected to increase as the overall population declines. The Ministry of Health is stressing the importance of offering comprehensive yet intermittent home nursing care to the elderly (1). Long-term care insurance systems provided in Japan to support elderly care currently classify patients based on their activities of daily life or level of dementia. The family structure is not considered for registration. Sudo *et al.* noted that in Japan, support for preventive care that encourages informal power including self-help and mutual aid has been spotlighted and strengthened by municipalities as authorized by support from the public, which may take the social cohesion for granted (2). Nevertheless, little evidence exists on whether social cohesion, an element of social capital, reduces the burden of caregivers who provide home nursing care (3). Our study aimed to clarify the relationship between social cohesion and family care burden.

We conducted a questionnaire survey in the isolated island of Tokunoshima. The study targets included caregivers living with patients aged 65 years or older who were visiting medical care services or using

visiting nursing care services registered in Tokunoshima Tokushukai Hospital (TTH). The research was conducted from 1 September to 4 October 2015.

The questionnaire was based on the social capital indicators of Kondo *et al.* (4) and the Japanese short version of the Zarit Care Burden Interview scale (J-ZBI\_8) (5,6). Confounding factors were the caregiver's sex, age, and occupation, length of caregiving, educational background, length of residence time, household, sex of the patient under care, and patient's age. Data were analyzed by multiple linear regression models.

The question items regarding social capital, especially on social cohesion, that were investigated were 1) Receipt of emotional support for the caregiver by the community, 2) Emotional support provided to others by the caregiver, 3) Instrumental support provided; care for the resident given by others when the caregiver cannot provide care, 4) Instrumental support provided by the caregiver and others, 5) Participant in organized activities – frequency of participation in the activities of a group organization, and 6) Caregiver's social network – using the frequency of meeting with friends and acquaintances. Questions 1)–4) were classified into two categories, Yes or No. Questions 5) and 6) asked for a frequency and were divided into two categories. We also conducted a logistic regression using dichotomous classification of

\*Address correspondence to:

Dr. Kenzo Takahashi, Graduate School of Public Health, Teikyo University, 2-11-1 Kaga, Itabashi-ku, Tokyo 173-8605, Japan.

E-mail: kenzo.takahashi.chgh@med.teikyo-u.ac.jp

**Table 1. Characteristic of the participants (N = 71)**

Items	Total	(Missing)	Number	%	Mean (SD)	Median (25–75th percentile)
Social Capital scale	64	7			4.8 (1.3)	5 (4-6)
1) Social support: receipt of emotional support	70	1				
No			5	7.1		
Yes			65	92.9		
2) Social support: emotional support provided	67	4				
No			10	14.9		
Yes			57	85.1		
3) Social support: receipt of instrumental support	71	—				
No			9	12.7		
Yes			62	87.3		
4) Social support: instrumental support provided	68	3				
No			13	19.1		
Yes			55	80.9		
5) Participant in organized activities	71	—				
No			39	54.9		
Yes			32	45.1		
6) Caregiver's social network	71	—				
No			11	15.5		
Yes			60	84.5		
Caregiver						
Gender	71	—				
Male			28	39.4		
Female			43	60.6		
Age (years)	71	—			69.9 (13.9)	66 (61-83)
Length of residence time	67	4			34	30 (11.7-50)
Length of caregiving time	69	2			5.79	5 (2.0-10)
Family members present (excluding care recipient)	65	6				
Have			45	69.2		
Not have			20	30.8		
Working Status	69	2				
Working <sup>†</sup>			25	36.2		
Unemployed/Homemaker			44	63.8		
Education	70	1				
High school			20	28.6		
Graduated high school			28	40.0		
Higher than high school			22	31.4		
Home-care patient						
Gender	70	1				
Male			27	38.6		
Female			43	61.4		
Age	70	1			85.9 (13.3)	87.5 (82-93)
Pattern of care	70	1				
Elder to elder			30	42.9		
Next-generation primary caregivers <sup>‡</sup>			40	57.1		
Gender pattern <sup>¶</sup>	70	1				
Male-Male			3	4.3		
Male-Female			25	35.7		
Female-Male			23	32.9		
Female-Female			19	27.1		

<sup>†</sup>Part-time job is included. <sup>‡</sup>Includes daughter, daughter-in-law, son, and grandchild. <sup>¶</sup>Gender pattern (A-B) means the relation between (gender of elderly cared for – gender of primary caregivers). SD, standard deviation; CI, confidence interval.

the total score of the J-ZBI\_8 (a variable of  $\geq 13$  vs.  $\leq 12$ ) and correspondence analysis.

Statistical analyses were conducted using SAS Ver. 9.3, and a two-sided level of 5% was considered to indicate statistical significance. Ethics approval was granted by Teikyo University (No. 15-038) and the ethics committee of TTH (TGE00526-018).

Ninety-nine people were approached to participate in the study, and 71 caregivers responded to the survey (response rate 72%). The average age of the primary caregivers was  $69.9 \pm 13.9$  years old (28 men, 43 women), and that of the person receiving care was  $85.9 \pm 13.3$  years old (Table 1). Cronbach's  $\alpha$  for the J-ZBI\_8 was 0.89. The results of the multiple regression analysis are shown in Table 2. In terms of social support, the

factors showing a significant difference included "receipt of emotional support" ( $p = 0.009$ ) and "instrumental support provided" ( $p = 0.010$ ).

The presence of "someone who heard the worries and complaints" resulted in a significant difference ( $\beta = 0.49$ ; Table 2). That "there are people who listen to the worries and complaints" was the result of increasing the care burden. This result suggests a link to self-disclosure (7).

We interpreted from the analysis of the correspondence that the next-generation primary caregivers (son, daughter, daughter-in-law, son-in-law or grandchildren) tended to rely on friends and neighbors for support, whereas the elderly primary caregivers tended to rely on relatives. A high care burden was a concern if the next-generation primary caregiver did not

**Table 2. Results of liner regression analysis**

Items	Simple regression analysis			Multiple regression analysis		
	$\beta$ (beta)	SE	p-value	$\beta$ (beta)	SE	p-value
Social Capital total <sup>†</sup>	-0.03	0.04	0.529			
1) Social support: receipt of emotional support	0.33	0.19	0.085	0.49	0.18	0.009
2) Social support: emotional support provided	0.03	0.14	0.823			
3) Social support: receipt of instrumental support	-0.33	0.14	0.024	-0.37	0.14	0.01
4) Social support: instrumental support provided	-0.1	0.13	0.433			
5) Participant in organized activities	-0.1	0.1	0.313	-0.13	0.09	0.171
6) Caregiver's social network	-0.07	0.14	0.602			
Caregiver						
Gender	0.02	0.1	0.84			
Age (10-year units)	0	0.04	0.922			
Length of residence time (1-year units)	-0.02	0.02	0.35			
Length of caregiving time (1-year units)	-0.01	0.12	0.901			
Family members present (excepting care recipient)	0	0.11	0.975			
Working status	-0.16	0.01	0.1			
Education						
High school	0.02	0.1	0.84			
Graduated high school	0.19	0.1	0.06			
Higher than high school	-0.17	0.1	0.1			
Home-care patient						
Gender	0.11	0.1	0.253			
Age (10-year units)	0.04	0.04	0.35			
Gender pattern <sup>*</sup>						
Age	0.03	0.1	0.8			
Gender				-0.42	0.22	0.066
Male-Male	-0.41	0.24	0.09			
Male-Female	0.05	0.1	0.6			
Female-Male	-0.04	0.1	0.7			
Female-Female	0.13	0.11	0.23			

<sup>†</sup>Not included in the linear regression analysis. A stepwise method was used for variable selection in the multiple linear regression analysis with the inclusion and exclusion criteria of 20%. A variable that was not selected in the stepwise method is indicated by "-". <sup>\*</sup>Gender pattern (A-B) means the relation between (gender of elderly cared for – gender of primary caregivers). J-ZBI\_8, short version of the Zarit Care Burden Interview scale in Japanese; SE, standard error.

receive support from friends and neighbors and did not participate in organized activities.

The Japanese Cabinet Office conducted "Consciousness research on elderly housing and living environment" in 2010. About 10% of single-person households were unable to form relationships with others in the neighborhood, responding that "there is no relationship" with the neighborhood. Households comprising one adult and a child also had few relationships with their neighbors (8). Considering a wide variety of family situations and backgrounds, the primary caregiver may well feel loneliness and a burden for caregiving. In addition, the gap between the loss of ideal world and the social role caused by the nursing care is also likely to increase the care burden (9). To support caregivers, maintaining social roles is important.

A community support system that includes not only medical personnel but also community residents is needed. Development of such a system is suggested to provide community support to patients and their families living at home.

## References

- Ministry of Health, Labor and Welfare. Toward a regional comprehensive health care system. [http://www.mhlw.go.jp/stf/seisakunitsuite/bunya/hukushi\\_kaigo/kaigo\\_koureisha/chiiki-houkatsu/](http://www.mhlw.go.jp/stf/seisakunitsuite/bunya/hukushi_kaigo/kaigo_koureisha/chiiki-houkatsu/) (accessed October 12, 2018) (in

Japanese)

2. Sudo K, Kobayashi J, Noda S, Fukuda Y, Takahashi K. Japan's healthcare policy for the elderly through the concepts of self-help (Ji-jo), mutual aid (Go-jo), social solidarity care (Kyo-jo), and governmental care (Ko-jo). Biosci Trends. 2018; 12:7-11.
3. Carrasco MA, Bilal U. A sign of the times: To have or to be? Social capital or social cohesion? Soc Sci Med. 2016;159:127-131.
4. Inaba Y, Kanamitsu J, Kondo K, Yamauchi N, Tsujinaka Y, Ohmari T. What is the science of social capital? Kyoto, Minerva Shobo, 2014. (in Japanese)
5. Arai Y, Nanako T, Yano E. The short version of the Japanese version of the Zarit Caregiver Burden Interview (J-ZBI\_8): its reliability and validity. Nihon Ronen Igakkai Zasshi. 2003; 40:497-503. (in Japanese)
6. Zarit SH, Reever KE, Bach-Peterson J. Relatives of the impaired elderly: Correlates of feelings of burden. Gerontologist. 1980; 20:649-655.
7. Hiroaki E. Psychological research of self-disclosure: No. 4 edition. Kyoto, Kitaoji Shobo, 2009. (in Japanese)
8. Cabinet Office. Consciousness research on elderly housing and living environment 2010; part 2. (in Japanese)
9. D'Ippolito M, Aloisi M, Azicnuda E, Silvestro D, Giustini M, Verni F, Formisano R, Bivona U. Changes in caregivers lifestyle after severe acquired brain injury: A preliminary investigation. Biomed Res Int. 2018; 2018:2824081.

(Received July 27, 2018; Revised October 27, 2018;

Accepted October 28, 2018)

## Prescription surveillance for early detection system of emerging and reemerging infectious disease outbreaks

Tamie Sugawara<sup>1</sup>, Yasushi Ohkusa<sup>1</sup>, Hirokazu Kawanohara<sup>2</sup>, Miwako Kamei<sup>3,\*</sup>

<sup>1</sup> National Institute of Infectious Diseases, Tokyo, Japan;

<sup>2</sup> EM Systems Co. Ltd., Osaka, Japan;

<sup>3</sup> School of Pharmacy, Nihon University, Chiba, Japan.

### Summary

Based on prescriptions filled at external pharmacies, prescription surveillance (PS) in Japan has been reporting the estimated numbers of influenza and varicella patients and people prescribed certain drugs since 2009. Every morning, this system estimates the numbers of patients from the numbers of prescriptions filled nationwide for neuraminidase inhibitors, anti-herpes virus drugs, antibiotic drugs, antipyretic analgesics, and multi-ingredient cold medications. Moreover, it can detect "unexplained" infectious diseases that are not explained as infectious diseases monitored by other surveillance systems. Such "unexplained" infectious diseases might be emerging and re-emerging infectious diseases including bioterrorism attacks, which are reportedly difficult to diagnose, at least in early outbreak stages. To ascertain the system's potential benefits, this study examined schemes to detect "unexplained" infectious diseases using PS information. The numbers of patients prescribed the respective drugs are first regressed on the known infectious diseases, time trends, and dummies for day-of-the-week, holidays, and days following a holiday. Known infectious diseases are defined as covered by the National Official Sentinel Surveillance for Infectious Diseases under the Infection Control Law. After the numbers of patients from PS are compared with the predicted numbers of patients, their probabilities of occurrence are calculated. We examined the system's prospective operation from January 2017 through July 2018. The criterion we used to define aberrations varied, from 0.01 to  $10^{-7}$ . For criteria of 0.01 and  $10^{-7}$  we found 254 and 15 aberrations, respectively. We confirmed its feasibility and effectiveness.

**Keywords:** Prescription surveillance, pharmacy, emerging and reemerging infectious disease, bioterrorism attack, National Official Sentinel Surveillance for Infectious Diseases

In Japan, the National Official Surveillance for Infectious Diseases (NOSSID) is operated based on a related Law. Except for some severe diseases, it requires only the sentinel medical institution to report the number of patients weekly. For many common pediatric infectious diseases, 3,000 sentinel pediatric care facilities, which account for about one-tenth of all pediatric care facilities throughout Japan, report the number of cases each week by NOSSID. For influenza, 2,000 internal medicine care facilities were added (1). The sentinel reports are regarded as reliable information

because it based on physician's diagnosis. Nevertheless, these reports are published weekly after a ten-day delay following diagnosis. For that reason, they probably cannot indicate emerging or re-emerging infectious diseases early.

Prescription surveillance (PS), as operated in Japan by the Japan Medical Association, Japan Pharmaceutical Association, School of Pharmacy, Nihon University, and EM Systems Co. Ltd., is a nationwide syndromic surveillance. Since 2009, it has been reporting the estimated number of influenza and chicken pox patients, and the numbers of patients prescribed drugs of certain types, based on prescriptions at pharmacies (2-7). It estimates the numbers of patients every day from the number of prescriptions by prefecture by age group. As of the end of April 2015, approximately ten

\*Address correspondence to:

Dr. Miwako Kamei, School of Pharmacy, Nihon University, 7-7-1 Narashinodai, Funabashi-shi, Chiba 274-8555, Japan.  
E-mail: kamei.miwako@nihon-u.ac.jp

thousand pharmacies were participating, collectively accounting for about 20% of all pharmacies. The estimated numbers of patients are presented on the web page the following morning (<http://prescription.orca.med.or.jp/kanjyasideki/>).

It is apparently useful to detect aberrational increases of patients with some symptoms that cannot be found by NOSSID. To examine its potential, we proposed and examined schemes to detect "unexplained" infectious diseases using PS information.

PS estimates the numbers of patients by multiplying the reciprocal of the pharmacy PS participation rate and the reciprocal of the proportion of prescriptions at external pharmacies in the prefecture by the total number of prescriptions issued in the prefecture. The numbers of patients prescribed neuraminidase inhibitors

(NI), anti-herpes virus drugs (AHV), antibiotic drugs (AB), antipyretic analgesics (AP), multi-ingredient cold medications (MIC), and antidiarrheal and intestinal drugs (AD) have been recorded. Antibiotics are classified into five types: penicillin (ABP), cephem (ABC), macrolide (ABM), new quinolone (ABQ), and others (ABO) (2,3).

To predict the numbers of patients taking those drug by well-known infectious diseases, we used the data for influenza, RS virus infection (RS), pharyngoconjunctival fever (PCF), group A streptococcal pharyngitis (A-SP), gastrointestinal infections (GI), varicella, hand, foot and mouth disease (HFMD), erythema infectiosum (EI), exanthem subitum (ES), pertussis, herpangina, mumps, and mycoplasma pneumonia(MP) from NOSSID. Except for RS, NOSSID provides numbers of patients per sentinel per week as the incidence of each disease. For RS, NOSSID provides only the total number of patients per week.

First, from known infectious diseases and calendar information, we predicted the numbers of patients prescribed each drug. The dependent variable was the number of patients prescribed drug  $i$  on day  $t$ . Explanatory variables were the NOSSID reported number of patients of disease  $j$ : the latest available data in day  $t$ . Because NOSSID publishes data in the prior week on Friday at noon, the latest available data are two weeks prior on Monday–Friday, and one week prior on Saturday and Sunday. Furthermore,

**Table 1. Criteria and numbers of detected aberration**

Criterion	Number of detected aberration
$10^{-2}$	254
$10^{-3}$	126
$10^{-4}$	66
$10^{-5}$	40
$10^{-6}$	30
$10^{-7}$	21
$10^{-8}$	15

*Note:* Total number of days and drug types was 5790. "Criterion" means that if the  $p$ -value was less than criterion, then we inferred that type of drug on that day as an aberration.

**Table 2. Detected aberrations when the criterion was  $10^{-5}$**

Year	Month	Day of week	Hol	Holw	ABP	ABC	ABQ	ABO	AP	MIC
2017	1	Mon								> 8
2017	1	Mon								> 8
2017	5	Mon	Yes							
2018	1	Fri								
2018	1	Tue	Yes							7.1
2018	1	Mon	Yes							> 8
2018	1	Tue								> 8
2018	1	Wed								7.3
2018	1	Thu								6.7
2018	1	Fri								> 8
2018	1	Mon	Yes							> 8
2018	1	Mon	Yes							> 8
2018	2	Mon	Yes							> 8
2018	2	Tue	Yes							5.3
2018	6	Fri								> 8
2018	6	Fri								> 8
2018	6	Sat								6.5
2018	6	Tue								7.1
2018	6	Wed								5.5
2018	6	Thu								6.2
2018	6	Fri								7.4
2018	7	Fri								5.2
2018	7	Fri								6.4
2018	7	Wed								5.4
2018	7	Fri								5.0
										> 8

*Note:* No aberration of neuraminidase inhibitors (NI), anti-herpes virus drugs (AHV), macrolide (ABM), and antidiarrheal/intestinal drugs (AD) was detected. ABC, cephem; ABO, other antibiotic drugs; ABP, penicillin; ABQ, new quinolone; AP, antipyretic analgesics; Hol, one for a day following a holiday or Sunday, otherwise zero; Holw, one for a day following two consecutive holidays or Sunday, otherwise zero; MIC, multi-ingredient cold medications.

explanatory variables included dummy variables of the epidemiological week, day of the week, holiday, and the day following a holiday, the day following two consecutive holidays, summer vacation (13-15 August), and the new year vacation (1-3 January).

Next, we calculated the probabilities at which they occurred if the numbers of patients from PS greater than the predicted number. If the *p*-value was lower than a criterion, it was regarded as aberration. We examine criteria from  $10^{-2}$  to  $10^{-7}$ . We applied this analysis prospectively from January 2017 through July 2018 using data from 1 October, 2010 to the day prior for prediction.

Table 1 presents association among criteria and the numbers of aberrations. When the criterion was 0.01, 254 aberrations were found. Its proportion was 4.4%. Conversely, when we used the criterion of  $10^{-7}$ , the number of aberrations decreased to 15, which is 0.26%.

Table 2 presents calendar information and the probability of detected aberrations if criterion was  $10^{-5}$ . In total, 40 aberrations were found in 25 days: ABP had 2 aberrations; ABC had 9; ABQ had 2; ABO had 10; AP had 12; and MIC had 5. No aberration was detected in NI, AHV, ABM, or AD.

Of 25 days, 7 were Monday, 4 were Tuesday, 3 were Wednesday, 2 were Thursday, 8 were Friday, and 1 was Saturday. Nine aberrations occurred on a day following a holiday. Only one aberration was detected on a day following two consecutive holidays.

Overall, we conclude that aberration seemed not to be biased to a particular day of the week or a day following a holiday. Therefore, we confirmed its feasibility and effectiveness. We expect to perform it prospectively and share the results to support public

health countermeasures against bioterrorism attack.

## References

1. Hashimoto S, Murakami Y, Taniguchi K, Shindo N, Osaka K, Fuchigami H, Nagai M. Annual incidence rate of infectious diseases estimated from sentinel surveillance data in Japan. *J Epidemiol.* 2003; 13:136-141.
2. Sugawara T, Ohkusa Y, Ibuka Y, Kawanohara H, Taniguchi K, Okabe N. Real-time prescription surveillance and its application to monitoring seasonal influenza activity in Japan. *J Med Internet Res.* 2012; 14:e14.
3. Sugawara T, Ohkusa Y, Kawanohara H, Taniguchi K, Okabe N. Chickenpox case estimation in acyclovir pharmacy survey and early bioterrorism detection. *Kansenshogaku Zasshi.* 2011; 85:632-637. (in Japanese).
4. Nakamura Y, Sugawara T, Kawanohara H, Ohkusa Y, Kamei M, Oishi K. Evaluation of the estimated number of influenza patients from national sentinel surveillance using national database of electronic medical claims. *Jpn J Infect Dis.* 2015; 68:27-29.
5. Nakamura Y, Kawanohara H, Kamei M. Evaluation of influenza patients in each prefecture estimated by prescription surveillance using national electronic medical claims. *Kouseinoshishyou.* 2015; 23-29. (in Japanese).
6. Nakamura Y, Kawanohara H, Kamei M. Evaluation of the number of varicella patients estimated by prescription surveillance. *Kansenshogaku Zasshi.* 2015; 89:23-29. (in Japanese).
7. Nakamura Y, Kawanohara H, Kamei M. Association between diarrheal infectious diseases and antidiarrheal drugs by prescription surveillance. *Kansenshogaku Zasshi.* 2015; 9:388-393. (in Japanese).

(Received August 24, 2018; Revised October 23, 2018;  
Accepted October 25, 2018)

### Guide for Authors

#### 1. Scope of Articles

BioScience Trends is an international peer-reviewed journal. BioScience Trends devotes to publishing the latest and most exciting advances in scientific research. Articles cover fields of life science such as biochemistry, molecular biology, clinical research, public health, medical care system, and social science in order to encourage cooperation and exchange among scientists and clinical researchers.

#### 2. Submission Types

**Original Articles** should be well-documented, novel, and significant to the field as a whole. An Original Article should be arranged into the following sections: Title page, Abstract, Introduction, Materials and Methods, Results, Discussion, Acknowledgments, and References. Original articles should not exceed 5,000 words in length (excluding references) and should be limited to a maximum of 50 references. Articles may contain a maximum of 10 figures and/or tables.

**Brief Reports** definitively documenting either experimental results or informative clinical observations will be considered for publication in this category. Brief Reports are not intended for publication of incomplete or preliminary findings. Brief Reports should not exceed 3,000 words in length (excluding references) and should be limited to a maximum of 4 figures and/or tables and 30 references. A Brief Report contains the same sections as an Original Article, but the Results and Discussion sections should be combined.

**Reviews** should present a full and up-to-date account of recent developments within an area of research. Normally, reviews should not exceed 8,000 words in length (excluding references) and should be limited to a maximum of 100 references. Mini reviews are also accepted.

**Policy Forum** articles discuss research and policy issues in areas related to life science such as public health, the medical care system, and social science and may address governmental issues at district, national, and international levels of discourse. Policy Forum articles should not exceed 2,000 words in length (excluding references).

**Case Reports** should be detailed reports of the symptoms, signs, diagnosis, treatment, and follow-up of an individual patient. Case reports may contain a demographic profile of the patient but usually describe an unusual or novel occurrence. Unreported or unusual

side effects or adverse interactions involving medications will also be considered. Case Reports should not exceed 3,000 words in length (excluding references).

**News** articles should report the latest events in health sciences and medical research from around the world. News should not exceed 500 words in length.

**Letters** should present considered opinions in response to articles published in BioScience Trends in the last 6 months or issues of general interest. Letters should not exceed 800 words in length and may contain a maximum of 10 references.

#### 3. Editorial Policies

**Ethics:** BioScience Trends requires that authors of reports of investigations in humans or animals indicate that those studies were formally approved by a relevant ethics committee or review board.

**Conflict of Interest:** All authors are required to disclose any actual or potential conflict of interest including financial interests or relationships with other people or organizations that might raise questions of bias in the work reported. If no conflict of interest exists for each author, please state "There is no conflict of interest to disclose".

**Submission Declaration:** When a manuscript is considered for submission to BioScience Trends, the authors should confirm that 1) no part of this manuscript is currently under consideration for publication elsewhere; 2) this manuscript does not contain the same information in whole or in part as manuscripts that have been published, accepted, or are under review elsewhere, except in the form of an abstract, a letter to the editor, or part of a published lecture or academic thesis; 3) authorization for publication has been obtained from the authors' employer or institution; and 4) all contributing authors have agreed to submit this manuscript.

**Cover Letter:** The manuscript must be accompanied by a cover letter signed by the corresponding author on behalf of all authors. The letter should indicate the basic findings of the work and their significance. The letter should also include a statement affirming that all authors concur with the submission and that the material submitted for publication has not been published previously or is not under consideration for publication elsewhere. The cover letter should be submitted in PDF format. For example of Cover Letter, please visit <http://www.biostencetrends.com/downncentre.php> ([Download Centre](#)).

**Copyright:** A signed JOURNAL PUBLISHING AGREEMENT (JPA) form must be provided by post, fax, or as a scanned file before acceptance of the article. Only forms with a hand-written signature are accepted. This copyright will ensure the widest possible dissemination of information. A form facilitating transfer of copyright can be downloaded by clicking the

appropriate link and can be returned to the e-mail address or fax number noted on the form (Please visit [Download Centre](#)). Please note that your manuscript will not proceed to the next step in publication until the JPA Form is received. In addition, if excerpts from other copyrighted works are included, the author(s) must obtain written permission from the copyright owners and credit the source(s) in the article.

**Suggested Reviewers:** A list of up to 3 reviewers who are qualified to assess the scientific merit of the study is welcomed. Reviewer information including names, affiliations, addresses, and e-mail should be provided at the same time the manuscript is submitted online. Please do not suggest reviewers with known conflicts of interest, including participants or anyone with a stake in the proposed research; anyone from the same institution; former students, advisors, or research collaborators (within the last three years); or close personal contacts. Please note that the Editor-in-Chief may accept one or more of the proposed reviewers or may request a review by other qualified persons.

**Language Editing:** Manuscripts prepared by authors whose native language is not English should have their work proofread by a native English speaker before submission. If not, this might delay the publication of your manuscript in BioScience Trends.

The Editing Support Organization can provide English proofreading, Japanese-English translation, and Chinese-English translation services to authors who want to publish in BioScience Trends and need assistance before submitting a manuscript. Authors can visit this organization directly at <http://www.iacmhr.com/iac-eso/support.php?lang=en>. IAC-ESO was established to facilitate manuscript preparation by researchers whose native language is not English and to help edit works intended for international academic journals.

#### 4. Manuscript Preparation

Manuscripts should be written in clear, grammatically correct English and submitted as a Microsoft Word file in a single-column format. Manuscripts must be paginated and typed in 12-point Times New Roman font with 24-point line spacing. Please do not embed figures in the text. Abbreviations should be used as little as possible and should be explained at first mention unless the term is a well-known abbreviation (e.g. DNA). Single words should not be abbreviated.

**Title Page:** The title page must include 1) the title of the paper (Please note the title should be short, informative, and contain the major key words); 2) full name(s) and affiliation(s) of the author(s), 3) abbreviated names of the author(s), 4) full name, mailing address, telephone/fax numbers, and e-mail address of the corresponding author; and 5) conflicts of interest (if you have an actual or potential conflict of interest to disclose, it must be included as a footnote on the title page of the manuscript; if no conflict of

interest exists for each author, please state "There is no conflict of interest to disclose". Please visit [Download Centre](#) and refer to the title page of the manuscript sample.

**Abstract:** The abstract should briefly state the purpose of the study, methods, main findings, and conclusions. For article types including Original Article, Brief Report, Review, Policy Forum, and Case Report, a one-paragraph abstract consisting of no more than 250 words must be included in the manuscript. For News and Letters, a brief summary of main content in 150 words or fewer should be included in the manuscript. Abbreviations must be kept to a minimum and non-standard abbreviations explained in brackets at first mention. References should be avoided in the abstract. Key words or phrases that do not occur in the title should be included in the Abstract page.

**Introduction:** The introduction should be a concise statement of the basis for the study and its scientific context.

**Materials and Methods:** The description should be brief but with sufficient detail to enable others to reproduce the experiments. Procedures that have been published previously should not be described in detail but appropriate references should simply be cited. Only new and significant modifications of previously published procedures require complete description. Names of products and manufacturers with their locations (city and state/country) should be given and sources of animals and cell lines should always be indicated. All clinical investigations must have been conducted in accordance with Declaration of Helsinki principles. All human and animal studies must have been approved by the appropriate institutional review board(s) and a specific declaration of approval must be made within this section.

**Results:** The description of the experimental results should be succinct but in sufficient detail to allow the experiments to be analyzed and interpreted by an independent reader. If necessary, subheadings may be used for an orderly presentation. All figures and tables must be referred to in the text.

**Discussion:** The data should be interpreted concisely without repeating material already presented in the Results section. Speculation is permissible, but it must be well-founded, and discussion of the wider implications of the findings is encouraged. Conclusions derived from the study should be included in this section.

**Acknowledgments:** All funding sources should be credited in the Acknowledgments section. In addition, people who contributed to the work but who do not meet the criteria for authors should be listed along with their contributions.

**References:** References should be numbered in the order in which they appear in the text. Citing of unpublished results, personal communications, conference abstracts, and theses in the reference list is not recommended but these sources may be mentioned in the text. In the reference list,

cite the names of all authors when there are fifteen or fewer authors; if there are sixteen or more authors, list the first three followed by *et al.* Names of journals should be abbreviated in the style used in PubMed. Authors are responsible for the accuracy of the references. Examples are given below:

*Example 1* (Sample journal reference):

Inagaki Y, Tang W, Zhang L, Du GH, Xu WF, Kokudo N. Novel aminopeptidase N (APN/CD13) inhibitor 24F can suppress invasion of hepatocellular carcinoma cells as well as angiogenesis. *Biosci Trends*. 2010; 4:56-60.

*Example 2* (Sample journal reference with more than 15 authors):

Darby S, Hill D, Auvinen A, *et al.* Radon in homes and risk of lung cancer: Collaborative analysis of individual data from 13 European case-control studies. *BMJ*. 2005; 330:223.

*Example 3* (Sample book reference):

Shalev AY. Post-traumatic stress disorder: diagnosis, history and life course. In: Post-traumatic Stress Disorder, Diagnosis, Management and Treatment (Nutt DJ, Davidson JR, Zohar J, eds.). Martin Dunitz, London, UK, 2000; pp. 1-15.

*Example 4* (Sample web page reference):

Ministry of Health, Labour and Welfare of Japan. Dietary reference intakes for Japanese. <http://www.mhlw.go.jp/houdou/2004/11/h1122-2a.html> (accessed June 14, 2010).

**Tables:** All tables should be prepared in Microsoft Word or Excel and should be arranged at the end of the manuscript after the References section. Please note that tables should not be in image format. All tables should have a concise title and should be numbered consecutively with Arabic numerals. If necessary, additional information should be given below the table.

**Figure Legend:** The figure legend should be typed on a separate page of the main manuscript and should include a short title and explanation. The legend should be concise but comprehensive and should be understood without referring to the text. Symbols used in figures must be explained.

**Figure Preparation:** All figures should be clear and cited in numerical order in the text. Figures must fit a one- or two-column format on the journal page: 8.3 cm (3.3 in.) wide for a single column, 17.3 cm (6.8 in.) wide for a double column; maximum height: 24.0 cm (9.5 in.). Please make sure that the symbols and numbers appeared in the figures should be clear. Please make sure that artwork files are in an acceptable format (TIFF or JPEG) at minimum resolution (600 dpi for illustrations, graphs, and annotated artwork, and 300 dpi for micrographs and photographs). Please provide all figures as separate files. Please note that low-resolution images are one of the leading causes of article resubmission and schedule delays. All color figures will be reproduced in full color in the online edition of the journal at no cost to authors.

**Units and Symbols:** Units and symbols

conforming to the International System of Units (SI) should be used for physicochemical quantities. Solidus notation (*e.g.* mg/kg, mg/mL, mol/mm<sup>2</sup>/min) should be used. Please refer to the SI Guide [www.bipm.org/en/si/](http://www.bipm.org/en/si/) for standard units.

**Supplemental data:** Supplemental data might be useful for supporting and enhancing your scientific research and BioScience Trends accepts the submission of these materials which will be only published online alongside the electronic version of your article. Supplemental files (figures, tables, and other text materials) should be prepared according to the above guidelines, numbered in Arabic numerals (*e.g.*, Figure S1, Figure S2, and Table S1, Table S2) and referred to in the text. All figures and tables should have titles and legends. All figure legends, tables and supplemental text materials should be placed at the end of the paper. Please note all of these supplemental data should be provided at the time of initial submission and note that the editors reserve the right to limit the size and length of Supplemental Data.

## 5. Submission Checklist

The Submission Checklist will be useful during the final checking of a manuscript prior to sending it to BioScience Trends for review. Please visit [Download Centre](#) and download the Submission Checklist file.

## 6. Online Submission

Manuscripts should be submitted to BioScience Trends online at <http://www.biostencetrends.com>. The manuscript file should be smaller than 5 MB in size. If for any reason you are unable to submit a file online, please contact the Editorial Office by e-mail at [office@biostencetrends.com](mailto:office@biostencetrends.com).

## 7. Accepted Manuscripts

**Proofs:** Galley proofs in PDF format will be sent to the corresponding author via e-mail. Corrections must be returned to the editor ([proof-editing@biostencetrends.com](mailto:proof-editing@biostencetrends.com)) within 3 working days.

**Offprints:** Authors will be provided with electronic offprints of their article. Paper offprints can be ordered at prices quoted on the order form that accompanies the proofs.

**Page Charge:** Page charges will be levied on all manuscripts accepted for publication in BioScience Trends (\$140 per page for black white pages; \$340 per page for color pages). Under exceptional circumstances, the author(s) may apply to the editorial office for a waiver of the publication charges at the time of submission.

(Revised February 2013)

## Editorial and Head Office:

Pearl City Koishikawa 603  
2-4-5 Kasuga, Bunkyo-ku  
Tokyo 112-0003 Japan  
Tel: +81-3-5840-8764  
Fax: +81-3-5840-8765  
E-mail: [office@biostencetrends.com](mailto:office@biostencetrends.com)

## JOURNAL PUBLISHING AGREEMENT (JPA)

---

**Manuscript No.:**

**Title:**

**Corresponding Author:**

---

The International Advancement Center for Medicine & Health Research Co., Ltd. (IACMHR Co., Ltd.) is pleased to accept the above article for publication in BioScience Trends. The International Research and Cooperation Association for Bio & Socio-Sciences Advancement (IRCA-BSSA) reserves all rights to the published article. Your written acceptance of this JOURNAL PUBLISHING AGREEMENT is required before the article can be published. Please read this form carefully and sign it if you agree to its terms. The signed JOURNAL PUBLISHING AGREEMENT should be sent to the BioScience Trends office (Pearl City Koishikawa 603, 2-4-5 Kasuga, Bunkyo-ku, Tokyo 112-0003, Japan; E-mail: [office@biosciencetrends.com](mailto:office@biosciencetrends.com); Tel: +81-3-5840-8764; Fax: +81-3-5840-8765).

### 1. Authorship Criteria

As the corresponding author, I certify on behalf of all of the authors that:

- 1) The article is an original work and does not involve fraud, fabrication, or plagiarism.
- 2) The article has not been published previously and is not currently under consideration for publication elsewhere. If accepted by BioScience Trends, the article will not be submitted for publication to any other journal.
- 3) The article contains no libelous or other unlawful statements and does not contain any materials that infringes upon individual privacy or proprietary rights or any statutory copyright.
- 4) I have obtained written permission from copyright owners for any excerpts from copyrighted works that are included and have credited the sources in my article.
- 5) All authors have made significant contributions to the study including the conception and design of this work, the analysis of the data, and the writing of the manuscript.
- 6) All authors have reviewed this manuscript and take responsibility for its content and approve its publication.
- 7) I have informed all of the authors of the terms of this publishing agreement and I am signing on their behalf as their agent.

### 2. Copyright Transfer Agreement

I hereby assign and transfer to IACMHR Co., Ltd. all exclusive rights of copyright ownership to the above work in the journal BioScience Trends, including but not limited to the right 1) to publish, republish, derivate, distribute, transmit, sell, and otherwise use the work and other related material worldwide, in whole or in part, in all languages, in electronic, printed, or any other forms of media now known or hereafter developed and the right 2) to authorize or license third parties to do any of the above.

I understand that these exclusive rights will become the property of IACMHR Co., Ltd., from the date the article is accepted for publication in the journal BioScience Trends. I also understand that IACMHR Co., Ltd. as a copyright owner has sole authority to license and permit reproductions of the article.

I understand that except for copyright, other proprietary rights related to the Work (e.g. patent or other rights to any process or procedure) shall be retained by the authors. To reproduce any text, figures, tables, or illustrations from this Work in future works of their own, the authors must obtain written permission from IACMHR Co., Ltd.; such permission cannot be unreasonably withheld by IACMHR Co., Ltd.

### 3. Conflict of Interest Disclosure

I confirm that all funding sources supporting the work and all institutions or people who contributed to the work but who do not meet the criteria for authors are acknowledged. I also confirm that all commercial affiliations, stock ownership, equity interests, or patent-licensing arrangements that could be considered to pose a financial conflict of interest in connection with the article have been disclosed.

---

**Corresponding Author's Name (Signature):**

**Date:**



